

123P

N64-18133 *gm*

CODE-1

CR-53466

OPTICAL SPACE COMMUNICATIONS

SYSTEM STUDY

FINAL REPORT

VOLUME III

SYSTEM TOPICS-PART TWO

OTS PRICE

XEROX

\$

1.10 per

MICROFILM

\$

3.89 incl.

CONTRACT NO. NASw-540
NATIONAL AERONAUTICS AND
SPACE ADMINISTRATION

SPACECRAFT DEPARTMENT

GENERAL  ELECTRIC

T
OPTICAL SPACE COMMUNICATION SYSTEM STUDY,

2#

T. suppl.
FINAL REPORT

VOLUME III :

SYSTEM TOPICS - PART TWO

(NASA Contract No. NAS w-540)

Office of Advanced Research and Technology

Headquarters

National Aeronautics and Space Administration

0 authors 7 February 1964

123 p

ref

(NASA CR-53466)

OTS: \$ 10.10
pL, \$3.89mf

0998914
2. Spacecraft Department
Missile and Space Division
General Electric Company
Valley Forge Space Technology Center
P. O. Box 8555
Philadelphia, Pa. 19101

TABLE OF CONTENTS

	<u>Page</u>
Part I. PHOTOMULTIPLIER DETECTORS	
I. The Photomultiplier	1
II. The Photocathode	2
A. Photocathode Structure	2
B. Quantum Efficiency	3
C. Temperature Effect	4
D. Collection Efficiency	7
III. The Electron Multiplier	7
A. Multiplier Structure	8
B. Resolving Time	10
C. Gain	11
D. Fatigue	14
IV. Dark Emission	15
A. Pulse Discriminator	15
B. Thermionic Emission	18
C. Experimental Evidence	19
D. Photocathode Discriminator	21
V. Pulse Counting	21
A. Circuit Characteristics	21
B. Information Rates	25
(a) Uncertainty in the Pulse Count	25
(b) Information Rate	26
(c) Counting Information Rate Advantage	27
C. Advantages	29
D. Limitations	29
VI. Current Measuring	30
A. Circuit Characteristics	30
B. Noise Analysis	30
C. Types of Noise	33
(a) Johnson	33
(b) Shottky	33
(c) Flicker	34
(d) Current	34
(e) Photon	35
(f) Secondary Emission (Photomultiplier)	35
(g) Pattern	36
(h) Breakdown	36
(i) Microphonics	36
D. Frequency Characteristics	37
(a) Photocathode with Decay Emission	40
(b) Light Mixing	41
E. Advantages	42
F. Disadvantages	42

	<u>Page</u>
VII. Optimization of a Photomultiplier's Physical Parameters	43
A. Internal	43
(a) Noise Discrimination	43
(b) Integrating Sphere Effect	43
B. External	43
(a) Shielding	44
(b) The Dynode Chain	44
(c) The Power Supply	45
(d) Signal Cables	46
Part 2: EFFECT OF ATMOSPHERIC TURBULENCE ON LASER PROPAGATION .	48
Part 3: LASER OPTICS	98
I. Transmitting Optics.	99
II. Receiving Optics	101
III. Filtering.	102
IV. Detection of Faint Sources	110

PART 1

PHOTOMULTIPLIER DETECTORS

PHOTOMULTIPLIER DETECTORS

The primary concern of this review is the performance of photomultiplier detectors on signals that are close to the noise level of the detector.

I. The Photomultiplier

The photomultiplier is a device for obtaining a relatively large electrical signal from a small amount of incident visible light radiation. Incident photons on a photocathode surface release photoelectrons which undergo cascade multiplication across dynodes within the tube to produce a current generator effect. If all photons release the same percentage of photoelectrons with identical velocities and the electron multiplier section acts equally on these electrons, pulses of exact equal size would occur to contribute equally to the signal current. Unfortunately, photocathode structure, photocathode efficiency, and dynode secondary emission ratio varies in an actual photomultiplier so that the multiplication is very different from one photoelectron to another. As a result, the stream of pulses coming out of a photomultiplier may vary by more than a magnitude in amplitude. Additionally, a variable time delay in the multiplier section broadens the pulses.

Since the electron pulses are not of equal size in amplitude and/or width, it is evident that the signal-to-noise performance of a photomultiplier will be larger in a pulse counting system where all pulses are given equal weight regardless of their sizes rather than in a current measuring system. However, when the pulses occur at a rate that allows pulses to overlap, current or charge integration measuring techniques must be used.

The photomultiplier is quite linear to a large range in the number of received photons, and is thus linear with power and could be called a square law device. If light is thought to be expressed in terms of wave equations, one would predict that two light waves could be mixed in a photomultiplier to produce a resultant beat frequency. This has been done at General Electric's Radio-Optical Observatory using two simultaneous modes of a gas laser as a light source, and the results are given under the Current Measuring section of this report.

II. The Photocathode

The object of the photocathode is to release a maximum of photoelectrons to the electron multiplier for a given number of incident photons while minimizing those photoelectrons released from self-excitation. The number of electrons entering the multiplier structure for a given number of incident photons is determined by:

- (a) The quantum efficiency of the photocathode.
- (b) The collection efficiency of the electron optical system.
- (c) The dark-current electrons.

A. Photocathode Structure

James P. Rodman and Harlan J. Smith² collaborated at Yale University Observatory, New Haven, Connecticut to measure the quantum uniformity of the photocathode of various photomultipliers by a linear scan with a 0.025-cm diameter spot moved by 0.063-cm increments. Extreme differences of 25% in sensitivity occurred over the cathode surface (Figure 1).

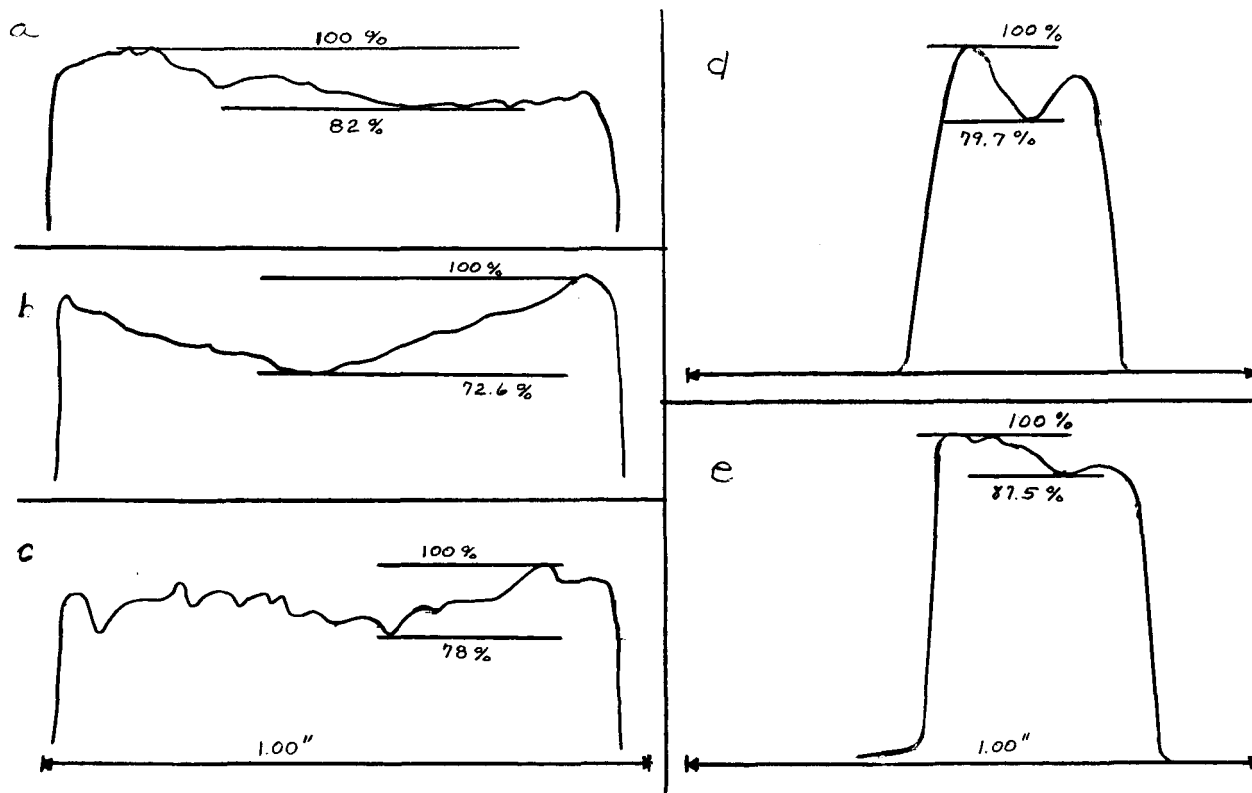


Figure 1. Photocathode Quantum Structure measured at Yale Observatory.

All scans made with 0.025-cm light spot moved in 0.063-cm increments except for 1c which was moved in 0.0063-cm increments. Scans a, b, c are of EMI 9558 A trialkali S-20, Nos. 584, 5833, and 5938; scans d and e of EMI 9502S CsSb No. 5598 and 6256SA No. 11519.

Notice how the photomultipliers seemed slightly more sensitive at the boundary where they most probably would not have been utilized. Structure variations are quite critical if star magnitudes are to be measured, for these scans indicate the need of requiring two comparison light sources to be imaged on identical sections of the photocathode.

B. Quantum Efficiency

Improvements in quantum efficiency basically rests on the discovery of new materials for sensitizing the photocathode or of new ways of activating known materials. A measure of the efficiency of conversion of light energy is in general the ratio of the number of distinct events (photoelectrons) produced in a radiation sensitized process to the number of quanta (photons) absorbed -- the intensity distribution of the radiation wavelength should be specified. For instance, the quantum efficiency of a dark-adapted human eye is found to be a maximum of about 3% in the vicinity of 5100 Å. This means that the signal-to-noise performance of the eye is equivalent to that of an ideal detector which produces one recorded photo-event for each 33 incident photons within the wavelength band to which it is sensitive. The approximate quantum efficiencies of three photoemissive cathodes, of the dark-adapted eye, and of two photographic emulsions are shown in Figure 2. Particularly notice the multialkali photo-

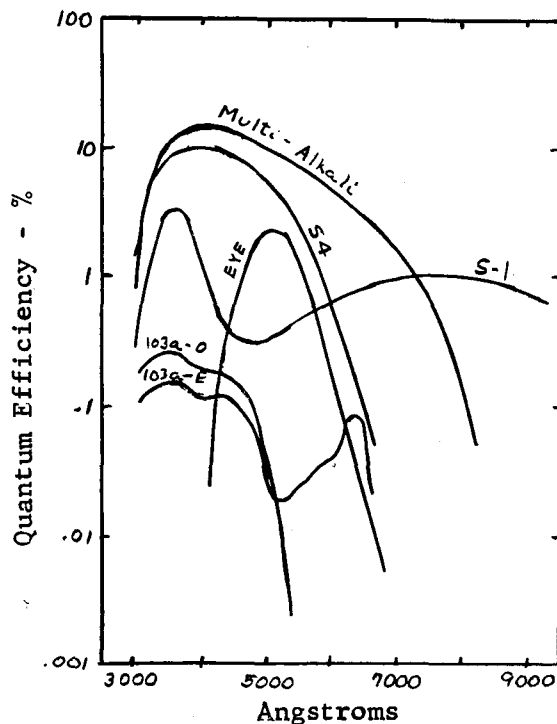


Figure 2. Quantum Efficiencies of three photoemissive cathodes, of the dark-adapted human eye, and of two photographic emulsions.

cathodes, which also have a relatively low dark emission along with high quantum efficiency. Astronomically they are attractive because of their sensitivity in the red region.

The quantum efficiency of a detector is not only a function of material, but it may also vary with temperature and time. When quantum efficiency is dependent upon exposure time, this is known as reciprocity failure. That is, the reciprocity law of a constant product of intensity and exposure time is not obeyed. This effect is common with photographic emulsions but only at high light levels may a photomultiplier produce similar results and the cause is either light fatigue or improper dynode biasing. The temperature effect, however may be striking.

C. Temperature Effect

Users of photomultipliers are universally familiar with the fact that cooling is effective in reducing a tube's thermionic dark current, but they are not always aware that the sensitivity of most photomultipliers have a large, wavelength-dependent temperature coefficient. Of those aware of these temperature effects, the feeling is that a temperature decrease will likewise decrease sensitivity. Confusion does exist with even the published data in conflict, and many low light level tubes that astronomers use have never been measured.

One of the better articles on the cooling of multipliers and their effect is written by Andrew T. Young of Harvard College Observatory.² Only the photomultipliers were cooled, with the voltage dividers mounted external to the cold chamber and the anode currents amplified by an electrometer. Particularly significant of his experiment was the impossibility of cooling to dry ice temperature without the addition of ethyl acetate and the importance of using a cold window to allow the radiation heat balance to drop the cathode to cold box temperature.

Different tubes of the same type show different spectral sensitivities, but there is very little in the published literature to indicate how much variation the user can expect. Lontie-Bailliez and Meessen¹ summarized a large number of observations on temperature coefficient of Sb-Cs photocathode (Figure 3). The temperature coefficient of Sb-Cs retains practically the same shape, and only becomes more positive as the temperature decreases. This means that at some temperature between 20°C and 80°C a Sb-Cs cathode has maximum quantum efficiency at wavelengths shorter than 5500 Å.

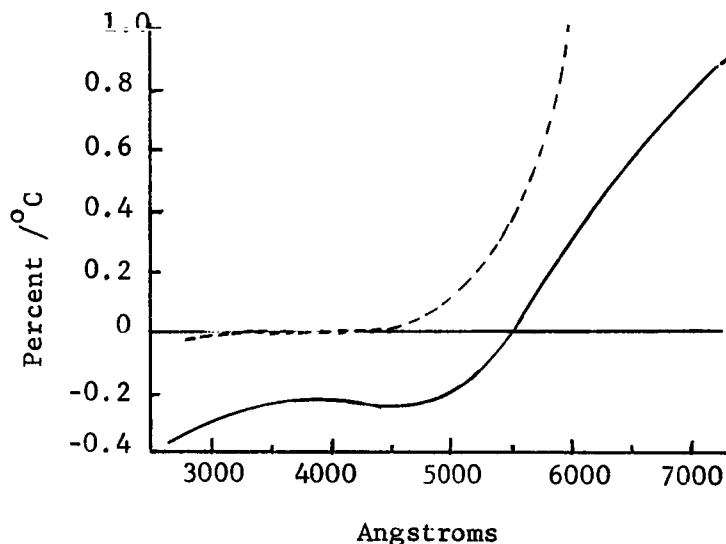


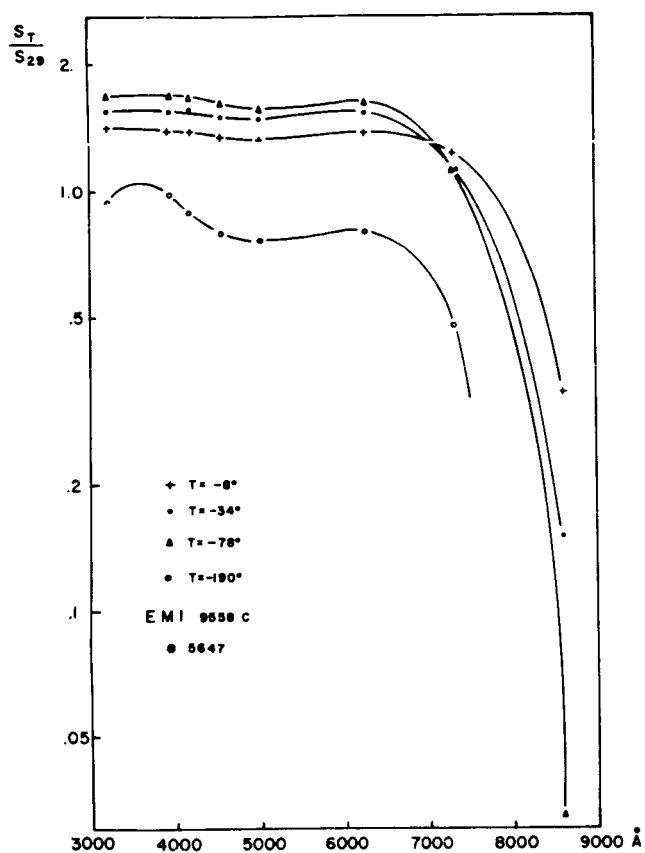
Figure 3. Temperature Coefficient of Sb-Cs cathodes

Solid Curve: $T = + 20^{\circ}\text{C}$

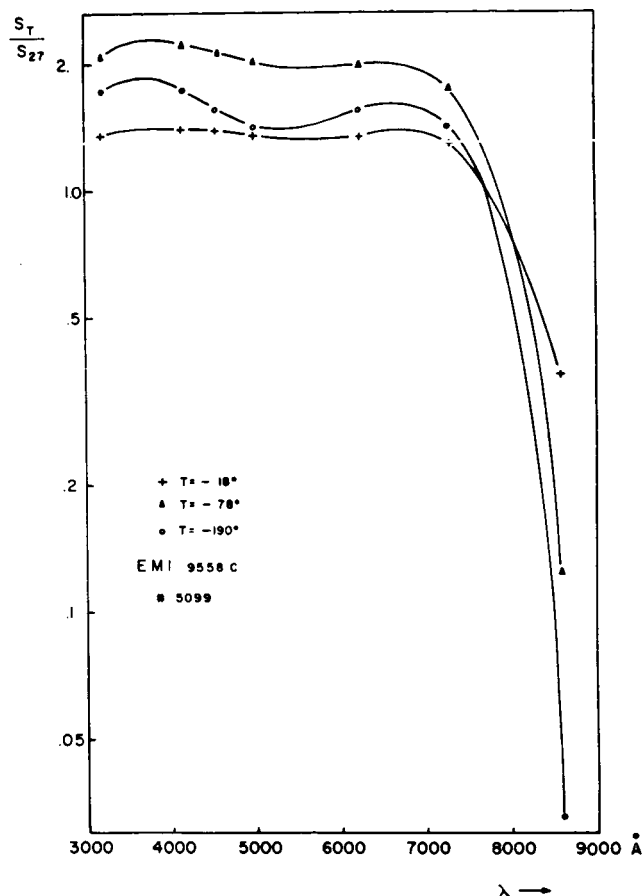
Dashed Curve: $T = - 80^{\circ}\text{C}$

Young also observed the effects of cooling two trialkali EMI 9558C photomultipliers to various temperatures where the ratio of anode response at a given temperature to that at room temperature was plotted - Figure 4. The results on two Ag-O-Cs Farnsworth FW-118 photomultipliers cooled with dry ice and with liquid nitrogen is given in Figure 5.

Young found that antimony-alkali photocathodes lost sensitivity below -100°C , and showed large variations in the red, but generally being well-balanced in the blue. Tubes with sharp red cutoffs become sharper when cooled, while those with long red tails of low slope - and hence higher relative far-red sensitivity - lose a smaller fraction of their long-wavelength response on cooling. This correlation is understandable in terms of W. E. Spicer's³ description.



(a)



(b)

Figure 4. Ratio of Cooled to Room-Temperature Anode Sensitivity for two EMI 9558 Photomultipliers - (Young)

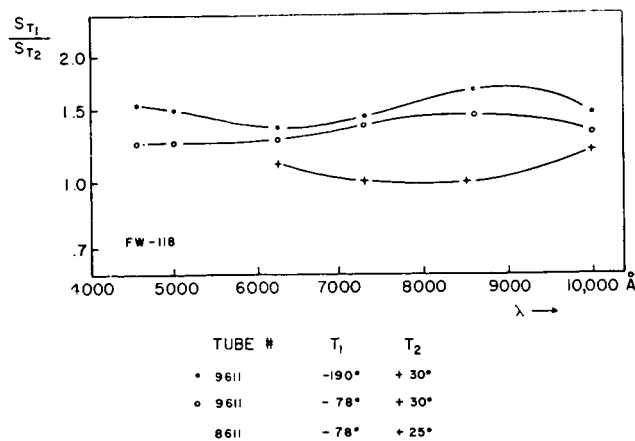


Figure 5. Ratio of Cooled to Room-Temperature Anode Sensitivity for Two Farnsworth FW-118 Photomultipliers - (Young)

D. Collection Efficiency

The efficiency of photoelectron collection in a photomultiplier is primarily a matter of the electrode design. A multiplier which is faulty in this important aspect cannot be made to perform well regardless of how it is used. If we assume that the mechanical structure is well designed, collection efficiency may be reduced by poor usage with operation in the presence of a magnetic field in the neighborhood of the photocathode or by incorrect voltages on the multiplier. Occasionally a multiplier will incorporate magnetic materials in its structure which may become permanently magnetized to cause poor collection efficiency.

If a given scintillation yields N photon at the photocathode of a photomultiplier, the number of electrons n which enter the multiplier and are useful in determining the size of the output current pulse will be

$$n = \gamma \eta_p N \quad (1)$$

It is evident that the quantum efficiency γ of the photocathode and the collection efficiency η_p are equally important in determining the effectiveness of the multiplier.

A good photoemissive cathode by itself is nearly a perfect detector since the photoelectron flux is a linear function of the incident light flux over a very broad range of light-levels. The photo-events are independent of one another and are all of the same size. In other words, any incident photon is just as likely to eject a photoelectron as any other incident photon and the photoelectrons all contribute equally to the cathode current.

III. The Electron Multiplier

The electron multiplier section consists of a series of electrodes known as dynodes which have been so surfaced that electrons striking them produce secondary emission. The electrodes of a multiplier are so shaped that electrons from the photocathode are directed onto the first dynode. The secondary electrons produced at the first dynode are in turn focused on the second dynode until finally the electrons resulting from this cascading process are collected at the last dynode, or anode. The reason for the multiplier section is that only a few photoelectrons are ejected from the

photocathode. This minute photocurrent must be amplified with an amplifier having an extremely short rise time and a low noise figure. A photomultiplier has the required rapid rise time, a very high input impedance, and an almost completely noise-free amplifier.

A. Multiplier Structure

The different classes of structures differ primarily in the means for directing the electrons from one dynode to the next. The classes are the dynamic, static, and unfocused.

The dynamic multiplier usually has only two plates with an alternating electric field used to accelerate the electrons. This type is not common.

Static multipliers use either a magnetic or electrostatic focus. The magnetic multiplier depends upon crossed magnetic and electric fields which produce cycloidal-like electron trajectories for directing the electrons from one stage to the next - Figure 6. The magnetic amplifier is quite critical in adjustment and requires a magnetic field which must be accurately controlled in intensity and orientation if the multiplier is to operate satisfactorily.

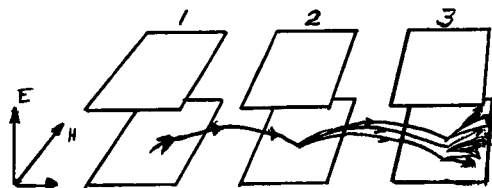


Figure 6. Magnetically Focused Multiplier.

The electrostatically focused multiplier is the most widely used type. The dynodes are so shaped as to produce an electrostatic potential distribution between successive dynodes to:

- (a) accelerate electrons from the working surface of one dynode to the working surface of the other.
- (b) draw the emitted secondary electrons away from the surface and towards the next dynode.

The dynodes may physically be placed in any manner. Figure 7 shows schematically two arrangements.

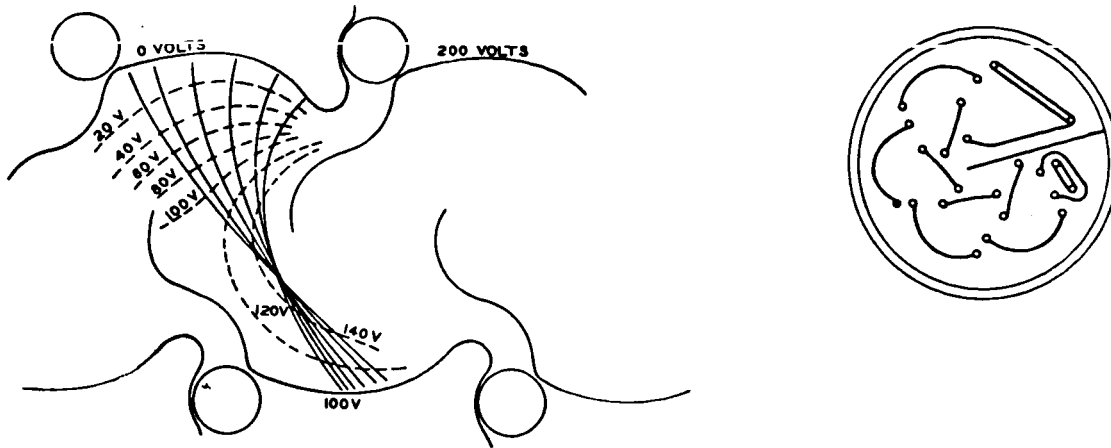


Figure 7. Typical Electrostatic Multiplier Structures

An unfocused multiplier makes no attempt to cause the electrons to follow unique predetermined paths. A typical example is a venetian blind type of multiplier - Figure 8 - in which electrons strike the dynode, and release secondary electrons which are drawn through the dynode by the potential existing between the mesh screen and the next venetian blind-like dynode.

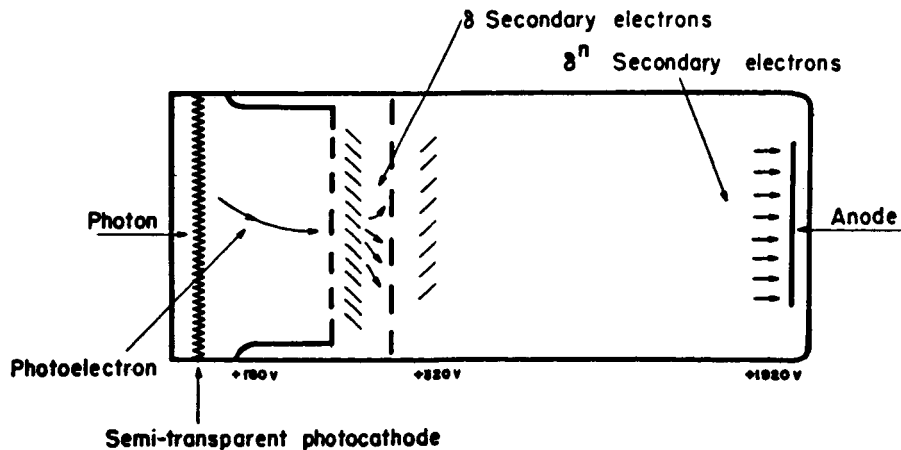


Figure 8. "Venetian Blind" Multiplier

Regardless of multiplier structure, the cascading process is continued for as many stages as required to obtain the desired overall current gain which is

usually in the range of 10^6 . This requires good electrode design. That is, sharp points and close spacings must be avoided to eliminate cold cathode discharge effects, ion feedback must be prevented by side electron path separation, etc.

B. Resolving Time

The photomultiplier has a very short resolving time; 10^{-8} sec. is easily obtained. The limit is set by the broadening effect on the signal as the cascaded electrons are emitted through the tube, thus causing a variable transit time. Transit time delays are the result of:

- (a) initial velocity effects
- (b) emission time of secondary electrons
- (c) electron trajectory differences
- (d) space charge effects

The photocathode surface is a good detector so that the velocity distribution of the cathode electrons is quite uniform. However, once they enter the multiplier section the cascading electrons have a variable delay between dynodes because a certain portion are just reflected primaries, others are variable velocity secondaries, and others may be just noise impulses. A dynode emits secondaries with initial velocities in the range of 0-5 v, so certainly the larger velocity electrons will reach the next dynode before a lower velocity electron. The fractional decrease in transit time of electrons with initial velocities of ΔV over zero initial velocities can be shown to be

$$\Delta t = t_0 \sqrt{\Delta V/V_0} \quad (2)$$

where V_0 is the voltage potential between dynodes and t_0 is the transit time of a zero velocity electron between the dynodes.

Since the entire process is random, a statistical variation in transit time to initial velocity effects will occur down the cascading tube. When an electron impinges on an emissive substance a certain time is required before secondaries are released. Estimates on this time are from 10^{-12} to 10^{-10} seconds. However considering that a few primaries are immediately elastically repelled with velocities greater than zero, the delay time and velocity distribution becomes important.

Electron trajectory differences leaving the dynode surface are considered to cause the largest spread in the transit time. Consider a multiplier structure as shown in Figure 7 where calculations have shown possible time delay differences of 2×10^{-9} sec/dynode.⁶ The mean of the spread per dynode is certainly less but for a sixteen-stage multiplier an average time delay of 4×10^{-9} seconds may be expected. This effect is especially pronounced in tubes that use little focusing, such as the venetian blind multiplier.

Space charge effects alter the potential lines and velocity distributions of the electrons so that random time delays exist depending on signal and emission characteristics. This effect is particularly noticeable when first applying voltage to the dynodes, for the residual current may become very large. Probably the redistribution of electric charges on the internal parts, insulators, and walls of the glass envelope cause minute currents to flow and eject secondaries from the dynodes. Generally the main effect decreases to a normal value within a half-hour.

C. Gain

Certain materials are capable of emitting in a vacuum several electrons when struck by an electron with sufficient velocity. This release of electrons known as secondary emission, depends upon the nature of the surface, the energy of the primary, and on the angle of incidence of the primary electrons. The rate of the number of electrons leaving the surface to the number arriving is designated as the "secondary emission ratio, δ ". The secondary emission ratio of a dynode is in itself a statistical quantity and the multiplier simply cascades the values of δ . Three group types of electrons are re-emitted from the dynode: primaries elastically reflected without a loss of energy, back diffused primaries which have lost varying amounts of energy, and low energy secondaries.

As a rule the true secondary electrons have energies with an approximate Maxwellian distribution between 2-50 ev. Diffused primaries exist around 50-150 ev, while reflected primaries appear near 150 ev. The typical secondary emission ratio as a function of primary electron energy for a dynode surface is shown in Figure 9.

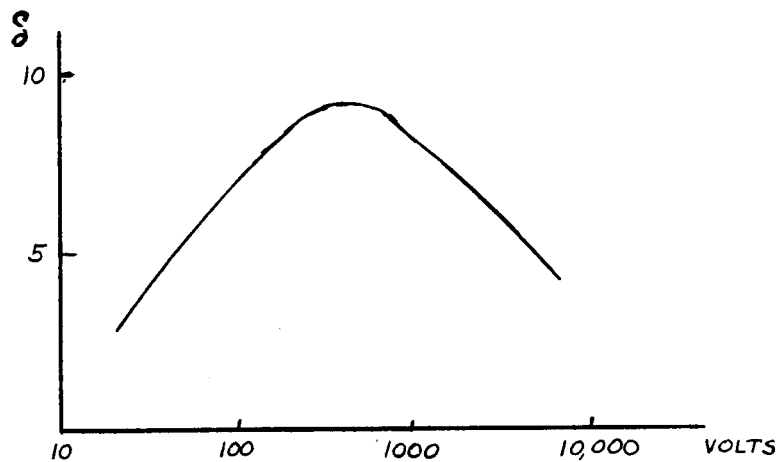


Figure 9. Secondary Emission Ratio as a function of Primary Electron Energy

Two classes of secondary emission surfaces exist:

- (a) Alkali metal compounds, e.g. cesium antimony, which have higher gain at low primary electron energy (≈ 75 v).
- (b) Metal oxide layers, e.g. magnesium oxide on silver-magnesium alloy, show less fatigue at high current density of emission (\approx several $\mu\text{a}/\text{cm}^2$).

Typical secondary emission ratios for various surfaces are tabulated in Table 1.

Surface	δ_{max}	V_{max}
Cs-Sb	8	500
Cs Ag O	5.8 - 9.5	500 - 1000
Mg O (on AgMg)	9.8	500
Be O (on CuBe)	3.5 - 5.5	500 - 700
Be O (on NiBe)	12.3	700
Al_2O_3	1.5 - 4.8	350 - 1300

Table 1. Maximum Secondary Emission Ratios

The actual emission value depends very much on the previous history of the material and the surface probably varies across the dynode as greatly as does the photocathode surface - Figure 1. Since the secondary emission ratio is a function of the primary electron energy, or the potential difference through which the primary bombarding electron falls, the overall gain of a multiplier is extremely sensitive to the overall voltage. This may readily be seen from the following equations:

$$\begin{aligned}\delta &\approx kV \\ G &= \delta^k \sim (kV)^k\end{aligned}\tag{3}$$

$$\Delta G/G \sim k \Delta V/V$$

Lallemand⁷ determined that to measure within one part in 1000 it is necessary to regulate the voltage supply to at least one part in 10,000. He obtained a total multiplication for 20 stages as shown in Figure 10.

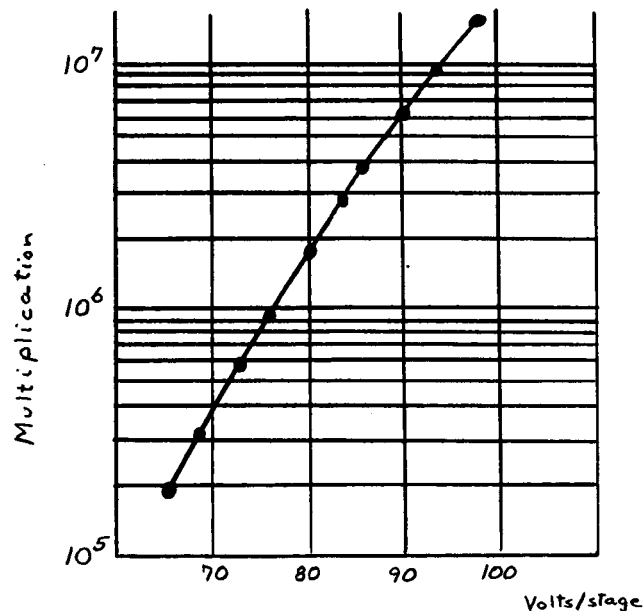


Figure 10. Over-all Gain of a Photomultiplier as a function of dynode voltage (Lallemand).

The gain of a multiplier used for scintillation counting is not critical as long as it remains constant throughout the measurement. The gain should be high enough so that the output pulses may be readily handled by the circuits following the multiplier, and not too high to become space charge limited.

The gain of a photomultiplier may vary drastically if it is used within a magnetic field environment, and under some circumstances it may be necessary to shield with mu-metal, -netic, or co-netic metal. This can be important in astronomical work where the photomultiplier may approach objects constructed of magnetic metal, such as the mount, dome, etc. Figure 11 shows the effect of a magnetic field on a RCA Type 5819 Photomultiplier.

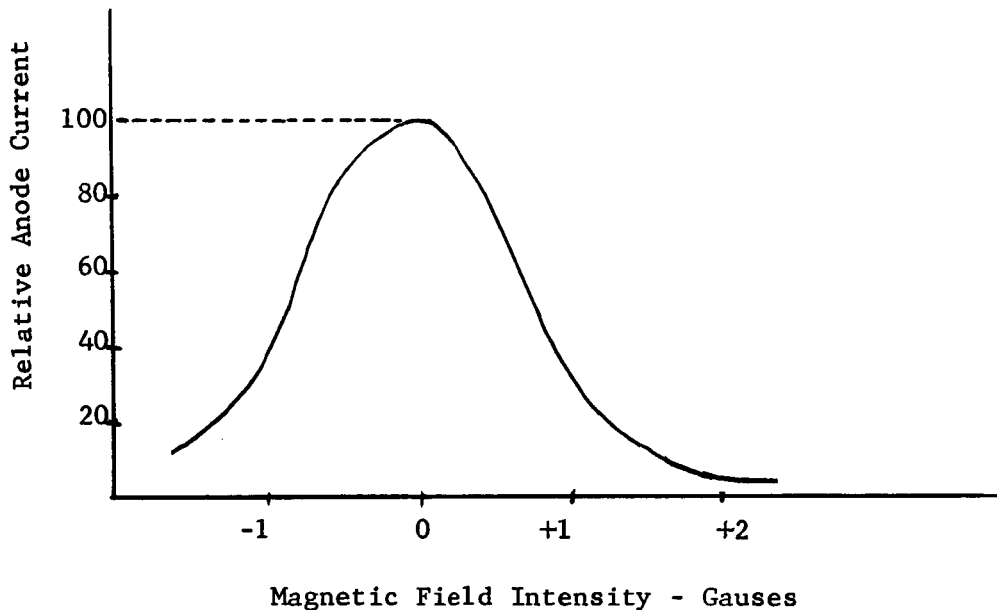


Figure 11. Effect of a Magnetic Field on a Photomultiplier (RCA 5819)

D. Fatigue

An increase in dynode potential may not always be expected to produce an increased gain because of fatigue. At higher current densities there is a falling off of secondary emission ratio as the bombardment continues. Complete recovery from this fatigue effect may only be expected if the emissive surface is allowed to remain at room temperature without bombardment for a period of several hours. If the photomultiplier delivers an excessive current to the last dynode (over 10^{-7} amp) a saturation fatigue will exist due to the variation in potential of the active surface of the dynode which moves in the direction of the potential of the collecting anode with the creation of a space charge.

IV. Dark Emission

If a photomultiplier output is observed under complete darkness a certain number of random pulses per second will be observed in the output. A few of these may be due to cosmic rays reaching the photocathode or dynode surfaces, but by far the majority are self-excited spurious pulses caused by:

- (a) Thermal emission from the photocathode and dynodes.
- (b) Field emission from the electrodes.
- (c) Leakage current across insulating supports.
- (d) Positive ion feedback to the photocathode.
- (e) Fluorescence from the dynode and insulating supports.

A. Pulse Discriminator

In a well-manufactured photomultiplier operated at the proper voltage, only thermionic emission from the photocathode and to a lesser extent from the dynodes will be present to add to the resistor noise at the output. The importance of thermionic emission from the photocathode to that of the dynodes depends upon the relative areas, relative work function, and the secondary emission ratio of the dynodes. That is, if an equal number of thermionic electrons are emitted by the photocathode and dynodes, the anode dark current count will be primarily a result of the photocathode emission since each of these electrons are multiplied through the entire dynode chain, while those emitted by the dynodes receive less amplification. In fact the thermal electrons emitted from the last dynode receive no amplification at all. This implies that those electrons being produced near the photocathode have the largest amplification so that pulse discrimination techniques may possibly distinguish between the source of these signals and thereby improve the overall signal to noise ratio from a photomultiplier.

A pulse discriminator is a device which passes all pulses above a set height level and absorbs all those pulses that are below that height. Counting circuits following the discriminator then only measures the pulse rate of those pulses with voltage heights capable of passing through the discriminator. A typical example of the use of pulse discrimination techniques on a photomultiplier where the dark current is primarily determined by dynode emission is shown in Figure 12.

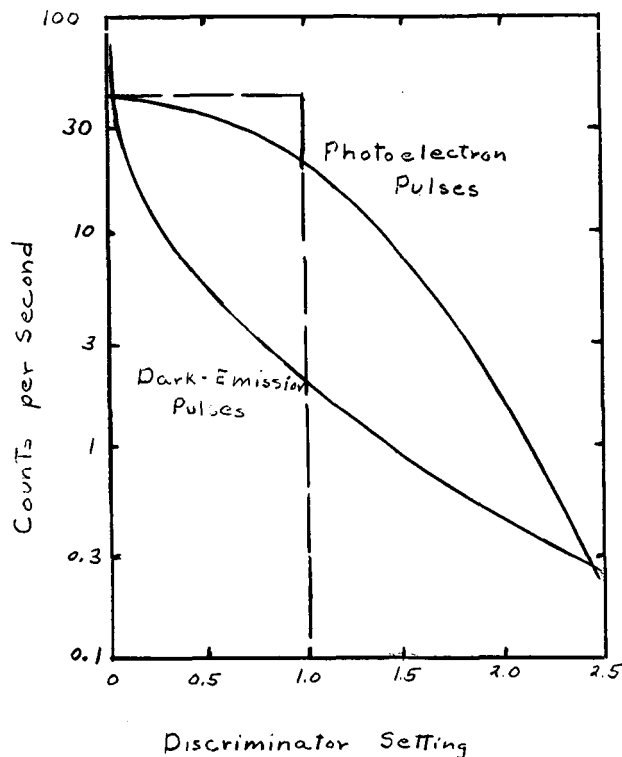


Figure 12. Pulse-height Distribution in a Dynode Emission Dark-Current Limited Photomultiplier

The count rate curve representing dark-emission pulses decreases with an increase in discriminator setting because relatively fewer of the electrons originate near the cathode to undergo multiplication through the entire multiplication chain. The curve rises asymptotically as it approaches zero minimum pulse height because the small pulses originating at the later stages of the multiplier become very numerous and blend eventually into ordinary resistor amplifier noise. For this reason, one cannot operate a pulse-counting system with a discriminator setting of zero. Now if a weak light flux is made to illuminate the photocathode, relatively more of the anode current will originate from the photocathode so that a pulse count rate shown by the curve of photo electron pulses occurs. Notice that if a discriminator setting of one electron-height unit is chosen, a maximum signal-to-noise ratio will occur. A properly functioning photomultiplier shows the following behavior: The dark current has a certain repetition rate and amplitude; on illumination of the photocathode with a very weak light-flux, the

signal increases as well as the amplitude. In a well-manufactured photomultiplier operated at the proper voltage, only thermionic emission from the photocathode and to a lesser extent from the dynodes will be present to add to the resistor noise at the output. If dynode pulses predominate, it is evident that the dynode area is relatively too large to the photocathode, and reduction at the dynode area would thereby reduce the dark-current. The best criterion for determining the suitability of a particular tube would probably be the overall signal-to-noise ratio at the required light level to be received, and the photocathode area needed. An example of two photomultipliers, one limited by photocathode dark current, and another by dynode pulses is shown in Figure 13. Notice that if the light signal and secondary emission ratio produces a large pulse height, the 5819 will be a better choice with a pulse discriminator setting of over 4.5. Actually, the two curves can not be directly compared because the photocathode area of the 5819 is approximately 7.5 times larger than the 931A photomultiplier. But considering that the nominal gain of the 5819 is 63% lower, a rough normalization may be done by reducing the pulse count rate of the 5819 by a factor of 5.

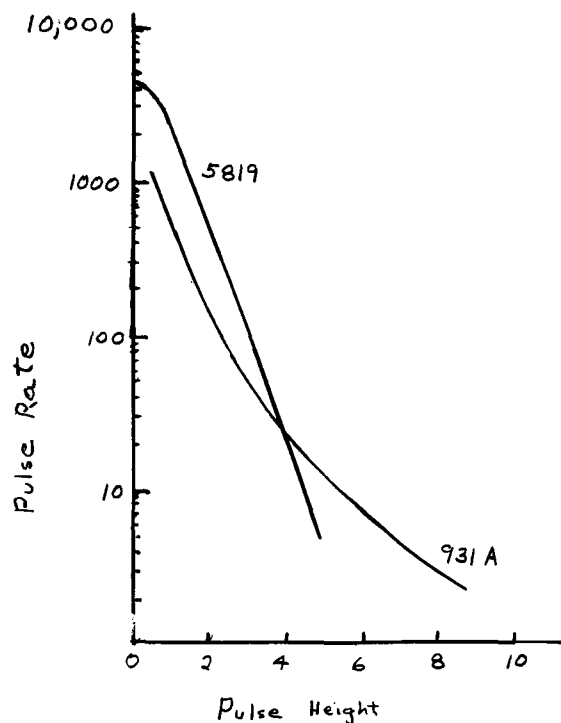


Figure 13. Spurious Pulse Output from Types 931A and 5819 Photomultipliers

B. Thermionic Emission

The emission from the photocathode and dynodes is of course thermionic, and for ideal metallic surfaces is given by Richardson's law as

$$j = A (1-r) T^2 \exp (-e\phi /kT) \quad (4)$$

where

j = is the current density of the electrons

A = is a combination of fundamental physical constants,

$$A = \frac{4\pi m k^2}{h^3} e/h^3 = 120 \text{ amp/cm}^2 \cdot \text{deg}^2$$

e = is the absolute value of electronic charge

k = is Boltzmann's constant

h = is Planck's constant

r = is the reflection coefficient for electrons crossing the potential barrier at the metal surface when the electric field just outside the metal surface is zero. For pure metals r is of the order of 0.05 and is thought to be rather insensitive to temperature changes.

ϕ = is the electronic work function and is defined so that ϕe is a characteristic amount of work required to remove an electron from the interior of the metal to a position just outside the metal. In general ϕ is dependent on temperature and the normal component of electric field intensity at the metal surface.

For practical applications an electric field will probably exist at the metals surface so that Richardson's law must be corrected to

$$j = A (1-r) T^2 \exp \left(- \frac{e\phi - e\sqrt{eE}}{kT} \right) \quad (5)$$

where this equation is the same as Equation 4 and E is defined as the applied electric field. For very small applied fields and appreciable electron emission, the space-charge field in the neighborhood of the cathode is such as to repel many of the electrons emitted with the lower energies. For applied fields sufficient to overcome the space-charge fields, all electrons emitted can be collected on a collecting electrode. Notice that at constant temperature the emission current will increase with the applied field. This increase in emission current is known as the Schottky effect and is due to the lowering of

the potential barrier. If the applied field exceeds 10^5 volts/cm the barrier thickness of the surface begins to approach the order of magnitude of a wavelength of the most energetic electrons in the metal. Some electrons then tunnel through the barrier, and the dependence of the emitted current on temperature and field is entirely different from Equation 5. Under this condition the emission is referred to as "field emission".

Richardson also demonstrated that the electrons emitted from a metal possess a Maxwellian distribution of velocities, even though the velocity distribution law inside the metal is that of Fermi. That is, the number of electrons emitted per unit time are distributed as

$$dn = (1-r) \frac{2m^3}{h^3} \exp(-e\phi/kT) \exp\left[-\frac{\frac{1}{2}m(v_x^2 + v_y^2 + v_z^2)}{kT}\right] v_x dv_x dv_y dv_z \quad (6)$$

where the velocities of the electrons outside the metal are v_x , v_y , v_z . The actual emission may not be exactly determined in practical cases because of patchy surface effects. Conyers Herring¹¹ has done a critical treatment of emission in general and especially in the categories of: the electron and ion emission from uniform pure metal crystals, the electron emission from polycrystalline metals, and the emission from metals with various absorbed monolayers.

C. Experimental Evidence

James P. Rodman and Harlan J. Smith² tested trialkali photo cells and found that over the range of $+20$ to 0°C , thermal emission is the primary noise, Figure 14. Below -20°C , residual noise overrides the thermal dark current. This non-thermal noise was somewhat burst like and non-statistical in character. Possibly resembling $1/f$ flicker noise. For photocathodes sensitive to the infrared, cooling is often insufficient to reduce the dark current so only an improvement may be made by using a photomultiplier with a very small photocathode, or artificially limiting the active surface of the photocathode - implying a photocathode dark noise limited tube.

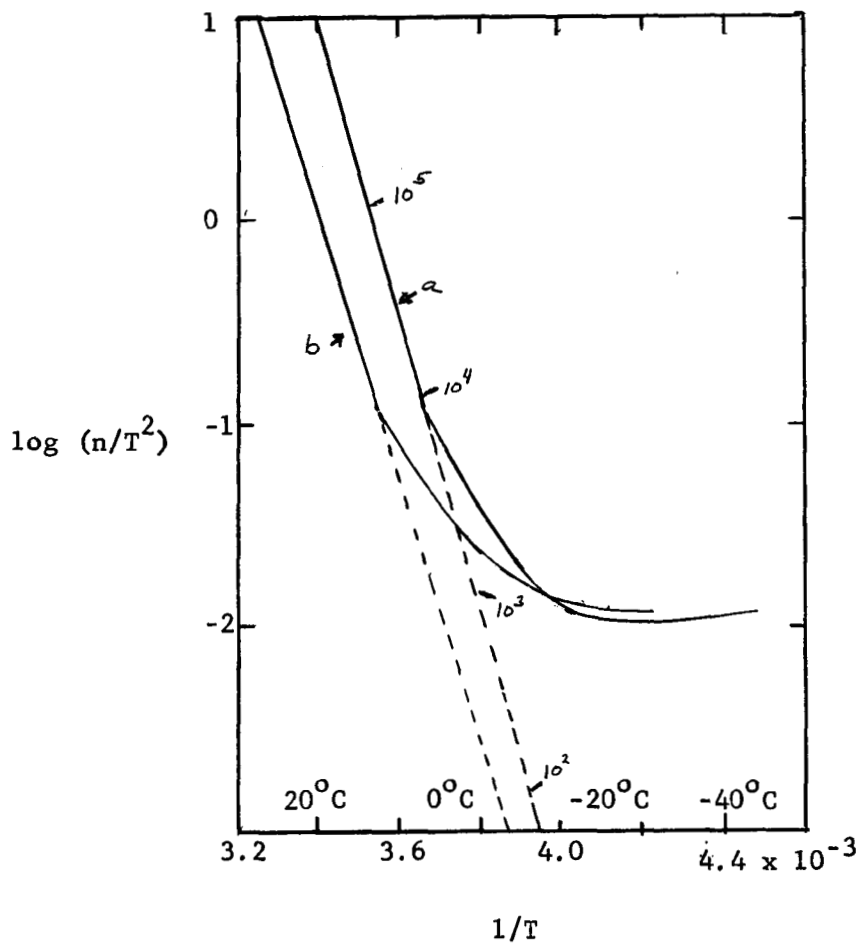


Figure 14. Richardson's Law Curves showing 50-second integrated dark counts as a function of temperature for two EMI Trialkali cells. Solid Curves: observed data for (a) 9559A No. 5844, (b) 9558C No. 5462. Dotted lines indicate extrapolated thermal emission based on primary work function; parenthetical numbers refer to the thermally originating pulses assumed to be associated with that work function for each temperature of No. 5844 (Rodman and Smith)

D. Photocathode Discriminator

If a photomultiplier has a dark current basically limited by photocathode thermionic emission, the place at which there is the greatest distinction between thermal electrons and photoelectrons is naturally at the cathode. At room temperature the average energy of thermal emitted electrons is 0.02 electron volts. The average energy of photoelectrons released is of the order of 1 electron volt¹². Therefore a retarding potential of less than 0.1 volt near the cathode surface would considerably reduce the number of thermal electrons reaching the first dynode. Obviously an internal modification to present photomultipliers would need to be made. Some astronomers have found that a close fitting metal shield near the cathode, maintained either positive or negative with respect to the cathode, would reduce the dark count without reducing the count due to photoelectrons^{12, 13}.

V. Pulse Counting

The photomultiplier is one of the first stable devices capable of precise measurements of light intensity which could indicate by a sizable pulse at its anode, the emission of a photoelectron. Pulse-counting techniques then merely count the time rate of occurrence at these discrete events.

A. Circuit Characteristics

A pulse counting technique requires seven basic function units as blocked out in Figure 15. These may be described as follows. The desired radiation is optically brought to incidence on the cathode of the photomultiplier cell to release photoelectrons. The dynodes supplied by the high voltage power supply multiply the photoelectrons to produce an output pulse at the anode of the cell which is fed into a fast pulse amplifier of stabilized

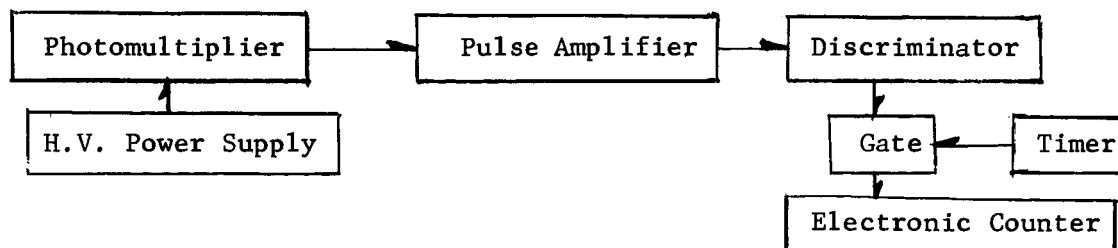


Figure 15. Block Diagram for Pulse Counting

gain. All pulses which are greater in amplitude than a selected reference level causes the discriminator to generate a standard pulse. The timer opens the gate for a specified counting time interval to allow the discriminator pulses to enter the counter. The count indicated on the scaler is then proportional to the sum of the dark current pulses and the intensity of the incident radiation. The requirements for an accurate comparison of the intensity of two light sources must include the gain of the multiplier, the gain of the amplifier, the level of the discriminator, and the counting time to remain constant over the measuring period.

The circuitry surrounding the photomultiplier may be divided into two parts. First the network needed to supply bias to the photocathode, dynodes and focusing electrodes. In general this consists of an extremely well regulated voltage supply capable of delivering one to four thousand volts, depending upon the multiplier used. This high voltage is then divided down into the required voltage steps to supply the electrode system. For a multiplier whose output current is less than a milliamp and requires about 100 to 200 volts per stage, it is common to use 100 k ohm bleeder resistors between stages in the divider - Figure 16. It is frequently advisable to place high value resistors in series with each of the dynodes to limit the maximum current that can flow for protection. Shunt capacitors in the range of 0.001 to 0.1 μ f may also be put on each dynode to reject AC pick up voltage.

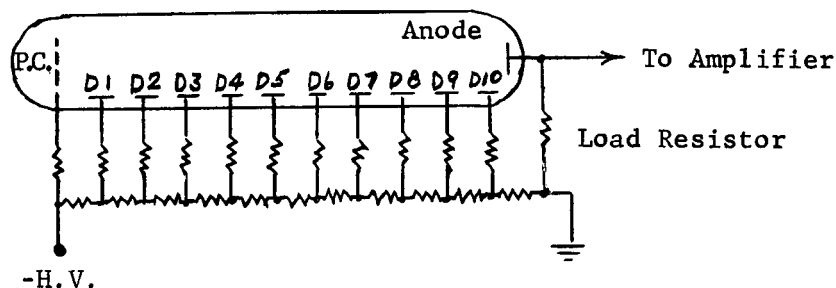


Figure 16. Bleeder and Protective Resistors

The second part consists of an amplifier and assorted analyzing circuits. The output circuit of a photomultiplier cell is shown in Figure 17. Basically the Thevenin equivalent of a photomultiplier is a high impedance current generator. As a result of the cascading dynode emission, an average burst of 10^6 electrons enter the anode for each electron emitted from the cathode.

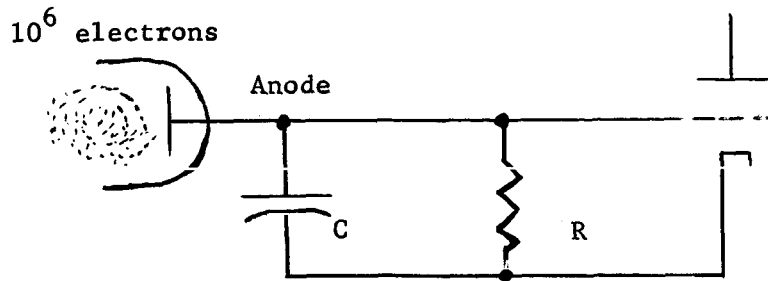


Figure 17. Output Circuit of a Photomultiplier

Depending on the RC time constant of the load impedance, two conditions arise. Either the anode is charged to its maximum in a short time (as a rule of thumb, approximately the electron transit time from the last dynode to the anode), and then discharges relatively slow because of a large RC time constant; or the RC time constant is short as compared to the pulse time spread so that the capacitance may be neglected. In any case the RC time constant should be much less than the average pulse rate so that the resistor may discharge the capacitance before the next pulse which may come quite randomly unless the light source is chopped.

The capacitance C which one must minimize is composed of the stray capacities to ground of the photocell anode, any associated wiring, and transistor or vacuum tube grid. The signal voltage is directly proportional to the output resistance R, but since the shunt capacitance always is a minimum limit, the resistance has an upper bound determined by the RC time constant. An example may easily show this effect.

A phototube generally has a gain and time spread of

$$\begin{aligned} G &= 5 \times 10^5 \text{ electrons/photoelectron pulse} \\ \tau &= 15 \times 10^{-9} \text{ seconds} \end{aligned} \quad (7)$$

If we assume the pulse is rectangular we obtain a peak current pulse of

$$i = \frac{Ge}{\tau} = 5.3 \times 10^{-6} \text{ amps-peak} \quad (8)$$

A typical minimum capacitance is $20 \mu\mu\text{f}$, and the cutoff resistance is given by

$$R = \frac{1}{2\pi C B} = \frac{7960}{B_{\text{Mc}}} \quad (9)$$

Also the rms resistor noise voltage is

$$N_{\text{rms}} = \sqrt{4kTBR} \quad (10)$$

But since the signal pulses are always negative and we wish them to exceed the peak noise pulses, we can say that the three sigma level of the noise peak is

$$N = 3N_{\text{rms}} \quad (11)$$

Thus the signal to noise ratio is

$$S/N = \frac{iR}{3N_{\text{rms}}} \quad (12)$$

Now substituting equation (9) and (10) into (12) produces

$$S/N = \frac{i}{6B_{\text{Mc}}} \sqrt{\frac{7.96 \times 10^{-3}}{kT}} \quad (13)$$

Knowing that

$$k = 1.38 \times 10^{-23} \text{ joules/}^{\circ}\text{K}$$

$$K = 300 \text{ }^{\circ}\text{Kelvin}$$

and with the current peak from equation (7) we have

$$S/N = \frac{1230}{B_{\text{Mc}}} \quad (14)$$

and the complete results are tabulated in Table 2.

Bandwidth Mc	$S/N = \frac{1230}{B_{\text{Mc}}}$	$R = \frac{7960}{B_{\text{Mc}}}$ Ohms	Signal = iR mv
100	12	80	.4
50	24	160	.8
20	61	400	2.1
10	123	800	4.2
1	1230	8000	42

Table 2. Limits on a pulse-counting system. The counting rate in pulses per second should be at least 100 times less than the cycles of bandwidth if pulse-height is to be retained. The shunt load capacitance is 20 μ mf.

The pulses at the anode have a wide distribution in amplitude; measured values sometime show ranges of greater than 100 to 1. Since the pulses are distributed randomly with these height variations the first dc amplifier must have a time constant of at least 100 times the expected pulse rate, and to be capable of accepting a wide range of pulse amplitudes without

blocking. Since the minimum time spread of a given pulse is probably 10×10^{-9} seconds, the largest counting rate that could be expected if one pulse followed another would be 10^8 pulses/second or roughly 100 Mcps. Actually the practical counting rate is below 10 Mcps. The conventional amplifier may have one or more preamplifier stages possibly in the form of cascaded pairs followed by a linear amplifier that does not block under load, nor change gain with pulse rate. Designing the pulse amplifier can be difficult, especially if pulse height is important since the dc zero reference must be retained until the height discriminator has clipped the signal. Otherwise the clipping level will vary with pulse rate.

B. Information Rates

(a) Uncertainty in the pulse count

When a very faint object is observed photoelectrically many of the counts are not caused by the desired image, but are also due to the addition of background noise and dark-current. If we use a photomultiplier and pulse counting system in observing a faint star, a pulse count of

$$C_{(S + N)} = (S_1 + N_1) t \quad (15)$$

will exist when the faint star image is centered in the focal-plane diaphragm, where

C = the total pulse count in time t

t = the time of measurement

S = the pulse count due to the star

N = the pulse count due to noise, where the noise is from the sky background and photomultiplier dark emission

When the focal-plane diaphragm is offset from the star to a vacant section of the neighboring sky a pulse count of

$$C_N = N_2 t \quad (16)$$

will be measured, and the mean difference between the two measurements will give an indication of the star intensity as

$$C_{(S + N)} - C_N = (S_1 + N_1) t - (N_2) t \approx ST \quad (17)$$

with a statistical variance in the difference of

$$\begin{aligned}\sigma^2 [ST] &= \sigma^2 \left[(S_1 + N_1) t - (N_2) t \right] \\ &= t \left[\sigma^2 (S_1) + \sigma^2 (N_1) + \sigma^2 (N_2) \right]\end{aligned}\quad (18)$$

Let us further assume that the count due to the star is small with respect to the noise, so that

$$\sigma^2 (S) \ll \sigma^2 (N) \quad (19)$$

and

$$\sigma [ST] = \sqrt{2} \sigma (N) (t)^{\frac{1}{2}} \quad (20)$$

For a large number of pulses the standard deviation is approximately the square root of the number so that

$$\sigma [ST] = (2Nt)^{\frac{1}{2}} \quad (21)$$

Therefore the probable error in the difference, or uncertainty is

$$0.67 ST \sigma = 0.95 (Nt)^{\frac{1}{2}} \quad (22)$$

(b) Information Rate

Some authors define a quantity called the "information rate" which is defined as

$$R_C = \frac{S^{*2}}{S^* + D^*} \quad (23)$$

where

S^* - is the component of the noise count

D^* - is the component of the noise count from photomultiplier dark-current

If equation (22) is manipulated the relationship of

$$\frac{2}{\sigma^2} = \left(\frac{I^*}{S^*} \right)^2 \left(\frac{S^{*2}}{S^* + D^*} \right) t = \left(\frac{I^*}{S^*} \right)^2 R_C t \quad (24)$$

may be found where

I^* - is the signal component from the star

Notice that for a given value of (I^*/S^*) - a given star and diaphragm - the value of $2/\sigma^2$ depends on the information rate and total time t . The value of information rate is that it indicates how well the equipment is performing with respect to external noise. A photomultiplier that is basically dynode thermionic limited can have a large range of information rate with discriminator voltage - Figure 18.

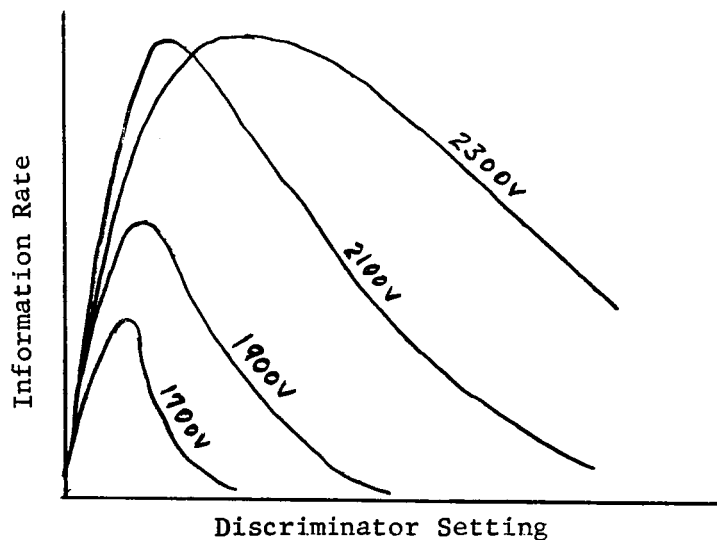


Figure 18. Information rates of a function of photomultiplier potential in a dynode thermal limited tube.

(c) Counting Information Rate Advantage

As a comparison of pulse-counting to current-measuring we will derive the rms noise produced in a continuous probability system. The variance from the average is given as

$$\sigma^2 = \int_{-\infty}^{\infty} h^2 d(S^*t) + \int_{-\infty}^{\infty} h^2 d(D^*t) \quad (25)$$

which reduces to

$$\sigma^2 = t \int_0^{\infty} h^2 dS^* + t \int_0^{\infty} h^2 dD^* \quad (26)$$

since the pulse height h is greater than zero. By analogy to equation (21) we may write that

$$\sigma \left(\int_0^{t_0} h \, di \right) t = 2^{\frac{1}{2}} (S^* + D^*)^{\frac{1}{2}} \quad (27)$$

from which we obtain an equation similar to equation (24).

$$2/\sigma^2 = \left(\frac{1}{S^*} \right)^2 \frac{\left[\int_0^{\infty} h \, dS^* \right]^2}{\int_0^{\infty} h^2 \, dS^* + \int_0^{\infty} h^2 \, dD^*} t \quad (28)$$

and may say that the information rate is given as

$$R_i = \frac{\left[\int_0^{\infty} h \, dS^* \right]^2}{\int_0^{\infty} h^2 \, dS^* + \int_0^{\infty} h^2 \, dD^*} \quad (29)$$

$$= S_0^2 \left(\int_0^{S_0} h^2 \, dS^* + \int_0^{\infty} h^2 \, dD^* \right)^{-1} \quad (29)$$

The advantage of pulse-counting over current-measuring is then

$$R_c/R_i = (S_c/S_0^*)^2 \frac{\int_0^{S_0} h^2 \, dS_c^* + \int_0^{\infty} h^2 \, dD_c^*}{(S_c^* + D_c^*)} \quad (30)$$

and is graphically illustrated in Figure 19.

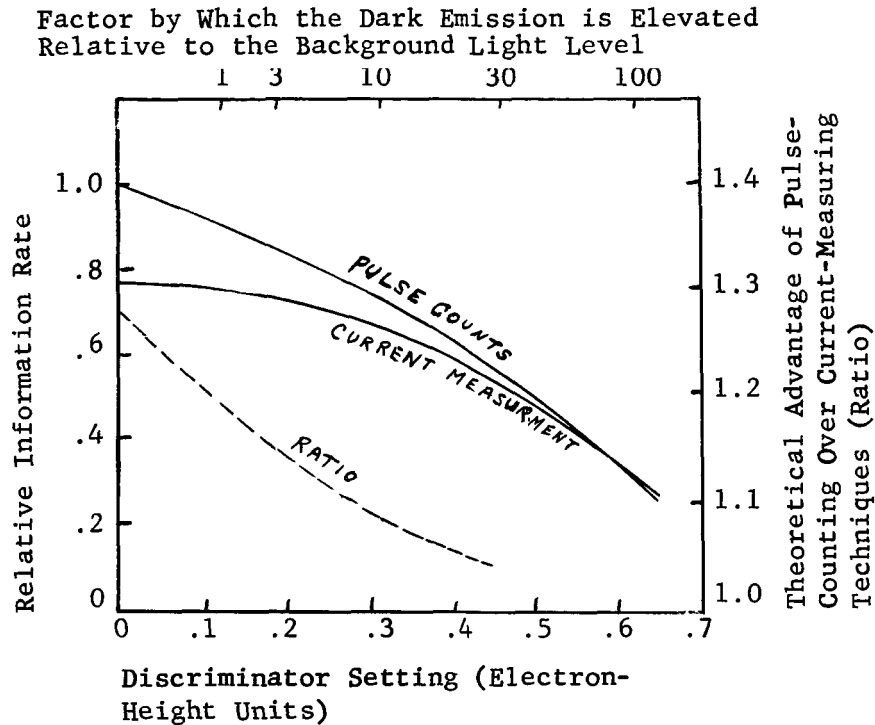


Figure 19. Typical theoretical advantage of pulse-counting over current-measuring for faint objects. An actual curve depends very critically on the relative importance of dark emission to background noise.

C. Advantages of Pulse-Counting

1. Exact integration of a fluctuating light source
2. Observations are directly available in digital form
3. The theoretical limits on information rate is approached
4. Drift problems are small
5. Dark-current pulses may be discriminated
6. High speed and better time resolution

D. Limitations

1. Affected by extraneous pulses - relays, slow-motion motors, etc.
2. Expensive recording equipment - counter, print-out, etc.
3. Very non-linear at high counting rates since pulses may overlap so that the maximum count rate practical is about 10 Mcps - finite resolution

VI. Current Measuring

Current measuring techniques are the most commonly used because of the simplicity in the signal processing equipment. Included under this category is the monitoring of the DC output voltage level, or resulting changes, and also any AC signal measurements caused by a pulsating or chopped light source. In a sense only gross effects are usually measured, such as a large signal to noise due to a chopped light source, or a long time average due to a current integration of a dim star under a poor signal to noise ratio.

A. Circuit Characteristics

The circuitry surrounding the photomultiplier is identical to that in pulse-counting in terms of dynode networks, etc. Basically the difference is in the analog technique of analyzing the output voltage. This signal processing is so varied that a general description is useless unless some desired output besides voltage signal is to be discussed. In any case a few comments may be made as to the output signal.

Usually a longer RC time constant (even up to minutes) is used with current techniques than with pulse-counting. The bandwidth needed is usually less than 1000 cps, so a large signal level is produced because of a larger load resistor. That is, if a long time constant is allowed, and the fixed stray capacitance is approximately $20\mu\text{pf}$, a load resistor in the megohm range may be used as compared to a load resistor below 1000 ohms in pulse-counting. The higher impedance circuits are more subject to electrical pick-up, and the noise spectrum becomes more important. Pulse-counting just requires a low dark count whose distribution made little effect. However, the noise frequency spectrum is much more important in measuring an analog current or voltage signal buried in noise.

B. Noise Analysis

Any detection system contains noise in its output which basically sets the lower limit on the energy that can be detected. If the noise has non-fundamental components, such as 60 cycle pickup, etc. rejection techniques may be capable of choosing the information signal from the noise. In the broadest sense, "noise" means that fluctuation which interferes with the transmission

of a message, or that disturbance which limits the precision of a measurement.

A message, on the other hand is best thought of as a surprise, i.e., an event that can not be predicted in advance. If any interference to the signal can be predicted, it is non-fundamental and may be rejected. Noise that is basic to a system, but not the theoretical limit is best to be thought of as non-fundamental. For instance, an amplifier in a system may be resistor noise limited, but this does not mean that a different amplifier could not have a lower noise figure.

A great deal of confusion also exists in the way noise varies with frequency or bandwidth. Authors tend to state noise in both power and voltage units so that at times noise is proportional to bandwidth and at other times noise is proportional to the square root of bandwidth. Generally, noise power is directly proportional to bandwidth but to be strictly correct the limiting noise producer must be determined because the various type of noise vary as $1/f^n$, $1/f$, f , f^2 and f^n . If a photomultiplier is limited by flicker noise ($1/f$), we can expect poor operation at very low frequencies, but at a higher frequency range the phototube may operate extremely satisfactory.

For an accurate prediction at the noise response of a particular system the relative magnitudes of the various noise sources must be known. In any case, photomultiplier tubes are able to give a gain high enough to make shot noise the limiting factor in wide bandwidth measurements.

The importance of the dark current is also dependent on the method by which the signal is recorded. That is, if an integration-current method is used in determining the signal, we would be interested in the uncertainty between the difference between the integrated signal and noise, and the integrated noise. On the other hand if an AC current is being measured, we would be interested in how different one value of rms change would be to another. That is, if we consider the anode voltage to be a cause of a large number of independent random events following a Gaussian probability density function the analytic expression for a particular current is given as

$$P(I) = \frac{1}{\sqrt{2\pi}\sigma} \exp \left[-\frac{(I-I_0)^2}{2\sigma^2} \right] \quad (31)$$

where

I - is the instantaneous signal and noise current

I_0 - is the true average value of the signal and noise current

σ - is the true rms value of the observed signal and noise

In an integration device we are interested in how the measured averages of two I_0 's are different, and with an instantaneous current or AC method, the difference of σ_1 and σ_2 are of interest.

Current integration techniques actually approach those of pulse-counting if the noise in a long time integrated interval is low and the pulse rate is so rapid that pulse techniques cannot be used. This indicates that most of the integrated output is the signal because a practical photomultiplier circuit should show a relatively low dark-current. Generally this is the case, thus most noise analysis is done for large bandwidth instantaneous current measuring techniques where the fluctuation in the output current due to noise is important.

It is necessary to mathematically describe the randomness, degree-of-independence, and mean-value characteristics of the amplitudes of the fluctuations and relate them to a cause. If a quantity varies sinusoidally in time, there is no difficulty in assigning a suitable measure to its amplitude. If the amplitude and frequency are randomly fluctuating the method of auto correlation is resorted to in defining the noise spectrum of any fluctuation when one has defined a model of its origin. The concept of mean value as an average over a long period of time is the most generally used method of defining a mean noise, mean square noise, and finally the noise frequency power spectrum. Three simple interrelations relating the mean noise (q), the mean square noise (q^2), and the noise frequency power spectrum $w_q(f)$ are defined as

$$\frac{\overline{q^2}}{2} = \int_0^{\infty} w_q(f) df \quad (32a)$$

$$\frac{\partial}{\partial \tau} (\tau^2 q^2) = \int_0^{\infty} w_q(f) \frac{\sin 2\pi f \tau}{\pi f} df \quad (32b)$$

$$w_q(f) = 4\pi f \int_0^{\infty} \frac{\partial}{\partial \tau} (\tau^2 q^2) \sin 2\pi f \tau d\tau \quad (32c)$$

C. Types of Noise

The noise in the output of a photomultiplier is generated by the anode load, internal noise in the tube, and random photon noise caused by the energy-rate distribution of the incoming photon quanta. We shall talk about noise current for definitiveness, although voltage might equally well have been chosen. The random current will be described by a one-dimensional continuous random-variable stockastic model with time as the continuous parameter. Spectrum equations are given for the various types.

(a) Johnson Noise

Johnson noise, or Nyquist noise is the voltage fluctuation that occurs across the terminals of any resistor. The magnitude of the fluctuations is independent of the structure of the resistor and is due to the fact that each electrical mode of vibration has a mean energy kT , thus Johnson noise may be considered a manifestation of black body radiation. The spectrum of the noise in the current I that flows in the circuit is given by a one-dimensional mode of

$$w_j(f) = 4kT/R(f) \quad (33)$$

where

k = Boltzmanns constant

T = the temperature of the resistor

R = the resistance of the anode load

(b) Shot Noise

Shot noise, or Schottky noise is produced by the mean square fluctuation of the thermal electrons emitted randomly from the cathode and dynodes. The noise spectrum of the shot noise is given by

$$w_s(f) = 2 e \bar{I} \quad (34)$$

where

e - is the electron charge

\bar{I} - is the average thermal anode current

The finite transit time of the electron from cathode to dynode, and dynode to dynode, causes the shot noise spectrum to decrease at high frequencies.

(c) Flicker Noise

The spectrum of shot noise tends to rise at very low frequencies. The extra noise at low frequencies is usually attributed to a fluctuation of the cathode surface or ionization, and will be called flicker noise. The noise is usually burst like and nonstatistical in character with possibilities of even disappearing for long periods in a particular tube. This behavior indicates that these noise pulses are not fully independent, but rather are triggered by random events. Investigators have found that flicker effect seems to obey the current spectrum of

$$w_f(f) = 2e\bar{I} \frac{F\bar{I}}{fA} \quad (35)$$

where

$2e\bar{I}$ - is the shot noise spectrum

F - is a constant characterizing the emission surfaces

f - is the frequency

A - is the surface areas of the emission surfaces

This equation is quite empirical and perhaps a more general formula would be

$$w_f(f) = \frac{K \bar{I}^\beta}{f^\alpha A} \quad (36)$$

where β , and α are constants for a particular material. This noise is not fundamental, but varies greatly from tube to tube and seems to be due to structural defects which may be practically unavoidable.

(d) Current Noise

Current noise again is non-fundamental, and is also known as contact noise. Current noise is the additional current fluctuation that exists in a resistor in addition to shot noise when a steady current I passes through the resistor. Similar to flicker noise, the current spectrum obeys

$$w_i(f) = C I^\beta / f^\alpha \quad (37)$$

where β usually is about 2 and α is about 1.2. The theory of both current and flicker noise has been poorly understood.

(e) Photon Noise

Photon noise is that part of the noise caused by the fluctuation in the rate by which radiation quanta act on the detector. Photon noise, as shot noise, is caused by random radiation so that the current fluctuations are indistinguishable experimentally from shot noise. Photon noise consists of two parts in photomultipliers since the cathode responds to the energy of the photon as well as the number of quanta. The spectrum of the photon noise energy that will cause the temperature fluctuation of the cathode is

$$w_p(f) = 16 A \epsilon_1 k \sigma T^5 \quad (38)$$

where

ϵ_1 - is the effective emissivity of the cathode

A - is the area of the photocathode

σ - is a constant (5.67×10^{-12} watt/cm² - deg⁴)

Additionally the number of photons have a noise spectrum of

$$w_{pn}(f) = 2.74 A \epsilon_2 \sigma T^3 \quad (39a)$$

where ϵ_2 is defined by

$$\epsilon_2 = \frac{3}{\pi^2} \int \frac{\epsilon(\zeta) e^{\zeta} \zeta^2}{(e^{\zeta} - 1)^2} d\zeta \quad (39b)$$

and

$$\frac{1}{\sigma} = 1.521 \times 10^{11} / \text{cm}^2 - \text{deg}^3 - \text{sec} \quad (39c)$$

and zeta is

$$\zeta = \frac{h\nu}{kT} \quad (39d)$$

(f) Secondary Emission (Photomultiplier)

The process of multiplication by secondary dynode emission contributes somewhat to the noise of the photomultiplier. Because the process of secondary emission is statistical in nature each photocathode electron does not exactly receive a gain G by the time it reaches the anode. If the distribution of secondary electrons may be approximated by Poisson's law, that is that the probability of Z electrons leaving the surface from a primary electron is given by

$$p(z) = \frac{e^{-\delta} \delta^z}{z!} \quad (40)$$

where δ is the average secondary emission ratio, then the noise spectrum of the anode current is

$$w_a(f) = 2eI_a \cdot \frac{G\delta - 1}{\delta - 1} \quad (41)$$

where G is the total average gain of the multiplier chain and I_a is the average anode current.

(g) Pattern Noise

For convenience we will consider secondary emission noise to include photocathode pattern noise. Irregularities in the sensitivity of the photocathode structure, in other words quantum non-uniformity across the photocathode releases a number of photoelectrons per light photon dependent on photocathode image position. Little analysis or measurement of this noise has been done, even with scanned detectors such as the TV image orthicon. Generally this retinal variation in image tubes gives rise to a graininess which is a form of noise in the picture they produce. This noise is analogous to the effect of grain on photographic film. In a photomultiplier the effect is an output signal that is dependent on image size and image position on the photocathode.

(h) Breakdown Noise

When large potential differences are developed across electrical elements, sharp spikes of noise may be generated. This may occur from a dynode to some part of the photomultiplier structure, but more often the cause will be capacitor breakdown on the potential divider feeding the dynodes.

(i) Microphonics

Mechanical vibrations often produce small motions of conductors or other parts so that changes in capacitance, inductance, or electric fields induce an output noise. The trend to small, rigid, potted electronic assemblies has reduced the importance of this effect. Primarily connecting cables are the source of microphonic noise today. Shielded, insulated cables such as the coaxial type may easily illustrate the noise. Flexing the cable changes the capacitance between the inner conductor and outer shield, and may also induce frictional electrostatic charge on the dielectric insulation. This fluctuation noise becomes progressively worse as the cable becomes longer and the cable terminations become of higher impedance. Special "noise-free" coaxial cables

have been developed which will remain electrically neutral under conditions of shock and vibration. The reduction of inherent noise is achieved on these cables by the application of a high resistance semi-conductive coating on the dielectric surfaces which tends to maintain the capacitance nearly constant and dissipates any electrostatic charge with cable movement.

A unique noise source which may be included under the microphonic title is the cooling noise often found in photomultipliers due to the boiling of the coolant liquid. Many times a different mounting of the detector in the dewar, or small pieces of blotting paper inserted at strategic points have been found to reduce this cooling noise.

D. Frequency Characteristics

Each photoelectron leaving the photocathodes produces a pulse of charge at the anode of average amplitude Ge , where G is the tube gain and e is the electron charge of 1.6×10^{-19} coulombs per electron. For a gain of 10^6 , the pulse is 1.6×10^{-13} coulombs, or sufficient to charge a capacitance of 20pf to a voltage of 8 millivolts. The electrons forming this pulse will not all arrive at the anode simultaneously, but owing to the time dispersion of electrons in their transit through the tube the current will tend to have a normal distribution. The pulse has a positively skewed distribution since the current rises more rapidly and falls more slowly than a Gaussian curve, nevertheless it often is convenient for the purposes of calculation to assign a standard time deviation

$$\sigma_2 = \frac{\tau_2}{2.36} \quad (42)$$

where τ_2 is the pulse width at half amplitude. On this basis the peak current is

$$I_P = \frac{2.36}{\sqrt{2\pi}} \frac{Ge}{\tau_2} \quad (43)$$

For the example already quoted this becomes

$$I_P = \frac{150}{\tau_2} \text{ microamps} \quad (44)$$

when τ_2 is measured in nanoseconds.

If in place of a single electron, the input consists of N photoelectrons produced simultaneously over the whole cathode, the time spread τ_2 will be increased by the transit time difference due to the electrical distance difference between points on the photocathode to those on the first dynode. This resultant time spread sets an upper limit to the frequency response. If the skewness of the pulse is neglected (skewness tends to increase the frequency response since it narrows the pulse) we may give the time response as

$$f(t) = \frac{1}{\sqrt{2\pi}\sigma_2} e^{-\frac{(t - \tau_0)^2}{2\sigma_2^2}} \quad (45)$$

where

$f(t)$ - relative pulse height at a given time t

τ_0 - time delay from photoelectron release to peak of pulse

σ_2 - standard time deviation of the pulse

If we take the Fourier transform of Equation 45 to change into the frequency domain we obtain

$$F(\omega) = e^{-\frac{1}{2}\omega^2 \sigma_2^2} e^{j\omega\tau_0} \quad (46)$$

which consists of a phase function

$$\phi(\omega) = e^{j\omega\tau_0} \quad (47)$$

that states that angular phase is directly proportional to frequency and transit time delay. And an amplitude function

$$A(\omega) = e^{-\frac{1}{2}\omega^2 \sigma_2^2} \quad (48)$$

If we substitute relationship 42 and $\omega = 2\pi f$ into Equation 48 we have a frequency amplitude of

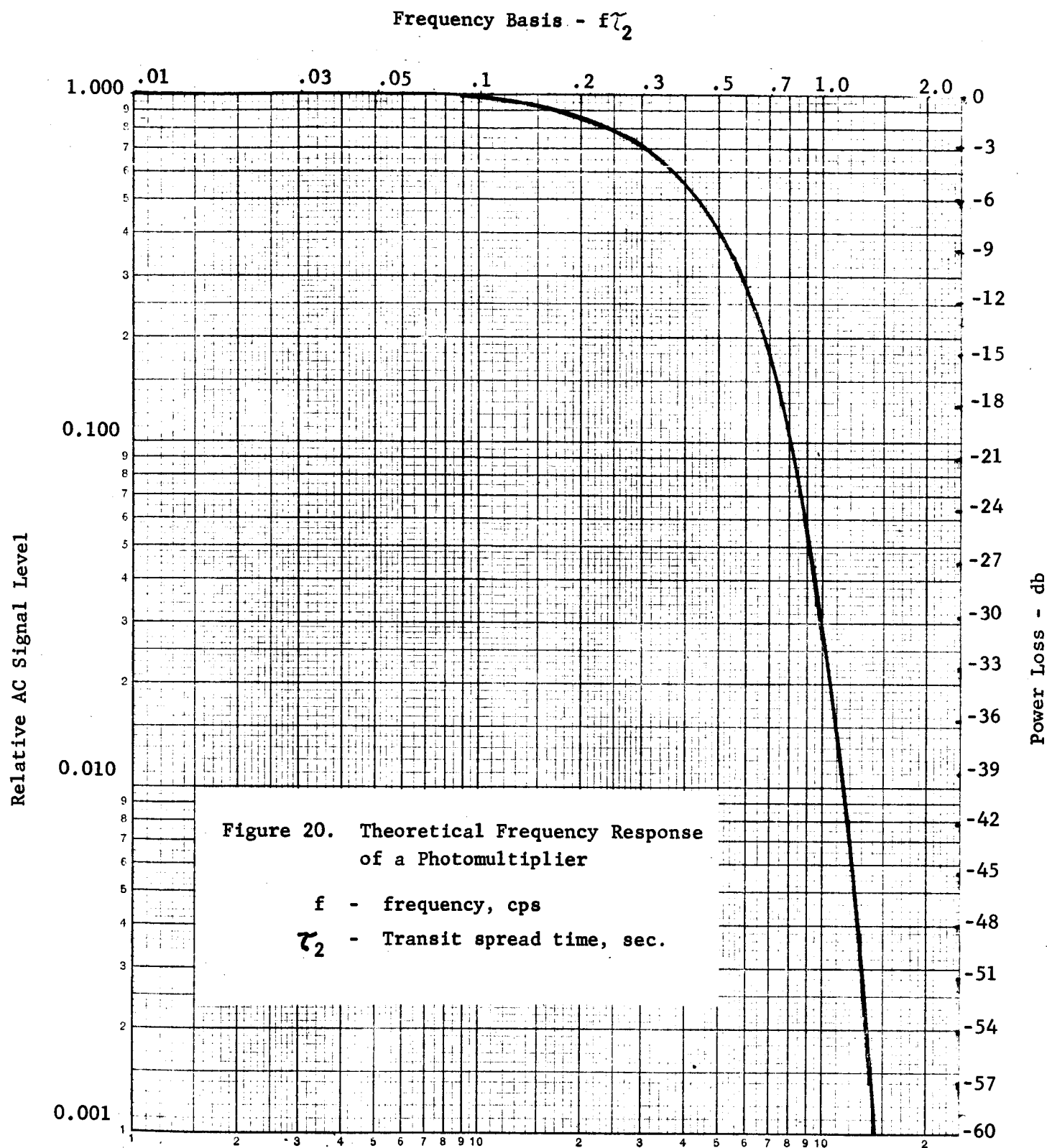
$$A(\omega) = e^{-3.55 (f \tau_2)^2} \quad (49)$$

where

f - frequency in cps

τ_2 - half amplitude pulse time spread in seconds

Figure 20 plots this function to illustrate the frequency response curve of a photomultiplier limited by pulse time spread. Notice that the slope of the curve becomes steeper with frequency and does not approach a fixed slope such as 20, 40, 60, etc. db/decade as in a normal frequency Bode curve.



This is particularly significant for if the value of $f\tau_2$ is reduced from 1.2 to 0.6 the improvement in signal is about 34 db. This merely comes about by halving the signal frequency or the spread time of the tube. The skewness of the actual pulse may also raise the response curve slightly. Manufactured values on time spread must also be taken with "a grain of salt". Some even omit giving a value, but only specify rise time which may be measured from 10% to 90%, or from a noticeable signal to peak amplitude. Needless to say the time spread can also vary with dynode voltage so that if the nominal time spread value, or equivalently twice the rise time is taken as τ_2 a response can be determined. After the tube is in operation the spread time can be indirectly determined from the actual response by checking at least one frequency above and below cutoff.

a. Photocathode with Decay Emission

Additionally, if the N photoelectrons are produced by an exponentially decaying time constant τ_1 , the photocathode current is:

$$I_{pc} = \frac{Ne}{\tau_1} \exp(-t/\tau_1) \quad (50)$$

as a function of time, and a peak anode current of

$$I_p = \frac{K N G e}{\tau_1} \quad (51)$$

where K is a function of the ratio τ_1/τ_2 and is shown by Figure 21.

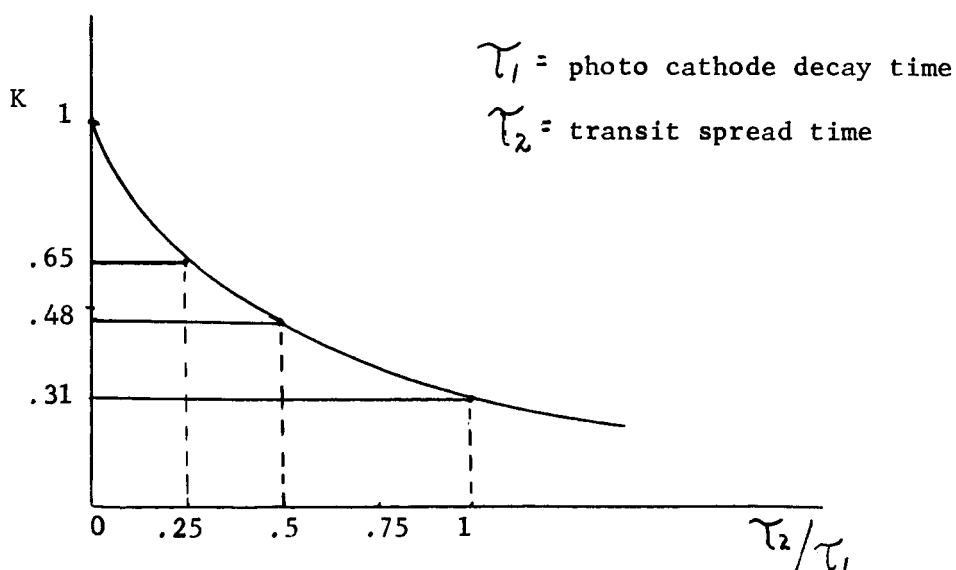


Figure 21. Correction Curve for Peak Anode Current

(b) Light Mixing

Two simultaneous modes from a gas laser operating at 6300 Å were heterodyned in an EMI 9558-B (S-20) photomultiplier to give a 126 Mc output frequency. The RF signal to the DC level of the photomultiplier is shown in Figure 22. The output load which shunted the anode capacitance was

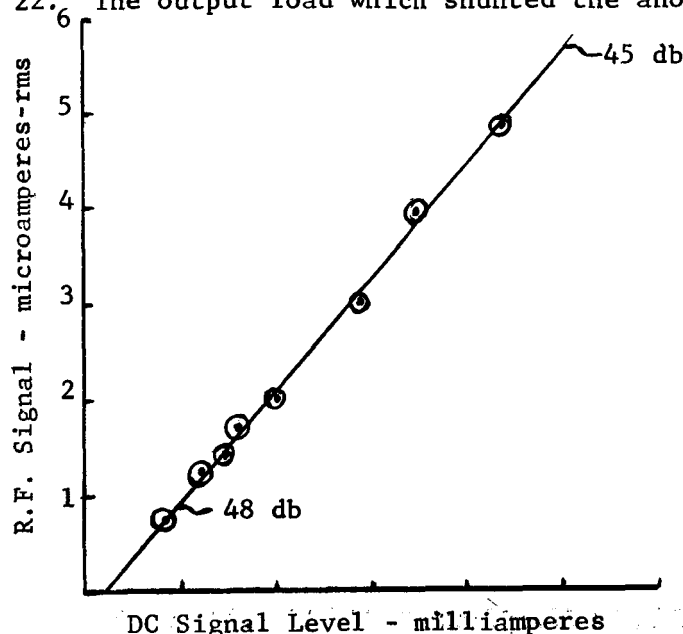


Figure 22. 126 Mc Heterodyned Signal

50 ohms so that the RC time constant was well above 126 Mc. Thus the pulse time spread should have been the determining factor of the frequency response.

If the light beam was assumed to be 100% modulated, zero time spread would produce a relative AC to DC signal ratio of one. The received signal was 45 to 48 db below this value so from Figure 20 we would expect a $f\tau_2$ value of 1.2 or

$$\begin{aligned}\tau_2 &= 1.2/126 \text{ Mc} \\ &= 9.5 \text{ nanoseconds}\end{aligned}\tag{52}$$

The tube manufacturer gives a value of 16 nanoseconds. More work needs to be done in the area of photomultiplier frequency response. Perhaps modulated light beams in the 100 Mc region may be possible by laser light diodes so that response curves may easily be obtained. We are planning a future experiment using a RCA 7265 (S-20) photomultiplier that is stated to have a 7 nanosecond spread time. Other photomultipliers with good high frequency characteristics are the 1P21 - 931-A (S-4) and the 5819 (S-11) which do not have as good a red response as the S-20 photocathode.

When the light was focused on a spot instead of over the entire photocathode a 6 db increase in signal was observed. This was the effect of the photocathode - first dynode transit difference.

E. Advantages

1. Simple circuitry as opposed pulse amplifiers, especially if AC signals are desired.
2. Good signal-to-noise signals are possible if the light is modulated since narrow bandwidths are possible.
3. Repetitive noise such as 60 cycle pick-up may be easily rejected.
4. Usually higher signal levels and the amplifier is used as an impedance transformer.
5. A large dynamic range in signal level.
6. The linear response allows differential photometry where direct subtraction of two quantities of light from two photomultipliers is possible, such as the difference between sky and sky plus star.

F. Disadvantages

1. Lower speed than pulse counting.
2. Resolution limited by bandwidth.
3. Drift problems when monitoring the DC level.
4. A modulated light source or chopped photomultiplier supply rejects half of the received quanta if an AC signal is needed.

VII. Optimization of a Photomultiplier's Physical Parameters

A. Internal

Improvements can be made internal to a photomultiplier to increase its sensitivity. Some ways are by

(a) noise discrimination. As discussed in Section IV-D, the thermal photoelectrons have much less energy than those emitted by photon excitation. If a field mesh could be installed directly behind the photocathode at a potential slightly negative to the photocathode, only those electrons - photon emitted - could climb the potential barrier to be multiplied in the dynode chain. Thus the dark current would be lowered and the signal to noise ratio is increased.

(b) an integrating sphere effect. Roughly only 40% of the light photons reach the photocathode surface, 30% are reflected and 30% are absorbed in the glass and optics. If a reflecting surface could be designed internally and externally to the tube so that all photons reflected or passing through the photocathode could be returned for another chance at photo-electron conversion, the signal may even be increased up to 20% which could drastically affect the signal-to-noise at low signal levels.

B. External

The photomultiplier is a very simple, reliable and efficient device that many times is limited in practice by supporting parameters such as inadequate shielding, excessive ripple on the dynode supply, etc. Additionally a different type of tube may have produced better results because the photocathode area had been many times the image area so that more photocathode dark current existed. At very low signal-to-noise ratios noise pickup suppression becomes an art and principles such as one point grounds must be used, especially if high impedance levels are used with proximity effects such as 60 cycle, power surges, and r.f. noise which can destroy the desired signal. One cannot give a general solution to the pick-up problem until the chief noise offender is known. It may be a simple case of requiring a magnetic shield when the photomultiplier changes orientation to the earth's magnetic field because of mounting on an astronomical telescope to a more complex electric magnetic field problem that may be set up when the

photomultiplier is used in close conjunction with a pulsed ruby laser. Therefore only a few of the common trouble spots will be discussed.

(a) Shielding

Recently a magnetic pair, known as -netic and co-netic shield, has become available which can be machined, cut or bent without requiring any annealing. This material is particularly good for experimental or temporary set-ups. Mu-metal shields are superior in insuring adequate shielding but must always be annealed after stressing. If the metal shield, or any part of the mounting contact the glass envelope of the photomultiplier tube, the potential distribution on the inner surfaces may be disturbed, and give rise to electron bombardment of the glass, causing fluorescence which, "seen" by the photocathode, increases the dark current. Tube manufacturers usually recommend that the phototube to be operated with the cathode at earth potential, or have the conducting shield at cathode potential. A small metal shield near the cathode that is at a slightly different potential also seems to reduce the dark count.

(b) The Dynode Chain

For maximum stability of gain under DC conditions the anode current should be limited to approximately $10\mu\text{a}$. Very often, however, high values of anode current (up to 200 ma) may be drawn under pulsed conditions and still keep a linear relationship. In all cases the dynode chain current should be at least 5 times the mean anode current. To improve the performance, suitable decoupling capacitors should be used on the last stages when high peak currents are drawn. Electrolytic capacitors must definitely be avoided because of the random breakdown and healing of the thin dielectric insulation which causes pulses of noise. For general operation disc ceramic capacitors are satisfactory and may be desired because of their small size. However, discs do produce some spikes and for real low noise operation, plastic film glass encased capacitors seem superior. Breakdown noise can usually be attributed to the capacitors of the bias network feeding the dynodes or any anode coupling capacitors. The gain of the electron multiplier section may be made independent of the over-all voltage, covering a wide range of voltage change. Figure 23 shows a circuit arrangement for accomplishing this. The fixed voltage may be obtained from a battery, zener, or gas discharge regulator tube. When the photomultiplier has a large number of stages, it may be necessary to apply

compensation to two or three sets of dynodes instead of one in order to obtain sufficient regulation.

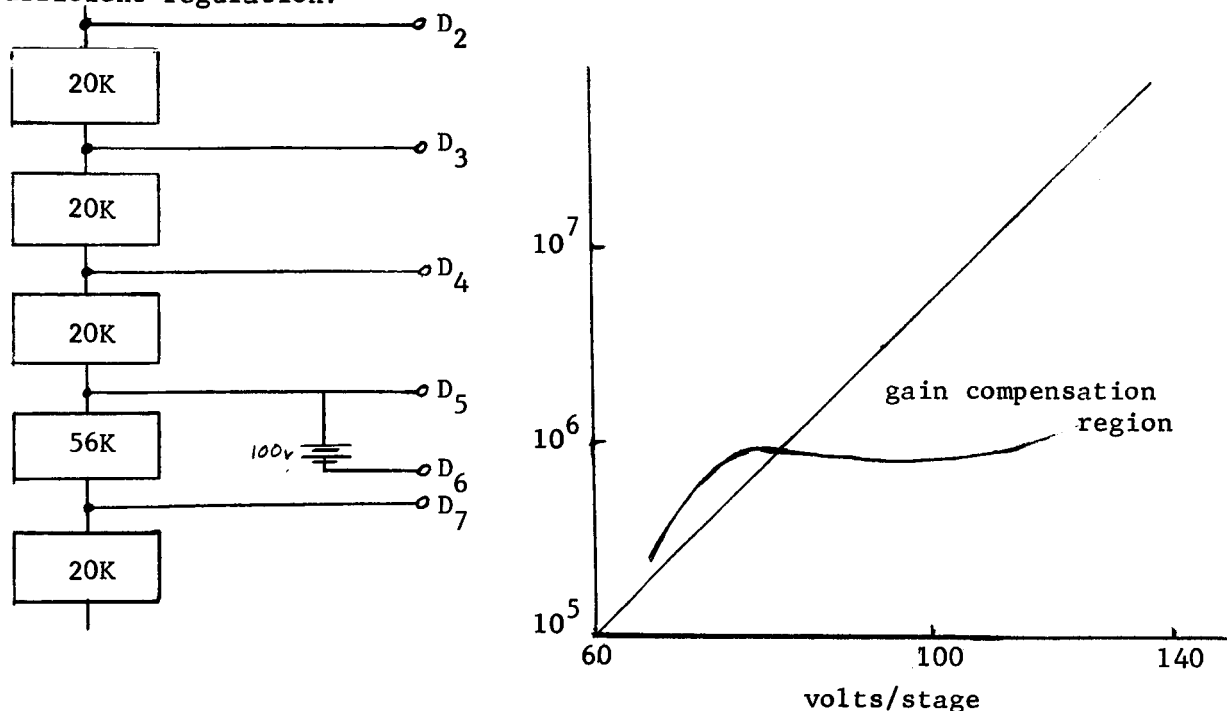


Figure 23. Gain Compensation

(c) The Power Supply

Very light weight power supplies can presently be purchased such as a 5 ounce unit that operates on -20 ma @ 28 v from Pulse Engineering Inc. that is built into a socket to attach directly to the phototube. Either a 2 kv or 4 kv unit power supply is available, and a companion two-stage pre-amplifier with a 50 ohm output is also offered. The only requirement on a power supply are stability, low ripple, and the capability of providing at least 5 times the peak anode current.

(d) Signal Cables

"Noise-free" coaxial cables such as those shown in Table 3 should be used in transmitting the photomultiplier signals to reduce microphonic noise pickup.

<u>Type</u>	<u>RG No.</u>	<u>Imp. Ohms</u>	<u>Overall Diameter</u>
21-467	149/U	75	.405
21-537	58A/U	50	.195
21-539	8/U	52	.405
21-541	59/U	73	.242
21-553	54A/U	58	.250

Table 3. Noise-Free Amphenol Coaxial Cable

REFERENCES

1. Andrew T. Young, "Temperature Effects in Photomultipliers and Astronomical Photometry", *Applied Optics*, Vol. 2, No. 1, pp. 51-60; January 1963.
2. James P. Rodman and Harlan J. Smith, "Tests of Photomultipliers for Astronomical Pulse-Counting Applications", *Applied Optics*, Vol. 2, No. 1, pp. 181-186; February 1963.
3. W. E. Spicer, "Photoemissive, Photoconductive, and Optical Absorption Studies of Alkali-Antimony Compounds", *Physical Review* 112, p. 114; 1958
4. Albert van der Ziel, Noise, Prentice-Hall Inc., 1954.
5. R. Clark Jones, "Performance of Detectors for Visible and Infrared Radiation", *Electronics and Electron Physics*, Vol. V, p. 196; 1953.
6. G. A. Morton, "The Scintillation Counter", *Electronics and Electron Physics*, Vol. IV, pp. 69-107; 1952
7. Edited by William A. Hiltner, Astronomical Techniques, Vol. II of Stars and Stellar Systems.
8. Frank Bradshaw Wood, Astronomical Photoelectric Photometry, American Association for the Advancement of Science, Washington D.C., 1953
9. J. H. Freeman, Principles of Noise, J. Wiley & Sons, 1958.
10. Lloyd P. Smith, Thermionic Emission, *Handbook of Physics*, pp. 8-74 to 8-83, Condon and Odishaw; 1958.
11. Conyers Herring, "Thermionic Emission", *Reviews of Modern Physics*, Vol. 21, pp. 185-267; 1949.
12. A. L. Hughes and L. A. DuBridge, Photoelectric Phenomena, McGraw-Hill Book Co., New York; 1932.
13. G. A. Morton, *RCA Review*, 10, 525; 1949.
14. Scintillation Counters RB-109, RCA Laboratories, 1957
15. J. Sharpe, "Vacuum and Gas Photocells", *Industrial Electronics*, pp. 70-74, November 1962.
16. Ye. A. Kolenko, Kh. V. Protopopoz, "The Thermoelectric Cooling of Photomultipliers", Aerospace Tech. Information Center, Wright-Patterson AFB, AD-256 611 Div 8; 26 May 1961.
17. Jamieson, McFee, Plass, Gube, Richards, Infrared Physics and Engineering, McGraw Hill Book Company Inc., 1963.
18. A. B. Gillespie, Signal, Noise and Resolution in Nuclear Counter Amplifiers, London Pergamon Press, Ltd., 1953.
19. Athanasios Papoulis, The Fourier Integral and Its Application, McGraw Hill Book Company, Inc.; 1962.

Part 2

EFFECT OF ATMOSPHERIC TURBULENCE
ON LASER PROPAGATION

EFFECT OF ATMOSPHERIC TURBULENCE ON LASER PROPAGATION

In considering the propagation of laser radiation through the atmosphere the problem can be divided up in a number of ways. The basic effects which must be considered are as follows:

1. Absorptive Attenuation
2. Scattering (non-absorptive attenuation)
3. "Seeing" effects, caused by random fluctuation in the index of refraction of the air
4. Potential high energy effects

Absorption and normal scattering are well known effects, and data is available to estimate their magnitude. Although the data is not always consistent, neither is the atmosphere. The most serious of the known effects is that of "seeing" and it must be considered in some detail.

To be able to visualize the phenomenon involved is of some help. Imagine that one is looking through a telescope at a point source of light, such as a star. The first thing that is noticed is that the star twinkles - depending on the zenith distance - in a random fashion. It is soon noted that the amplitude and frequency distribution of this effect is also as function of the telescope aperture - it increases as the aperture decreases, and decreases as the aperture increases. This twinkling is commonly referred to as scintillation, and in this discussion the term will be reserved for this effect. It is sometimes given a wider meaning in the literature.

Now assume that one looks at the star with higher powers. The next thing that is noticed is that the star dances back and forth in a random manner about some mean position with an amplitude of several seconds of arc. Obviously, a time exposure with a photographic plate or other detector will give an averaged position that is fairly good, but the image size will be quite large, while a short exposure will yield a sharp image but indefinite position. Fixing attention again on the star it is found that it is not just a dancing point, but is constantly changing shape like an amoeba under a microscope. One instant it is sharp, the next instant large, and changes shape continuously. Occasionally one can see a perfect diffraction limited image, but more frequently the image is blurred. One of the first impressions that is received about all these phenomena is that it is possible, within fairly bound limits, to trade space and time averages - space averages with the aperture, time averages with the exposure length.

As an extension of this, the effects of refraction must be noted. The DC component and the effects of the scattering of light, both in the instrument and in the atmosphere must be observed. Even with perfect seeing the latter would set a contrast limit.

The simplest model that can be made of seeing phenomenon is a modified form of the original work of Gavioli. He attributed the observed image structure to a wavelike structure in an inversion layer. This last is probably only partially correct, however, his model is still one of the clearest.

Assign a typical turbulent element size L , with a focal length F , moving with a velocity V at a height H , and a telescope aperture D (see Figure 1). Gavioli pointed out the following cases:

1. $D < L/2$
 - a. $H \ll F$ dancing of a fine image, little scintillation
 - b. $H \approx F$ scintillation and pulsation in phase
 - c. $H \gg F$ large, steady images
2. $L > D > L/2$
 - a. $H \ll F$ enlarged image, little dancing
 - b. $H \approx F$ large scintillation, little pulsation and dancing
 - c. $H \gg F$ large steady images
3. $D > L$ inversion layer spectra

These phenomenon are all well known. Case 3. (above) deals with diffraction effects, while the other effects are intuitively apparent.

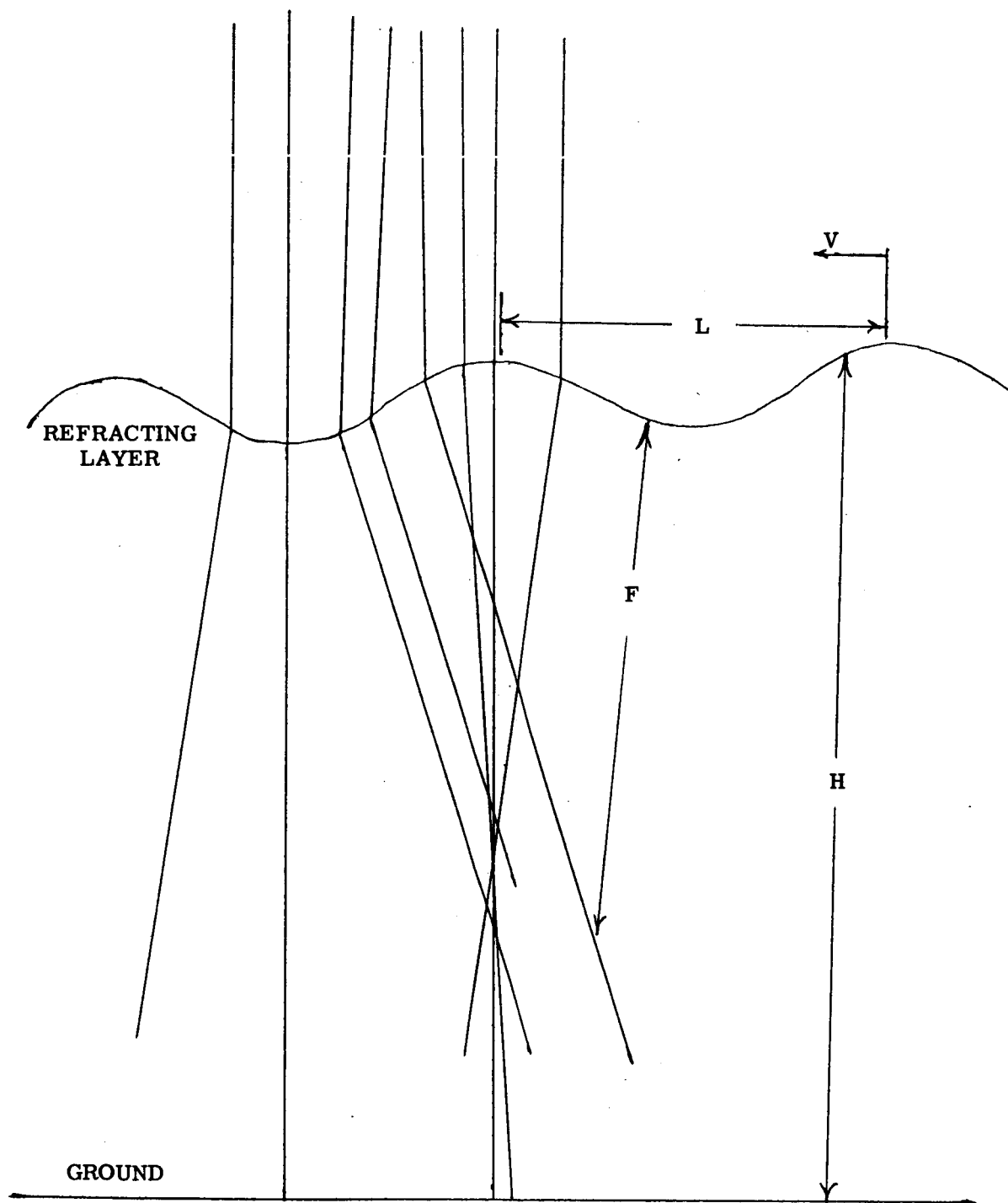


Figure 1

One of the consequences of this is that it is possible to separate some of the effects - most scintillation are due to elements at some distance from the observer, while image dancing and pulsation will be due to elements closer to the observer. The range of effects observed at one time indicates also that we are dealing with a range of sizes of elements.

Scintillation has been the most studied of all these phenomenon, and a series of papers by Keller and others, as noted in the bibliography, have rather thoroughly tied down this aspect of seeing. It has been established that scintillation is highly correlated with winds near the tropopause, diffraction effects dominate, and the elements are roughly from 2 to 20 cm in size. Scintillation frequency is dependent on both wind velocity near the tropopause and element size. However, the important effects of dancing and image pulsation and distortion are independent of scintillation, occurring primarily at lower elevations, so that these effects may be disregarded for the present. This does not mean that scintillation is not important, but rather that at present it does not affect our observations as much as closer effects, so that they are not the limiting factor. If the closer problem was completely solved, then reconsideration would be necessary. One limitation must be made explicit - these statements apply primarily to those elements of scintillation over 100 cps, much of the lower frequency scintillation is also a lower atmosphere phenomenon.

Chandrasekhar has treated the problems of the deviation of a ray of light by a thick turbulent layer, and his arguments were repeated in Photo-electric Observatory Report 3, to which reference is made, rather than repeating the rather lengthy arguments. However, his results may be used as a starting point for further discussion.

Consider a turbulent layer of thickness d , path length of a ray through the medium of $S = d \sec \theta$, and characterized by:

$$\sqrt{\bar{X}^2} = 1.74 \times 10^7 \sqrt{\delta^2 \mu} \left(\frac{d}{r_0}\right)^{1/2} (\sec \theta)^{1/2} \text{ (seconds of arc)}$$

$$\sqrt{\frac{-2}{\rho}} = 4.86 \times 10^5 \sqrt{\delta^2 \mu} \left(\frac{d^3}{r_0}\right)^{1/2} (\sec \theta)^{3/2} \text{ cm}$$

$$\sqrt{L^2} = 4.21 \times 10^2 \sqrt{\delta^2 \mu} \left(\frac{d}{r_0}\right)^{1/2} (\sec \theta)^{1/2} \text{ cm}$$

S in units of $10^4 \text{ cm} = 10^2 \text{ meters}$, r_0 the scale of the structure, in units of 10 cm. X is the angular deviation, ρ the radial displacement, L the change in phase, $\delta\mu$ the change in refractive index. For simplicity, assume that by observing normally through this layer, that it is at a distance h from us, and that a telescope of aperture D is used. See Figure 2.

Chandrasekhar considered 0.75" for $\sqrt{\bar{X}^2}$ as representative, and evaluated

$$\left(\frac{d}{r_0}\right)^{1/2} \sqrt{\delta^2 \mu} = 4.3 \times 10^{-8}$$

Since he assumed $\frac{d}{r_0} = 1$, this yields $\sqrt{\delta^2 \mu} = 4 \times 10^{-8}$. If it is assumed that $d = 10$ instead of 1, we have

$$\sqrt{\delta^2 \mu} = 1.4 \times 10^{-8}$$

For these two cases we have:

$$\sqrt{\frac{-2}{\rho}} = 4.86 \times 10^5 \times 4.3 \times 10^{-8} = 2.1 \times 10^{-2} \text{ cm}$$

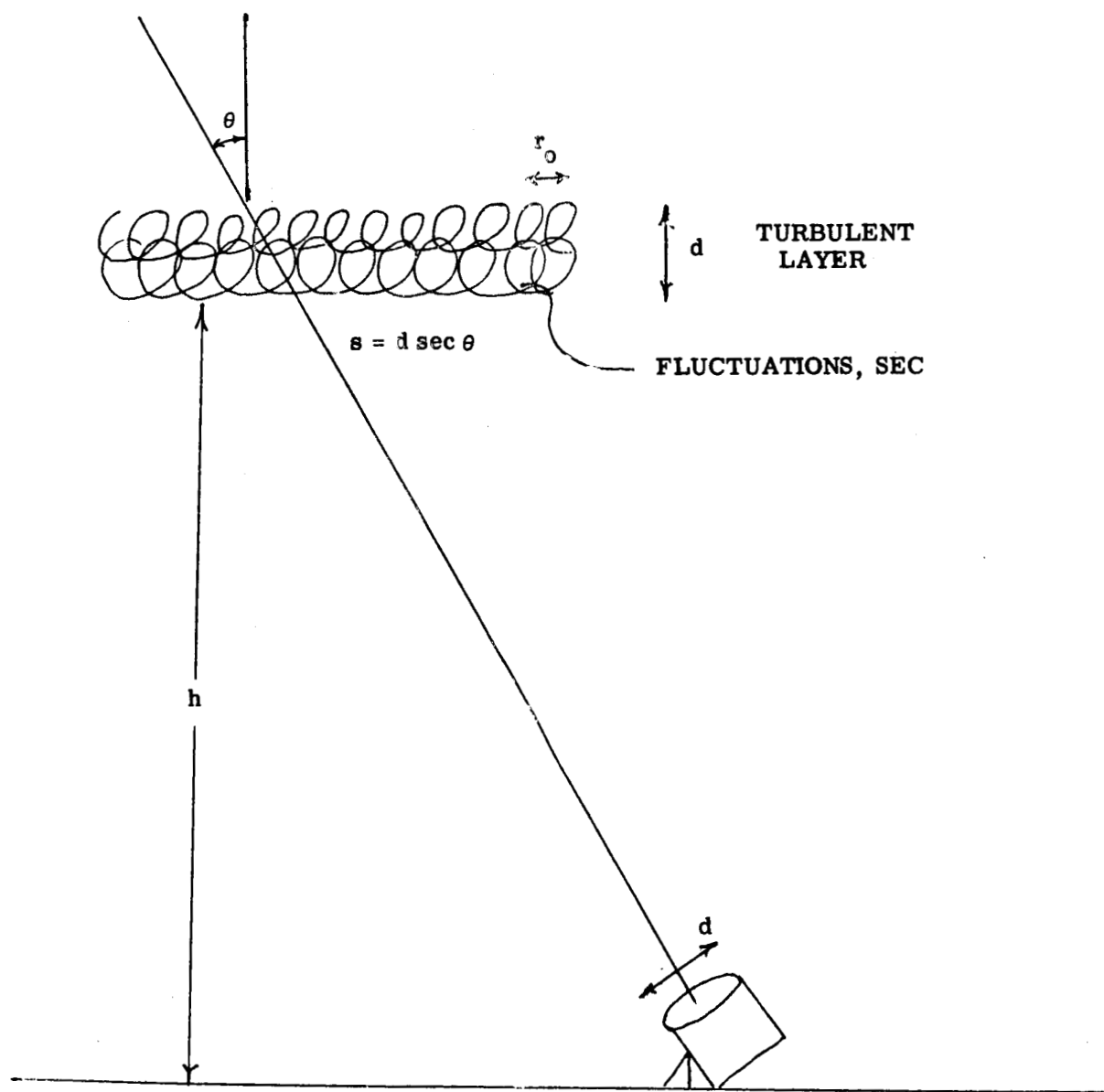


Figure 2

$$\sqrt{\frac{-2}{\rho}} = 4.86 \times 10^5 \times 4.3 \times 10^{-8} \times 32 = 6.4 \times 10^{-1} \text{ cm}$$

Thus, since this is the RMS deviation of the ray at the bottom of the turbulent layer, no scintillation would be expected until the aperture was reduced from 0.02 to 6 cm, depending on the thickness of the layer.

Consider now that the layer is at a height h . Shadow patterns on the ground would then have RMS values near $h\sqrt{\bar{X}^2} \times 4.8 \times 10^{-6}$, where the last term is a conversion from seconds to radians. If the layer was at a height of 10 km = 10^6 cm, and had deviation of 0.75 inch, the result would be

$$10^6 \times \frac{3}{4} \times 4.8 \times 10^{-6} = 3.6 \text{ cm}$$

which is the correct order for the smaller elements of observed shadow patterns.

Consider now angular deviations. If we are at the base of the turbulent layer, those will, of course, depend on our aperture. Let us vary the aperture, and note the correlation between extreme rays. Thus

$$\frac{X_1(0, s) X_1(x, S)}{X_1^2(S)} = \left(1 - 2 \frac{x^2}{r_o^2}\right) \exp(-x^2 r_o^2)$$

For simplicity let the aperture x be in terms of r_o . Thus

$$\text{Corr} = (1 - 2x^2) \exp(-x^2)$$

This may be readily evaluated, but precision is not necessary. It is noted that for $x = 0$, the function is 1, for $x = 0.1$ it is 0.98, at $x = 0.3$ it is close to 0.80, dropping to 0.5 between $x = 0.4$ and $x = 0.5$, and zero near $x = 0.7$, after which it goes negative and again approaches zero for longer values. Thus, for an aperture less than $\frac{r_0}{2}$ there will be a coherent dancing, then as the aperture increases, the superimposition of images will blur the resultant image.

What happens as the height of the layer is increased? A slight angular deviation will sweep the rays out of the telescope, and one will be looking at a different region. One second of arc, at ten kilometers, corresponds roughly to 5 cm, and thus, since this is large enough for there to be little or no correlation, the image will be steady, but of the order of a second of arc in size. There will also be an affect of aperture size here, since it controls the coherence of the individual regions that is being observed.

These arguments may, of course, be carried further but the returns at this point begin to diminish. One additional point should be made before closing this portion. There has been extensive discussion as to the dependence of seeing on zenith distance. Such measurements are difficult, and the literature is scanty, but deviations proportional to $\sec^{1/2} \theta$ are common, and values of $\sec \theta$ are also common, with occasional $\sec^2 \theta$. The theoretical derivation of Chandrasekhar yields $\sec^{1/2} \theta$ for $\sqrt{\bar{X}^2}$, and $\sec^{3/2} \theta$ for $\sqrt{\bar{\rho}^2}$. Now, $\sqrt{\bar{X}^2}$ is the important factor from the above argument in seeing (especially dancing) caused near the observer, and also in the non-dancing image caused at a distance. $\sqrt{\bar{\rho}^2}$ will be the major factor in scintillation. Low frequency (10-20 cps) scintillation varies with zenith distance, provided that the frequency between $\sec Z$ and $\sec^2 Z$ is not unreasonable. High

frequency scintillation (above 50-100 cps) seems to be relatively independent of zenith distance. An approach of this type might assist in separating the effects of the various sections of the atmosphere.

The relative independence of high frequency scintillation with zenith distance can be partially explained. If scintillation increases as $\sec^{3/2} \theta$, the high frequency components, which are caused by the shadow pattern being carried past the aperture, are reduced by the relative decrease in wind velocity perpendicular to the line of sight. Thus, it would be expected that

$$\cos \theta \sec^{3/2} \theta = \sec^{1/2} \theta$$

This is a little stronger dependence than would be expected. On the other hand, if the basic dependence was $\sec^{1/2} \theta$, the actual effect would then be $\sec^{-1/2} \theta$, and such an improvement is not observed.

The literature dealing with seeing is reasonably extensive, but it is not all well known. A bibliography will be found at the end of this report, which although not complete, is reasonably representative. Further references may be obtained from Nettelblad's Studies of Astronomical Scintillation, which is an extremely good review and introduction to the subject.

Chandrasekhar's arguments may also be modified in another way. A region may be taken near the ground of thickness of the order of 100 meters. \bar{X}^2 may be taken as 7.5 inches, then $\sqrt{\epsilon^2 \mu} = 4.3 \times 10^{-7}$, an order of magnitude greater than before. We now have

$$\sqrt{\bar{\rho}^2} \approx 5 \times 10^5 \times 4 \times 10^{-7} = 2 \times 10^{-1} = 0.2 \text{ cm}$$

This result is of special interest, even though it is only an order of magnitude argument, because of the break in scintillation at roughly a half centimeter beam. Experimental observations indicate a large jump in scintillation when a beam is only a half centimeter or less diameter at path lengths of 100 meters. Its values also correspond more closely to lower atmosphere effects as would be expected.

Unfortunately, it is difficult to relate data of the various investigators into a comprehensive picture. As one would expect there is a diurnal fluctuation in seeing - a maximum of "scintillation", in the broader sense, near noon; a minimum near sunset and sunrise; and a secondary maximum at night. This secondary maxima is much less intense than the daytime one. This is, of course, related to the thermal balance and is to be expected. On the other hand, stellar scintillation measurements show that at least some of the components do not go to a minima near sunrise and sunset - there are undoubtedly components caused at higher levels, while that portion due to turbulence near the surface is strongly effected by the thermal balance. The seeing also shows fluctuations with weather systems, being poorest during cyclone (low) conditions.

A full review of all the different correlations has been given by Nettelblad, and will not be repeated here, since his discussion is unsurpassed. However, some comments should be made about several recent papers appearing in The Journal of Geophysical Research, Volume 67, No. 8, devoted to the International Symposium on "Fundamental Problems in Turbulence and Their Relation to Geophysics". Especially to be noted is "Some Optical Properties of Turbulence in Stratified Flow Near the Ground" by Portman, Elder, Ryznar and Noble. This paper reports measurements of

scintillation along low horizontal paths from 120 to 600 meters in length. An extremely close relation was found between the temperature gradient near the ground and scintillation. Further, it was noted that under stable conditions the effects were intermittent, seemingly caused by the mixing of layers at different temperatures. It was also noted that the percent modulation, per unit temperature difference, was a strong function, the Richardson number, with a break in slope near $Ri = 0.35$. The modulation also increased with path length. The writers believe that they confirm Tatarski's path length to the 0.9 power relation, although the scatter of data could cover a number of other relations also. It should be noted that this relation appears to saturate near path lengths of 2 km, and the percent modulation then becomes independent of path length. As would be expected, shifts to higher scintillation frequencies were noted as the aperture is decreased. These observations correlate closely with observations made at the observatory.

This work seems to be quite significant, but it must be remembered that it deals with horizontal paths near the ground, and effects rising relatively near the observer. It shows the importance of thermal gradients near the ground, however, and establishes some of the properties of seeing as caused near the ground. Slant paths are, of course, a different matter. Some idea of the effects that will occur can be gained in another article in the same Symposium - "Turbulence in the Presence of a Vertical Body Force and Temperature Gradient" by R. Deissler. As would be expected, a negative temperature gradient will feed energy into the turbulence and have a distabilizing influence, while a positive gradient will tend to stabilize the atmosphere. The effects of these buoyancy focus on the turbulent spectra are also calculated. For Prandtl numbers less than 1, as is characteristic of the atmosphere, the buoyancy forces feed energy in throughout the spectrum,

while the dissipation region is relatively unaffected. The net effect is to emphasize the low wave numbers. It might be concluded that lower frequency effects will become more and more important as we leave the ground, so that although near the ground the effects are peaked at higher frequencies (smaller components), the buoyancy forces will tend to emphasize the lower frequencies as one looks away from the surface. It might be noted that the shift in the peak of the spectrum is not too strong, although the change of shape is.

A further check on Tatarski's assumption of isotropic turbulence is given in a paper in The Journal of Geophysical Research, March 1962, "Turbulence Measurements by Sailplane", and the "Inertial Subrange of Atmospheric Turbulence", by P. MacCready, Jr.

Since seeing is basically a meteorological phenomenon, it would seem wise at this point to consider some of the meteorological aspects of the problem, without going into too much detail.

First consider the daytime situation. There will be the incoming solar radiation, to which the atmosphere is essentially transparent, being absorbed by and heating the ground. The ground then re-radiates, but in this case the atmosphere is only partially transparent, the water bands having a strong effect. It can be shown that the transfer of energy by radiation is not strong, nor is conduction, so that the main diffusion of energy to the atmosphere has to be through turbulence.

The Reynolds number, R , is frequently used to determine if turbulence will occur. When $R = \frac{v l}{\nu} > 10^4$, it is usually assumed that flow will be

turbulent. Actually, the value of R , at which turbulence starts, depends on the roughness of the boundary layer, experimentally it starts between 10^3 and 10^5 depending on this factor. If l is taken as the height of the tropopause, and v as one meter per second, $R = 10^9$, and turbulence must exist. Obviously, l can be reduced radically, as can v , and turbulence will still exist in the atmosphere because of the low value of ν , the kinematic viscosity. Another relation can be obtained using the Reynolds number and dimensional analysis,

$$l = \sqrt{\frac{F(\dot{R})\nu}{\frac{\partial \bar{v}}{\partial Z}}}$$

where l is a characteristic length of a turbulent element, and $\frac{\partial \bar{v}}{\partial Z}$ is the mean vertical velocity gradient. $F(\dot{R})$ is dimensionless and unknown. Thus the size of an element is inversely proportional to the velocity gradient in the vertical. Low velocity gradients thus yield larger elements, high velocity gradients small elements.

With a wind, the eddy velocities relative to the mean wind must be considered. If the mean wind is U , with $V = W = 0$, and the eddy velocities are U' , V' , W' , it has been established that sufficiently far above the ground,

$$\overline{U'^2} = \overline{V'^2} = \overline{W'^2}$$

so that there is an equipartition of eddy velocities. The distance above the surface that equipartition of energy occurs has been variously estimated, but in general, isotropy begins to occur at a height of six to ten meters. In the anisotropic region below this height, the ratio of V'/W' varies from 3,

at less than a meter, to $1-1/2$ at two meters, approaching 1 at eight to ten meters. The lateral component decreases with height, and the vertical component increases. This eddy energy tends to be concentrated in periods of less than one second. There is a tendency for the faster moving air to go down and the slower to go up, so that the eddies tend to be in planes strongly inclined to the horizontal.

From the standpoint of the observer there are two driving forces for the turbulence - the wind, and thermal convection or instability. Ultimately, of course, both have the same energy source, but in a small area it is possible to distinguish between them. Neglecting the wind then, it is seen that from considerations of conservation principles there will be no net mass transfer. Thus, there is simply the transfer of thermal energy. As a rough approximation then,

$$\frac{\partial T}{\partial t} = K \frac{\partial^2 T}{\partial Z^2}$$

and the net upward flow of heat across a horizontal surface will be,

$$-K\rho C_P \left(-\frac{\partial T}{\partial Z} + \Gamma \right)$$

where K is the eddy diffusivity, ρ the density, C_P the specific heat, T the temperature, and Γ the lapse rate. If the dry adiabatic lapse rate Γ is greater than the lapse rate $-\frac{\partial T}{\partial Z}$, the expression is negative, the atmosphere stable, and the flow of heat is directed downward. It is noted that in the daytime the ground is hot and heats the nearby air, so the expression is positive, the adiabatic lapse rate being smaller. Now, as the ground cools off the heat transfer equals zero, where $-\frac{\partial T}{\partial Z} = \Gamma$, and we enter stable

equilibrium. At night, of course, a temperature inversion occurs, $-\frac{\partial T}{\partial Z} < \Gamma$, and heat is transferred to the ground from the air, and the ground becomes colder because of its radiation into space.

Another characteristic already mentioned is the Richardson number,

$$Ri = \frac{g \left(\frac{\partial T}{\partial Z} + \Gamma \right)}{T \left(\frac{\partial \bar{v}}{\partial Z} \right)^2}$$

the magnitude of which determines the stability of the air. If it is less than one, turbulence builds up, greater than one, turbulence dies out. It is noted that if $\frac{\partial T}{\partial Z} < -\Gamma$, Ri is zero or negative, and the atmosphere is very stable.

One question of importance is the height of the turbulent layer near the surface of the earth. It has been established that the turbulence will be proportional to $e^{-\beta Z}$, where empirically $\beta = 2.4 \times 10^{-5} \text{ cm}^{-1}$. Thus the turbulence will die down to $1/e$ of its initial value in about 400 meters, or 1200 feet. It will be roughly 10 percent of its initial value at between one and two km, and 90 percent between 70 and 80 meters.

From the discussion thus far it is apparent that in the ten meters closest to the ground, the turbulence will be anisotropic, and very rapidly changing in nature. Thus one would expect a large gain in seeing, when moving above the first ten meters of atmosphere. On the other hand, the improvement in the next 100 meters will be negligible, so that added height will do little, if any, good.

By reviewing the sources of poor seeing it is seen that there are several causes. The major ones are listed as follows. First, turbulence caused by convection currents. This, of course, will be primarily a day-time phenomenon, but can occur at night in poorly chosen locations. Secondly, winds will give rise to turbulence near the surface of the ground. This, of course, can occur at either day or night. A third source exists when there is a strong inversion and motion of the air. Then a wavy turbulence exists at the interface of the two air masses. A fourth source is the turbulence caused by the air moving past an obstacle, such as the observing dome or building. Other sources arise within the dome and telescope, but these are a separate matter.

Now consider the fluctuations in the index of refraction that give rise to the seeing problem. At zero degrees centigrade, 760 mm of mercury pressure and 4 mm of mercury water vapor pressure, assuming constant moisture content, the empirical formula for the index of refraction results,

$$\mu(t, p) = \frac{p}{760 + 2.9t} \mu(0, 760)$$

so that we have, assuming constant pressure,

$$\delta\mu = \mu(0, 760) \left(\frac{-2.9t}{760 + 2.9t} \right)$$

Assume that the temperature fluctuations about zero are of the order of 10^{-2} degrees, then

$$\delta\mu \sim 4 \times 10^{-5}$$

Tracing a ray

$$\frac{\partial \psi}{\partial s} = \frac{\partial}{\partial x} \delta \mu$$

and the gradient of μ might well be $4 \times 10^{-5}/10 \text{ cm} = 4 \times 10^{-6}$. Letting $s = 10 \text{ cm}$, results $\Delta\psi = 4 \times 10^{-5}$, or 8 seconds of arc.

Near the tropopause the pressure will be an order of magnitude lower, so that the index of refraction will be also, and it follows that $\Delta\psi$ will also be an order of magnitude lower.

The use of these formulas oversimplifies the problem, since pressure, density, and temperature are related. The usual estimates of fluctuations, in the index of refraction, vary from a few times 10^{-7} for the troposphere, to four times 10^{-8} for the tropopause. Tracing a ray with these values, and again assuming that $s = 10 \text{ cm}$, $\Delta\psi$ is found to be of the order of 10^{-7} to 10^{-8} . Near the ground $\delta\mu$ is larger, probably of the order of 10^{-6} to 10^{-5} , close to the calculated value. With a value of $\Delta\psi$ of 10^{-7} , assuming a random walk situation, a quarter of a kilometer is required to obtain an angular deviation of a second. Near the ground, observed values of 10 inches, in tens of meter, imply a $\Delta\psi$ of the order of a second, and correspondingly high values of $\delta\mu$, between 10^{-5} and 10^{-6} , as mentioned above.

All calculations of this type must be taken with a grain of salt - values varying an order of magnitude with the assumptions made. However, it is clear that usually, except for paths lying close to the ground, one element does not give an appreciable deflection - the effects are built up by a large number of elements. Close to the ground, in addition to the anisotropy of

the turbulence, large fluctuations are possible in the index of refraction, which can lead to one or a few cells being effective. These large fluctuations die out in the first few meters, and are normally not encountered.

It should also be noted that the RMS image fluctuations will be proportional to the square root of the path length, thus effectively weighting the nearer atmosphere in apparent importance. Another factor can enter here under some circumstances - deviations in the index of refraction caused by humidity fluctuations (fluctuations in the partial pressure of wave vapor). These can have strong effects, but we normally do not expect large deviations in this quantity.

One last important characteristic of the turbulence should be noted. That is, that sufficiently far from the ground (roughly 10 meters), it will be homogeneous and isotropic, decaying upward. Under these conditions we can expect to trade space and time averages.

Intuitively what has been said so far may be extended to lasers without too much difficulty, since the beam from a laser, assumed to be monochromatic coherent, and with a flat wave front, will display very strong scintillation effects, comparable to those of a star or perhaps even more extreme. Thus, consider stellar seeing.

There are two distinct problems associated with seeing. First, scintillation, or the changing intensity of a star at the aperture of a telescope, commonly known as twinkling; and secondly, the image shape and motion. The first is associated with the tropopause and the winds near it; the second is associated with the nearer atmosphere. The two effects are independent, and should not be confused.

Let us consider scintillation first. This is not so important from the standpoint of image orthicon techniques as it is for photomultipliers, because of the usually longer integration times associated with image orthicons. However, for star trackers, or the measurement of magnitudes, scintillation introduces a noise level that must be considered.

If one removes the eyepiece of the telescope and looks at the aperture, the turbulence causing the scintillation can be seen as a sort of schlieren. These are elements varying from roughly an inch or two in dimension to areas larger than six or eight inches. Because of our aperture limitation, it is not possible to definitely eliminate larger elements, but at least they do not appear to be too important. These elements, carried by the winds near the tropopause, can be seen to stream past the aperture. It is interesting to note though, that a frame by frame examination of motion pictures taken of the phenomenon reveals practically no correlation frame to frame. Thus the turbulent elements are changing size and shape more rapidly than they are carried past the aperture. It would appear that fluctuations in the elements take place in less than 30 milliseconds, so that there are two sources of the scintillation modulation. First, the turbulence itself, which we might regard as isotropic, and secondly, the streaming of the patterns across the aperture, as they are carried by the wind. As a first approximation, at least, these effects appear to be independent.

The accompanying figures give an idea of the frequency content of this modulation. Figures 3, 4, and 5 show the tendency when changing aperture, atmospheric conditions, and zenith distance.

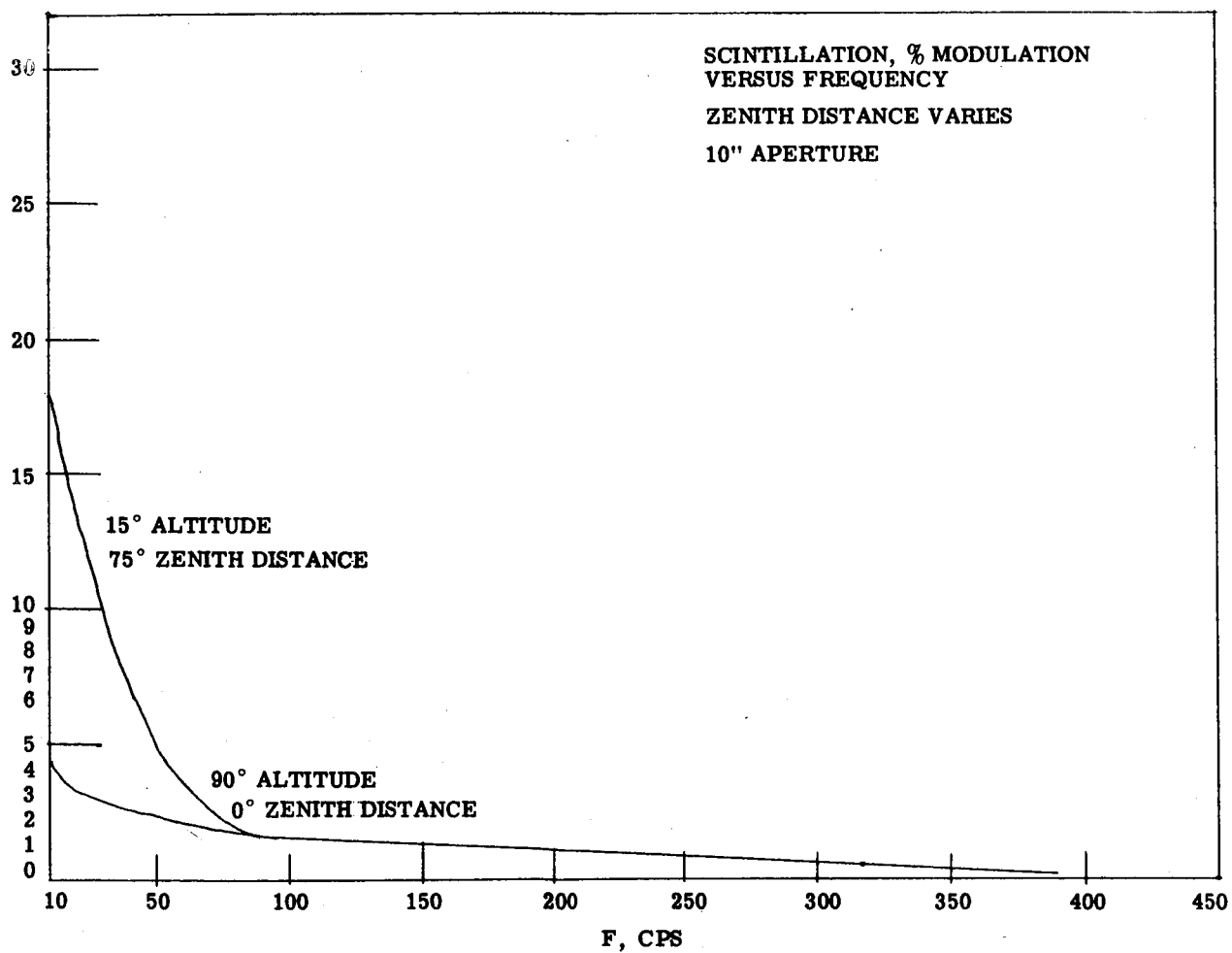


Figure 3

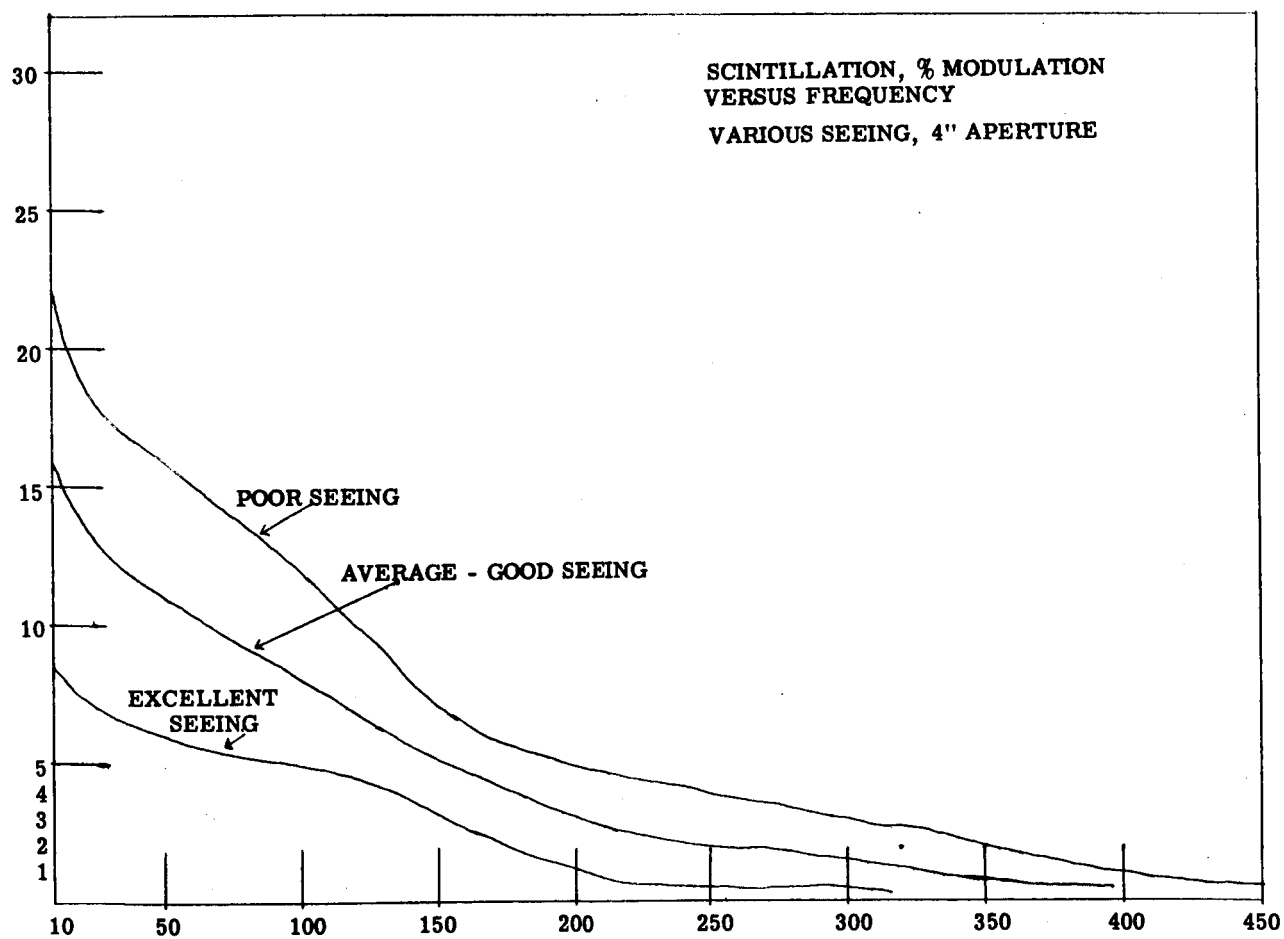


Figure 4

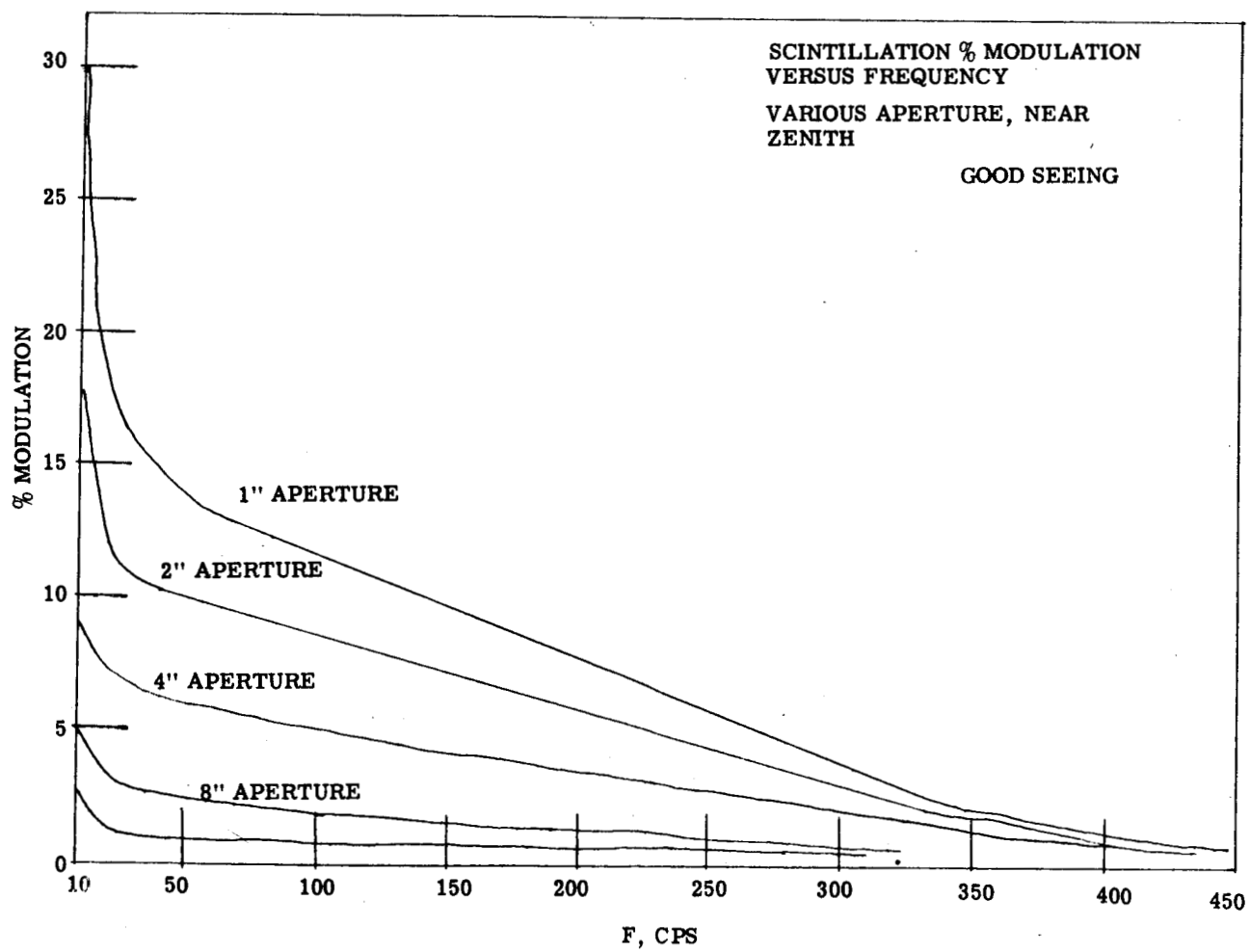


Figure 5

The most striking effect is the increase of low frequency modulation relative to high frequency modulation as conditions worsen. This effect is especially striking as high clouds move into an area. Prior to the clouds moving in the low frequency, components increase to the extent that the scintillation becomes quite apparent when observing with an image orthicon. The components observed are well below 10 cycles per second. The Observatory has obtained observations only at night to date, and it would be very interesting to observe during daytime hours. However, this is more difficult than night time observations. The observations mentioned here confirm the observations of others, the topic of scintillation having been considered more than any other topic in the seeing problem. For references see the bibliography.

The relative value of low and high frequency scintillation, and the shift in their importance can be readily understood when it is realized that most of the high frequency scintillation arises near the tropopause. Thus, when seeing conditions worsen, most of these being near the observer, the relative value of low frequency scintillation increases. The importance of the near atmosphere can readily be shown on a horizontal light path, where it is quite simple to get large low frequency (below 100~) scintillation.

There are two sources of noise associated with fluctuations in intensity. These are scintillation and photon noise. Fluctuations in the arrival of photons follow a Poisson distribution, and to a good approximation if n photons arrive, the fluctuations will be \sqrt{n} . Since, if when the aperture is D , n is proportional to D^2 , and the noise is proportional to D , the photon signal-to-noise will improve as D^{-1} . Considering scintillation, the number m of turbulent elements will be roughly proportional to D^2 , and the RMS fluctuations might be regarded as varying with the square root of the number of turbulent elements, or

proportional to D . Thus the situation will also improve as D^{-1} . However, as the number of photons decrease, as we go to fainter magnitudes, the scintillation will not get worse, while photon noise will. Thus at some point, as we go to fainter magnitudes, the problem of photon noise will become more serious than scintillation noise. This point, for the Observatory's 12-inch aperture and good seeing conditions, seems to be around the sixth or seventh magnitude, which is in line with the estimates of others. From this discussion it appears then that for the brighter stars, roughly those that can be seen with the dark-adapted eye, scintillation noise will be most important, while for fainter stars photon noise predominates, regardless of the telescope aperture. However, this point would vary with the transmission, or efficiency of the optical system, since this would effect the effective number of photons, but not the scintillation noise. If observations are to be made in the daytime or twilight, consideration should also be given to photon noise in the background.

To convert this last into data for laser beam, if one remembers that a 0 magnitude star gives a flux of 10^6 photons cm^2/sec at the observer (in the visible), and compare this to the number of photons in the beam, from $E = h\nu$, a direct comparison can be made.

Scintillation effects for a laser should be stronger than for a star, since it is monochromatic and no wavelength averaging is present. The only available data on this is given in "Astronomical Photoelectric Photometry" published by American Association for the Advancement of Science, and shows little lack of correlation. Thus from available data this increased effect should not be too strong.

Consider now the attenuation of light as it passes through the atmosphere, neglecting the effects of atmosphere turbulence. As light passes through a volume of air, there will be both an absorption and a scattering of light which will remove light from the beam. The equation of transfer in such cases is treated by Chandrasekhar in, "An Introduction to the Study of Stellar Structure" and in other works. The continuous attenuation of a signal may be considered as consisting of molecular (Rayleigh) scattering, absorption, and some scattering by longer particles. The total transmission of an atmosphere is given, for example, in Allen, Astrophysical Quantities. As given there, for a clear atmosphere, 1 air mass at 0.4μ the transmission is 63 percent, at 0.45, 73 percent; at 0.50, 80 percent; at 0.55, 83 percent; at 0.60, 84 percent; at 0.65, 88 percent; at 0.70, 91 percent; at 80, 94 percent; and at 1μ , 96 percent. These figures include Rayleigh scattering with a λ^{-4} dependence, absorption, primarily by water vapor, and scattering by dust particles in the clear air. Since one air mass is equivalent to roughly 8 KM of air at S.T.P., this data may be directly applied for an 8 KM path in clear air. Because of this high transmission this should not be an important factor in calculations, unless extreme ranges in the atmosphere are required.

Band absorption by atmospheric gases also exists, but at present wavelengths this is not a problem. Data on this will also be found in Allen.

When haze, fog, or clouds occur, the situation changes radically. When the particles scattering the light are molecules much smaller than a wavelength, the scattering function is $\beta(\phi, \lambda) = A \lambda^{-4} (1 + \cos^2 \phi)$ neglecting polarization effects, which is not completely valid but will do for this discussion. The actual scattering is fairly small, though it does account for the blueness of the sky, and has been included in the continuous attenuation given above. Small particles in the air, aerosols, can either act as scatters

and absorbers or as condensation nuclei for water vapor, leading to moisture droplets. These liquid droplets may occur in diameters from 10^{-8} to 10^{-3} meters. The critical item in scattering is the value $\alpha = \frac{2\pi a}{\lambda}$, where a is the radius of the droplet. Tables for indices of refraction of 1.33 (water) for various values of λ will be found in LaMer and Sinclair, O.S.R.D., Report No. 1857, and in National Bureau of Standards Applied Mathematics Series No. 4, "Tables of Scattering Functions for Spherical Particles". Some tables will also be found in Middleton's book, Vision Through the Atmosphere, which is basic. For large particles ($a \gg 3\lambda$) and small angles an optical approach can be made which gives good approximation.

A drop can interact with a wavefront in three ways. First, it can externally reflect light; next, light can enter and be internally reflected; and last, the light can be diffracted. These have all been examined in detail by various authors, with a number of good references given in Middleton's book.

The intensity at an angle ϕ due to diffraction by a spherical droplet is,

$$I = \frac{\pi^2 a^4 E}{\lambda^2} \left[\frac{2J_1 \left(\frac{2\pi a}{\lambda} \sin \phi \right)}{\frac{2\pi a}{\lambda} \sin \phi} \right]^2 \cos^4 \frac{\phi}{2}$$

where J_1 is the Bessel function of first order, a is the particle diameter, and λ is the wavelength. The light refracted through the drop will be,

$$I_2 = \frac{(1 - k)^2 E a^2}{2} \frac{\sin 2 i_1}{\sin \phi} \frac{d i_1}{d \phi}$$

where,

$$\phi = 2 (i_1 - r_1)$$

$$k_1 = 1/2 \left[\frac{\sin^2 (i_1 - r_1)}{\sin^2 (i_1 + r_1)} + \frac{\tan^2 (i_1 - r_1)}{\tan^2 (i_1 + r_1)} \right]$$

$$\frac{di_1}{d\phi} = \frac{\sin i_1 \cos r_1}{2 \sin (\phi/2)}$$

and i_1 and r_1 are the incident and refracted angles,

$$\sin i_1 = \mu \sin r_1$$

where μ is the index of refraction, $4/3$. The light reflected will be

$$I_3 = 1/4 k_2 E a^2$$

where k_2 differs from k_1 only in the angles considered. See Figure 6.

I_1 , I_2 , and I_3 cannot always be simply summed because the scattered light is not completely incoherent with normal light sources. It is possible to include absorption in these calculations if necessary. The absorption coefficient k is small, of the order of $2 \times 10^{-2} \text{ cm}^{-1}$ for water. The fractional flux absorbed will be $\frac{4\pi k a^3}{3\mu} = \pi k a^3$ for water. The scattered flux will be much greater than this, of the order of $2\pi a^2$ for drops in the region of 10μ . The ratio of these two is of the order of 10^5 . A large raindrop, of the

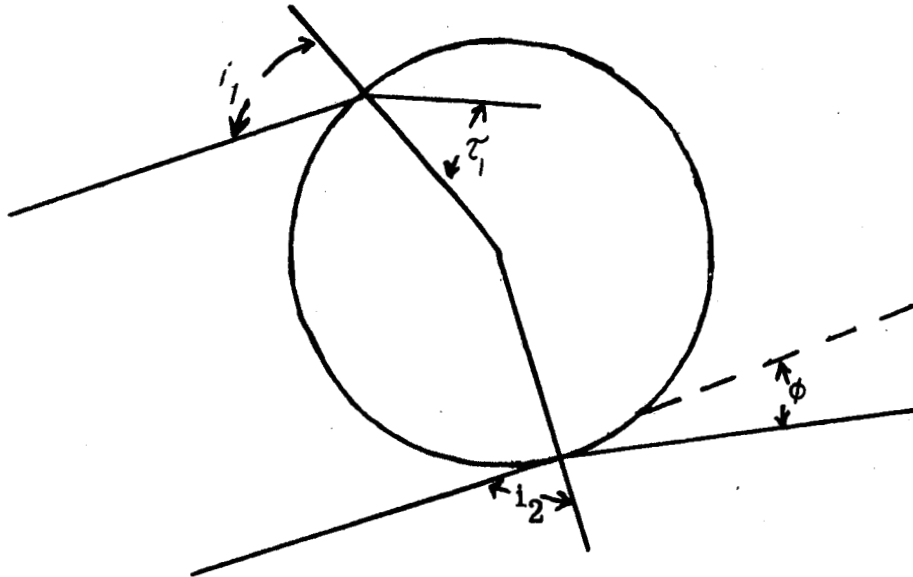


Figure 6

order of 0.5 cm, would have a ratio of 200. Thus absorption is normally neglected in atmospheric optics. This is probably not a justified assumption, though with high intensity laser beams of low divergence using the figure of $\pi k a^3$ for a 10 micron sphere, there is an absorption of 6×10^{-11} watts per watt/cm². Then one drop will absorb 6×10^{-2} watts. The volume of the 10 micron sphere is on the order of 10^{-9} cm³, so that the mass is 10^{-9} gm. 10^{-9} gm would be raised 100 centigrade degrees by $10^{-9} \times 10^2$ calories, or 4×10^{-7} joules. If the pulse lasted one millisecond, the drop would absorb 6×10^{-5} joules, much more than enough to not only raise its temperature, but also to vaporize it. On the other hand, if the pulse lasted

1 microsecond, the absorbed energy would only be 6×10^{-8} joules, or about a 15-degree raise in temperature. Depending on the meteorological conditions, the resulting change in vapor pressure of the droplet could give rise to a temporary clearing of the path.

There is one disadvantage in this type of calculation, and that is the short high energy pulse can easily lead to modifications of classical theory. Surface absorption could become a factor, which would increase the absorbed energy. This will probably have to be settled experimentally.

The variation of scattering with wavelength is of some interest here. For water droplets and opaque particles we may plot n versus a/λ . See Figure 7.

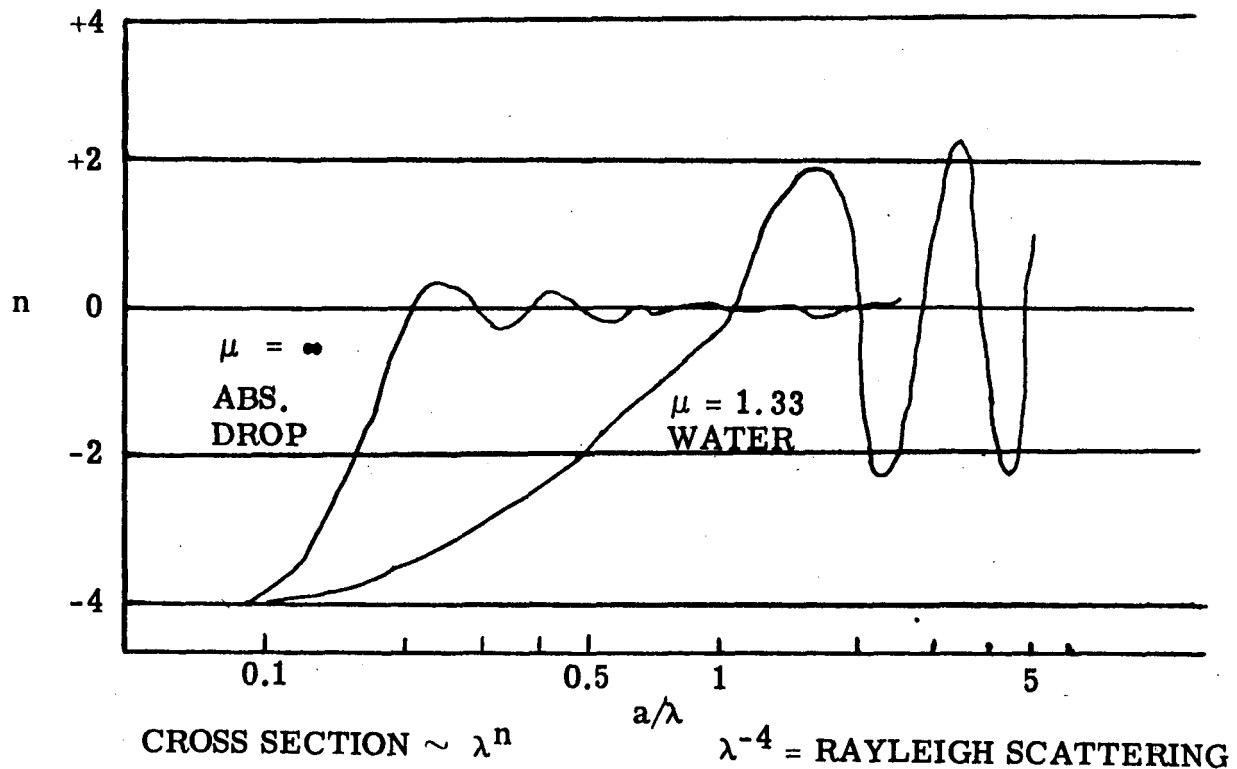


Figure 7

The most significant thing about this is that for absorbing particles (haze, smoke) n goes to 0 at about $a/\lambda = 0.2$, and for water particles it goes to 0 at $a/\lambda = 1$, with subsequent fluctuations. Thus for most fogs and clouds, and of course rain, there is no transmission advantage at longer wavelengths over shorter wavelengths. It is not possible to readily estimate attenuation by fog or clouds, much more work is required here.

The size of particles in clouds and fog is of interest. The mean will be about 10μ in nimbostratus, 8μ in stratocumulus, 5μ in cumulus, 4μ in stratus, and 2.3μ in valley, or low fogs. These sizes fluctuate though, and the width of the distribution can be as high as an order of magnitude. The number of particles per cm^3 varies from 300 in fair weather cumulus clouds to $50/\text{cm}^3$ in tropical cumulus. Another important factor in evaluating this problem is that the drops are frozen at the tops of temperate region cumulus clouds and other high clouds, so that scattering dominates over refraction. This topic is extremely complex and it would seem that almost any simple approach would lead one astray.

The following may be concluded:

1. The major problem in narrow beam laser systems will be atmospheric turbulence, or seeing. The theoretical treatments of Tatarski and Chernov are the best available at this time, but they do not extend far enough to make predictions in the case under discussion. In addition, much empirical data is needed. These effects are of the order of seconds of arc, and become negligible when beam widths go to minutes of arc. Thus most experimental data to date is useless.
2. Transmission of the clear atmosphere is not a major problem and, with available data, can be readily calculated.
3. Scattering and absorption by clouds and fog is not readily calculable, especially since we do not have a good description of cloud particle distributions. However, most of the effects appear to be amenable to experimental and theoretical treatment.

Combining experimental data and theoretical analysis it is possible to construct a model of what occurs when a laser beam is propagated through the clear atmosphere.

The effects are similar to those often experienced in astronomy. However, there are two principal differences. First, the laser beam has a wavefront with finite dimensions; this differs from the astronomical case where the wavefront is of infinite extent. In the latter case, there is essentially the same amount of light scattered into the "receiving" beam as there is scattered out, whereas for the finite diameter beam there is a greater loss caused by outward scattering. The second factor that is beginning to be investigated is the effect of the high energy or power density that is to be transmitted.

A factor determining the contrast of an image of a distant object is the time-varying distortion caused by inhomogeneities in the refractive index of the atmosphere. This shimmer of distant objects is caused by temporal and spatial variations in the index of refraction which disturb the propagation of high frequency electromagnetic radiation. This disturbance causes distortion and loss of resolution.

In order to determine the effects of atmospheric turbulence on the propagation of a laser beam, an experimental link was set up at General Electric's Radio Optical Observatory located on Crawford Road Hill eight miles west of Schenectady.

Gas Laser

A Perkin-Elmer Model 112 helium-neon gas laser emitting 0.63μ was employed and the beam was narrower than one minute of arc. The gas laser was mounted on a one-meter high concrete pier sunk to bedrock as shown in the foreground in Figure 10. A photograph of the propagation path is shown in Figure 9 with the gas laser in the foreground. The concrete piers at 25 and 400 meters are clearly visible with the 400 meter pier at the edge of the open field.

Measurements were taken with a 6" oval mirror on the farthest pier and a white diffuse cardboard near the transmitter; thus the path length was 800 meters, but since the cross-section of the beam exceeded the reflecting mirror, dancing can be attributed to a 400 meter path. During a night of reasonably good seeing, clear sky, and the earth radiating to the sky, 16 mm movies using Tri-X film were taken at 64 frames per second; a portion of this film (3 frames) is shown in Figure 8. Notice the changes in each frame. A

black cross of 1/2" wide tape for positional reference is barely visible in the top frame. The divergence of the beam was about 2×10^{-4} radians (≈ 40 secs of arc), and the beam danced randomly with amplitudes of 5×10^{-5} radian (≈ 10 secs of arc) with probably much greater instantaneous displacements. A 12 mph wind was directed at right angles to the beam; its effect can be seen in the anisotropy of the turbulent elements becoming elongated in the wind direction.

Collimated Arc Source

Some of the time varying effects are slow enough to be discernable to the eye, but much of the effect is so rapid that visual observations only time-averages the image radiance. One of the simplest ways of further examination of beam structure is to measure the scintillation. A tungsten arc point source was used in a 5" aperture f/16 collimator. Scintillation spectra of the laser and arc source beams were compared under identical conditions, and no difference was noted within the limits of experimental error imposed by the atmosphere. The arc source was selected for scintillation measurement use because of operational simplicity. Apertures of both the collimator and 12-inch reflecting telescope were controlled by the use of masks. A 6" oval quarter wave mirror was placed on the 50-meter pier so that the photomultiplier receiver was next to the collimated source. The photomultiplier at the focus of the telescope had its output recorded, either directly using a DC amplifier and a Sanborn recorder to measure total beam modulation or scintillation, or by using a tunable filter microvoltmeter combination feeding the recorder to measure frequency component data. Figure 11 shows a scintillation record taken under good seeing, clear sky conditions.

Several points are worth noting. First, conditions change radically from night to night, and with the wind. The worst beam modulation occurred when there was little or no wind, and this effect decreased with the wind which mixes the air. The data were taken during an evening in July. With a 5" diameter collimated beam and a 12" receiving aperture one might typically obtain 20 to 30 percent total beam modulation with no wind, dropping to 1 to 4 percent modulation with a 20 mph wind. See Figure 12.

Second, since the wind mixes the atmosphere, the low frequency components are reduced as well as the average fluctuations.

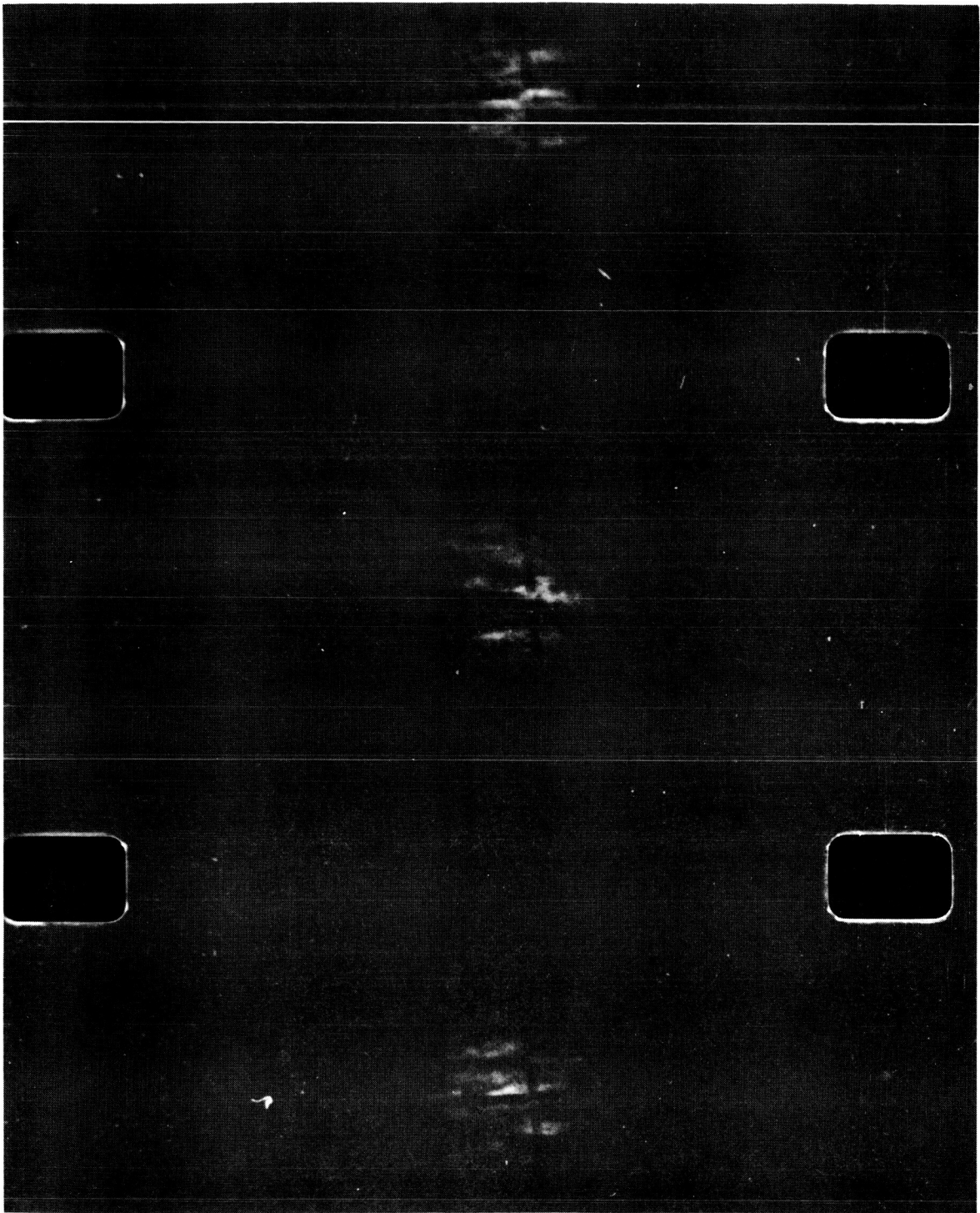


Figure 8



Figure 9

ORIGINAL PAGE
BLACK AND WHITE PHOTOGRAPH

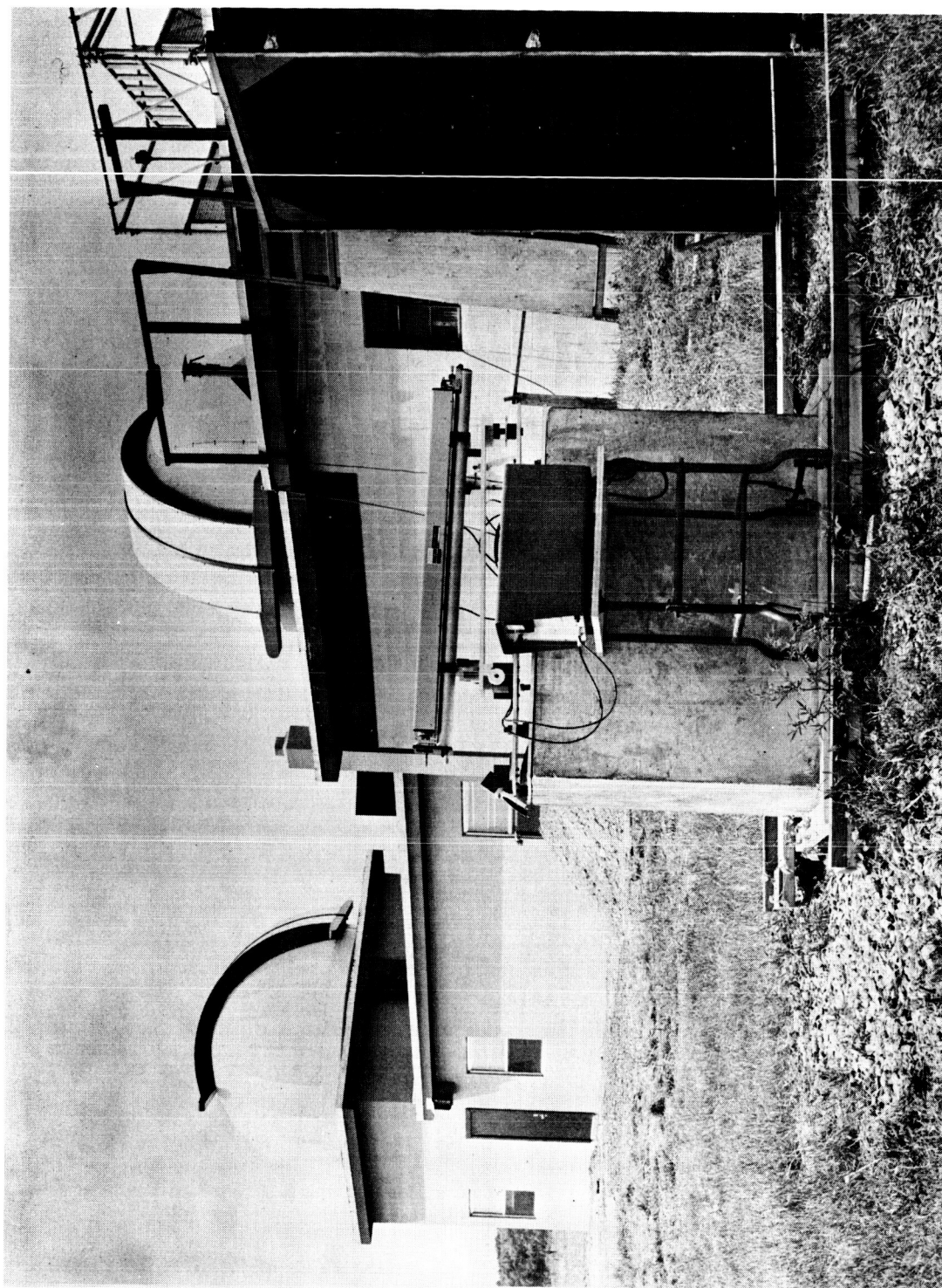
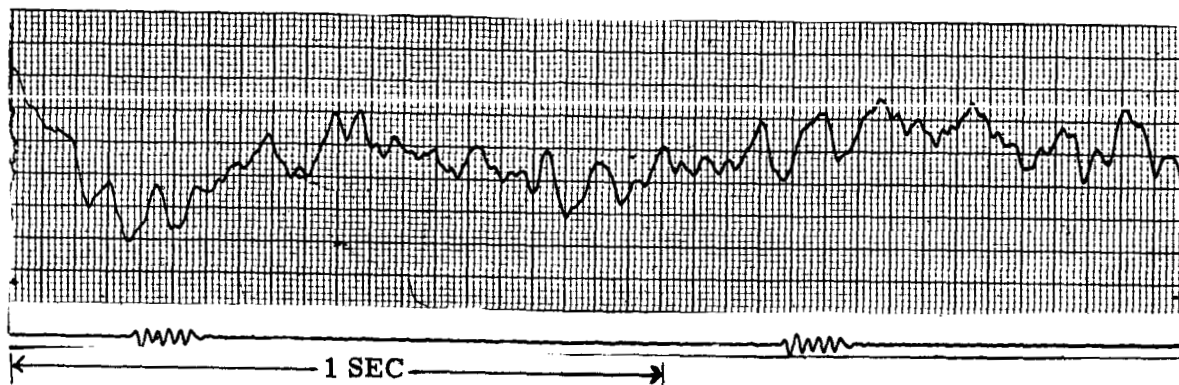
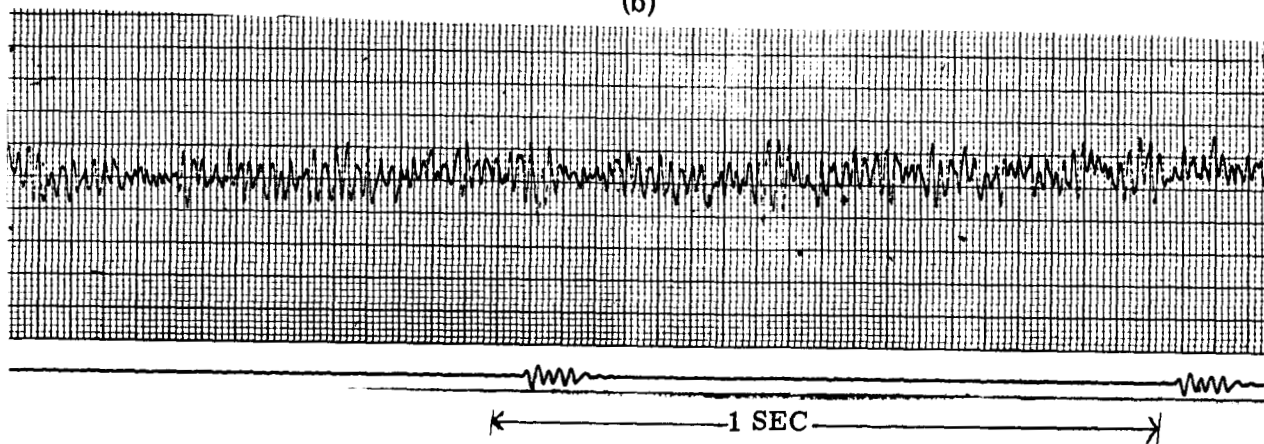


Figure 10

(a)



(b)



SCINTILLATION RECORD

- (a) 5-inch diameter beam, no wind,
Peak to Peak Modulation 1.6%
- (b) 5-inch diameter beam, 12 MPH wind,
Peak to Peak Modulation 2.2%

Note: Traces indicate increasing signal in the downward direction.

Figure 11

Third, with a receiving aperture smaller than the beam diameter (Figure 13) the low frequency components are relatively stronger than for a case of receiving aperture larger than the beam diameter (Figures 12 and 14). Furthermore the higher frequency components (100 to 1000 cycles) do not decrease as rapidly as when the receiving aperture is smaller than the beam. See Figure 13. On the other hand, a narrow beam and larger receiver (Figure 14) tend to give much greater fluctuations in the lower frequency components, and the total modulation is not as great as with a smaller receiving aperture. (Figure 13).

A fourth point, of some importance, is the difference between these data and those for stellar scintillation. These data show that the high frequency components fall much faster than do the stellar scintillation data. In stellar observations there is a correlation between 100 to 500 cycle scintillation and the winds near the tropopause; with this correlation, one can infer that much if not most of the low (10 - 100 cps) frequency stellar scintillation is caused by turbulence in the lower atmosphere.

A fifth point of interest is that a half inch diameter beam traversing 100 meters of atmosphere has twenty-five percent modulation when the receiver has a twelve inch aperture (See Figure 15). This implies that a portion of this small beam is deflected completely out of the receiver. The scintillation decreased with larger beams and apertures, and the smaller apertures accentuated the high frequency components.

Now a description of the atmospheric turbulence is needed. An article by S. Q. Duntley, W. H. Culver, F. Rickey and R. W. Preisendorfer on "Reduction of Contrast by Atmospheric Boil" in the Journal of the Optical Society of America, Vol. 53, No. 3, pp. 351-357, March 1963 assumes that ray transmission through a turbulent atmosphere may be derived by using a probability distribution model for a random walk problem. The result is that the probability of receiving light from an object viewed through a turbulent atmosphere follows a normal Gaussian distribution. Furthermore, the root-mean-square angular deflection of the points of any object will be proportional to the square root of the object-to-observer distance. From the derived relations described by the article, it is possible to predict the apparent contrast throughout a given scene provided the inherent contrast distribution, the optical air state, and the range of the target are known.

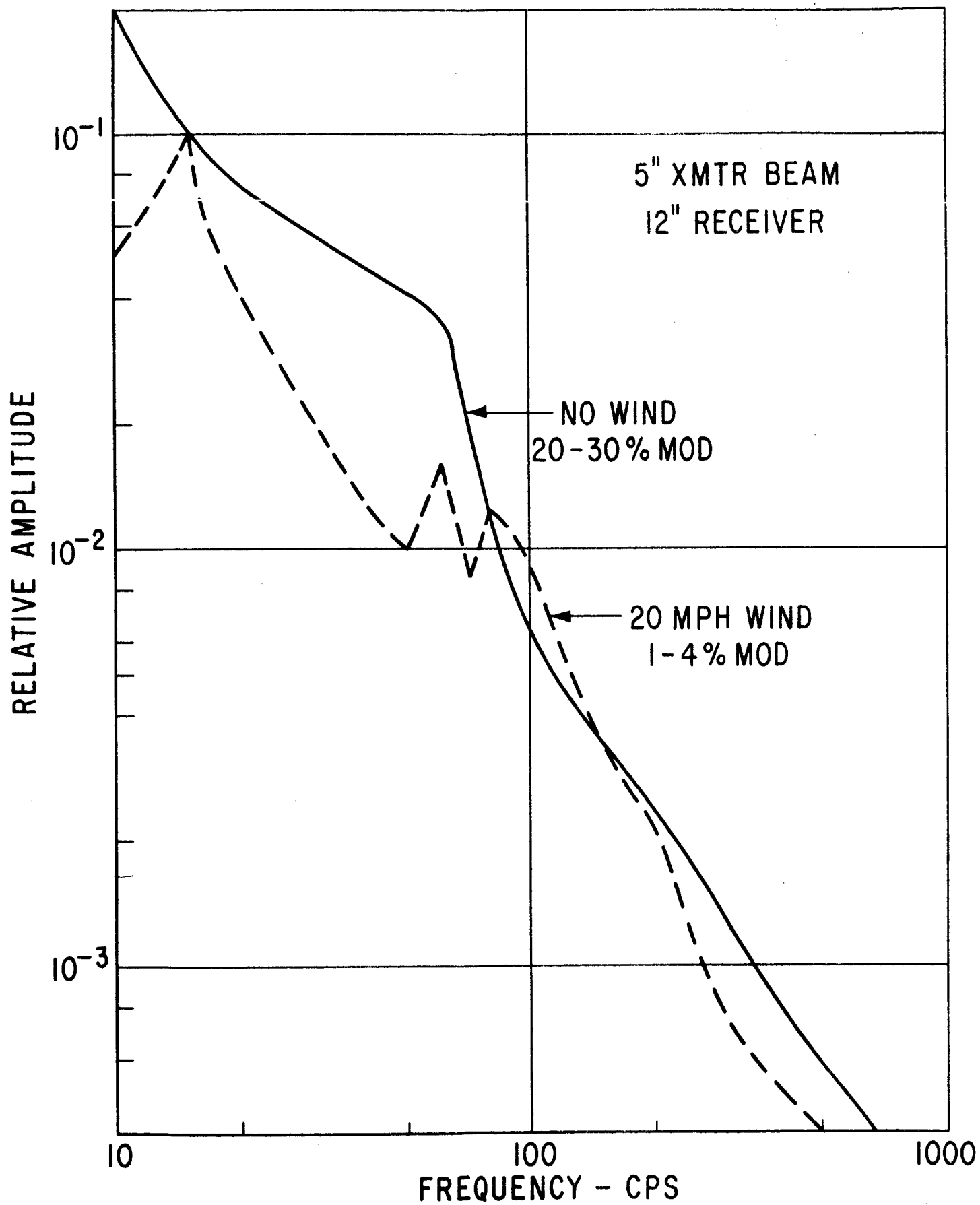


Figure 12

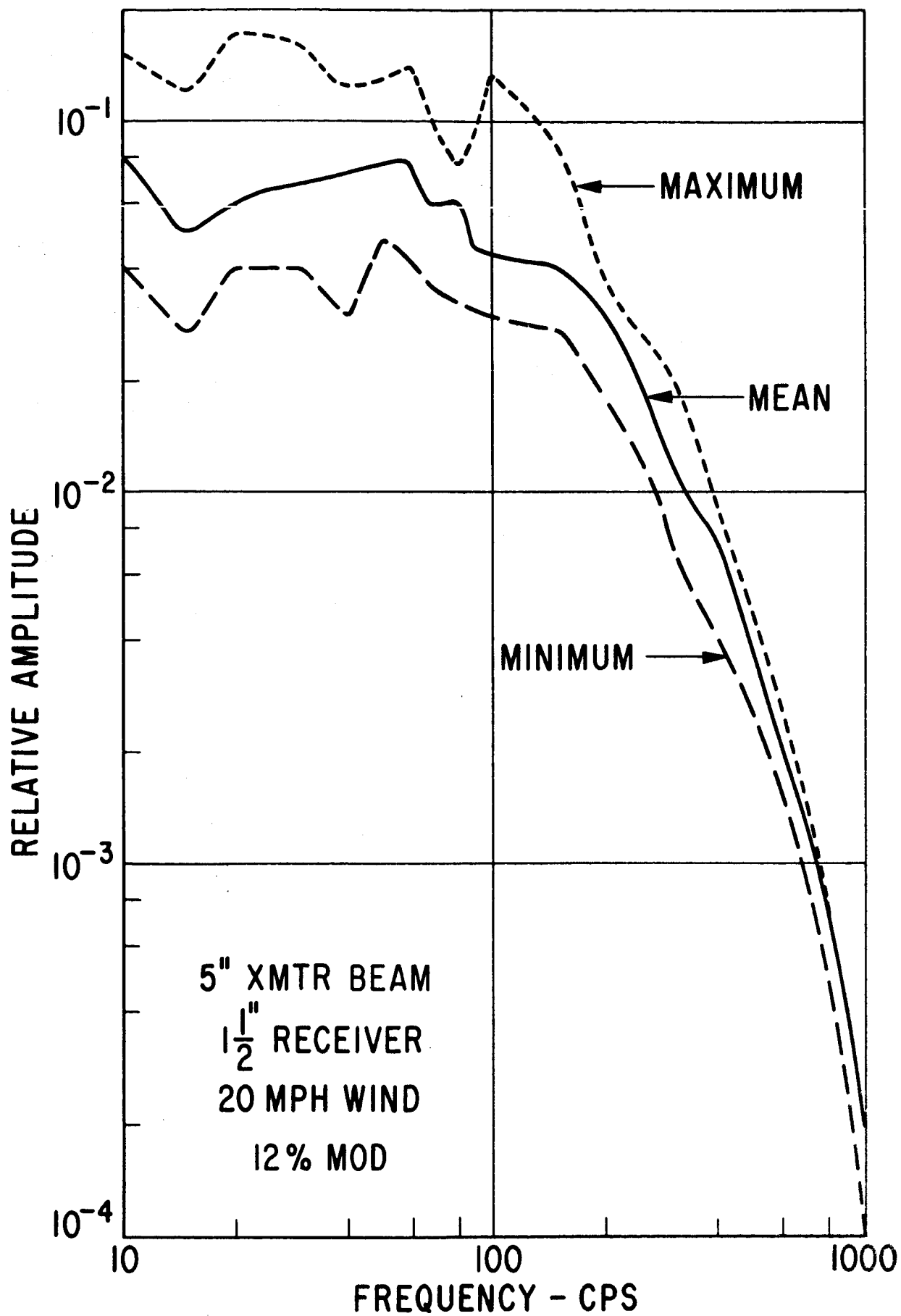


Figure 13

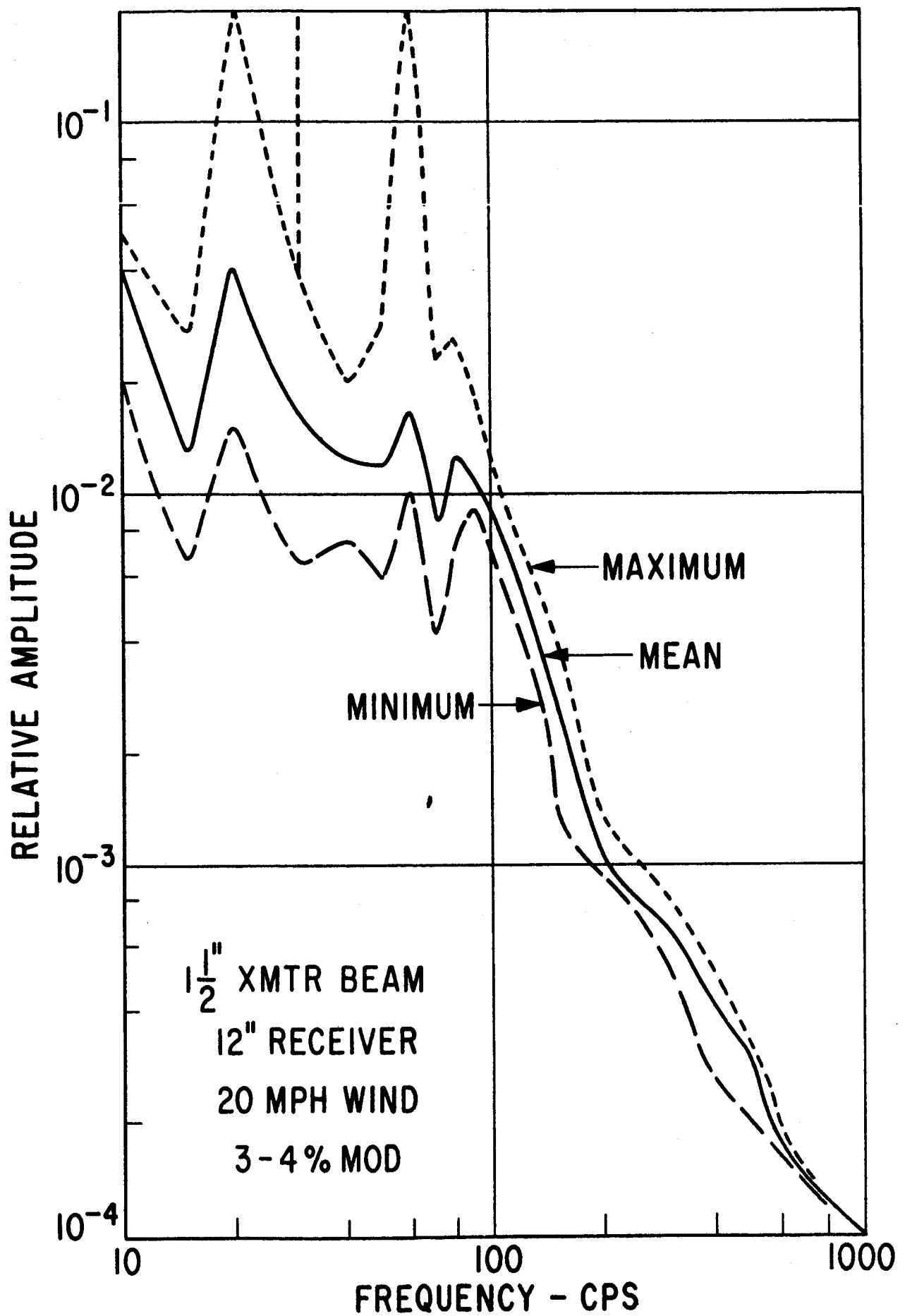


Figure 14

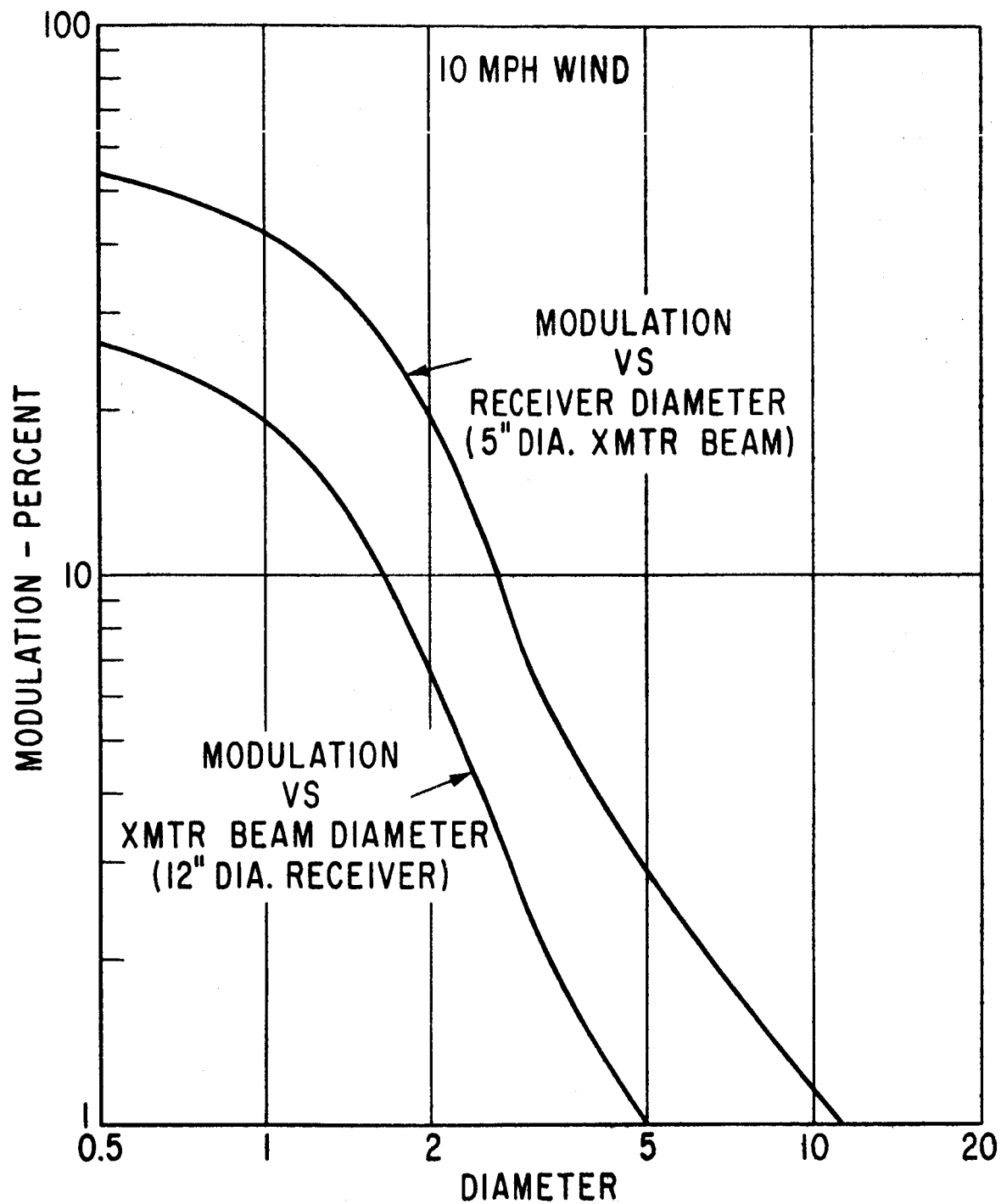


Figure 15

The optical state of the air should be able to be defined by using a telephotometer to measure scatter and a series of long thin black bars of varying widths for contrast. Experiments are needed to reduce this theory to actual measurements. A great need exists in defining an impulse function for the atmosphere in terms of scattering, turbulent elements, temperature, wind, etc.

For simplicity consider a perfectly collimated beam with isotropic turbulence. As the beam starts out, with a diameter of $d > \ell$ the size of the turbulent elements, it will be deviated an amount $\Delta\psi$ by each element. After a number of elements, the distribution of $\Delta\psi$ will be Gaussian. One difference between this and the astronomical case is immediately apparent. The wavefront coming from a star is effectively infinite, and on the average as much light will be scattered out of a beam as will be scattered into it, while with the laser beam light will be primarily scattered out of the beam. This leads to a new attenuation, which will be a function of the beam diameter and divergence. If the beam has less divergence than the divergence of the scattering observed, in many cases for a 1 KM path of the order of 10 inches at night, then it will suffer an apparent attenuation. This attenuation will also be larger for a small diameter beam than for a large diameter beam.

In examining a beam, as in Figure 9, care must be taken in interpretation. The large linear deviations will be due to angular deviations near the source, however, the large angular deviations are not apparent since they will occur near the detector. These large deviations near the detector lead to the light being scattered at large angles, which form a background around the point image in an optical system.

The case is somewhat different when considering a beam of light entering the atmosphere from outside and being detected at the ground. First, two cases must be distinguished. If the diameter of the beam is large, much larger than the detector aperture, the case resembles the astronomical case and there is a well known scintillation plus seeing phenomena. If the beam is narrow, light is scattered out by the small deviations and very strong scintillation and attenuation result. The dancing and other seeing effects caused by this layer will be small if measured as a focused image in a telescope. Also, seeing deviations will be less than in the horizontal case and will be a function of zenith distance. This effect is, of course, due to the exponential decay of the turbulence array from the ground.

Reversing the situation and sending a beam out from the ground leads to a different set of effects. The worst layers of the atmosphere are encountered first, leading to an enlarged beam and a broken-up internal structure. The layer near the tropopause, which usually yields scintillation, is now of negligible effect, since its angular deviations are small compared to those caused near the ground, and those near the ground also have the greatest lever arm. Thus the beam outside the atmosphere will exhibit a strong scintillation effect, and the cross section of the beam will be quite broken up.

This non-reciprocal nature of the difference between outgoing and incoming beams is quite important in any practical application of lasers.

One experimental fact should also be mentioned. In observing the broken-up pattern of a horizontal beam it has been noted that the pattern is locally coherent. Therefore, coherence of the beam has not been lost, the "sparkle" effect of the beam, caused by interference, still exists in the bright patches. This local coherence, of course, does not imply that there are no phase shifts across the wave front, but only that phase shifts are similar for nearby points.

This, of course, is of importance in the possible application of heterodyne detection, which does not seem too optimistic because of the necessity of matching the two beams, one from the local oscillator and one from the beam.

It is possible that some compensation for seeing effects can be made in a transmitting system. One such suggestion would be to track an object, and to optically correct for beam deviations. If, as has been established, the effects are primarily below 100 cycles, the situation in the atmosphere could not change in the time interval between incoming and outgoing light. Two reservations must be made about such a system. First, it would be necessary to track the object that the beam was being aimed at optically; and second, as Figure 8 illustrates, we are not dealing with a simple dancing of a beam, but rather with a breakup of the beam itself. Thus only part of the effect is compensated for.

Noise Effects of Scintillation

In addition to the photomultiplier or other detectors there are several sources of noise in photoelectric measurements. These may be divided as follows:

1. Photon noise, due to the statistical nature of the photon arrival.
2. Scintillation, due to atmospheric scattering by turbulent elements.
3. Transparency effects, low frequency variations in intensity.
4. Background noise.

For the time being, let us confine ourselves to photon noise and scintillation. Fluctuation in the arrival of photons follow a Poisson distribution, and to a good approximation if n photons arrive, the fluctuations will be $n^{1/2}$. Thus the photon signal to noise goes as $n^{1/2}$. If we let the aperture of a telescope be D , the number of photons increases as D^2 , so that the photon signal to noise ratio goes as $1/D$. To a first approximation for scintillation the number of turbulent atmospheric elements intercepting the aperture, m , will be proportional to D^2 , and assuming that the elements are independent the fluctuation due to scintillation will also go as $1/D$. Now assume that a signal, \bar{n} photons per second, is arriving. Let k be the percentage modulation introduced by scintillation. Then the photon signal to noise will be $\sqrt{\bar{n}}$, while the scintillation noise will be $k \bar{n}$. Thus the ratio, photon S/N / scintillation S/N will go, as a function of n , as $\sqrt{\bar{n}}/k\bar{n} = 1/k \times 1/\sqrt{\bar{n}}$. On the other hand, consider the flux as a constant, or the aperture D as the variable. Then the photon S/N will go as $1/D$ and the scintillation signal to noise will also go as $1/D$. Obviously, there will be a point, depending on the amount of scintillation, where scintillation noise becomes less important than photon noise. This point observationally occurs between 5 and 7.5 magnitude, or roughly at flux of 10^4 to 10^3 photons/cm²/sec, usually closer to the later.

Let us consider these factors in a little more detail. Let the flux of photons be f photons/cm²/second. Let the aperture of the telescope be D , its transmission t , and the quantum efficiency of the detector be ϵ . Assume that all operations are noiseless behind the photocathode. Further, let us as a convenient convention drop the factor $\pi/4$ in the area factor relationship to diameter (we might introduce a modified D' , for example to compensate for this).

Then the photon flux at the detector is fD^2 , and the average number of photoelectrons given off is ϵfD^2 , so that the noise is

$$N_p = (\epsilon f t)^{\frac{1}{2}} D \quad (53a)$$

and the signal to noise is

$$S/N \text{ photon} = \frac{\epsilon t f D^2}{(\epsilon f t)^{\frac{1}{2}} D} = (t \epsilon f)^{\frac{1}{2}} D \quad (53b)$$

Now consider scintillation noise. Assuming that it gives a percentage modulation k , for a unit aperture, then the scintillation noise will be

$$N \text{ scint} = k t \epsilon f D^2 D^{-1} = k \epsilon f D, \text{ and} \quad (54)$$

$$S/N \text{ scint} = \frac{\epsilon t f D^2}{k t f D \epsilon} = D/k \quad (55)$$

assuming the noises add in quadrature, we have

$$N = (N_p^2 + N_s^2)^{\frac{1}{2}} = (t \epsilon f D^2 + t^2 k^2 \epsilon^2 f^2 D^2)^{\frac{1}{2}} = (t \epsilon f)^{\frac{1}{2}} D (1 + k^2 \epsilon f t)^{\frac{1}{2}} \quad (56)$$

and the signal to noise ratio is

$$S/N = \frac{\epsilon f t D^2}{(\epsilon f t)^{\frac{1}{2}} D} \frac{1}{(1 + k^2 \epsilon f t)^{\frac{1}{2}}} = (\epsilon f)^{\frac{1}{2}} D \frac{1}{(1 + k^2 \epsilon f t)^{\frac{1}{2}}} \quad (57)$$

However, the two noises are not independent, since the scintillation noise is an amplitude effect, and the photon noise is a function of amplitude. Thus the photon noise should be considered as being added on after the scintillation, so that

$$N_p = (\epsilon D^2)^{\frac{1}{2}} (k^1 f t)^{\frac{1}{2}} \quad (58)$$

when k^1 is a random variable with a time average $(k^1) = 0$, and limits depending on the percentage modulation. We might thus use

$$N = N_p + N_s = (\epsilon f t)^{\frac{1}{2}} D + k \epsilon f t D = (\epsilon f t)^{\frac{1}{2}} D (1 + k \sqrt{\epsilon f t}) \quad (59)$$

and then the signal to noise would be

$$S/N = (\epsilon f t)^{\frac{1}{2}} D \frac{1}{1 + k (\epsilon f t)^{\frac{1}{2}}} \quad (60)$$

The difference in the two formulas - Equations 57 and 60 - assuming $k = 0.3$ is :

(a) if $\epsilon f t \sim 10^7$ - a strong signal

$$(57) \frac{1}{(1 + k^2 \epsilon f t)^{\frac{1}{2}}} = \frac{1}{(1 + 0.1 \epsilon f t)^{\frac{1}{2}}} \approx 10^{-3} \quad (61)$$

$$(60) \quad \frac{1}{1 + k (\epsilon f t)^{\frac{1}{2}}} = \frac{1}{(1 + 0.3 (\epsilon f t)^{\frac{1}{2}})} \approx 10^{-3} \quad (62)$$

or no difference

(b) If $\epsilon f t \sim 10$ - a weak signal

$$(57) \quad \frac{1}{(1 + 1)^{\frac{1}{2}}} = 0.707 \quad (63)$$

$$(60) \quad \frac{1}{1 + 0.3 (10)^{\frac{1}{2}}} = 0.51 \quad (64)$$

The crossover point of the importance of photon and scintillation noise may be found by equating equations 53a and 54.

$$N_p = N_s \quad (65)$$

$$(\epsilon f t)^{\frac{1}{2}} D = k t \epsilon f D \quad (66)$$

solving for f gives

$$f = \frac{1}{k^2 \epsilon t} \quad (67)$$

If the quantum efficiency is taken as

$$\epsilon = 25\% \quad (68)$$

and the optical transmission is

$$t = 60\% \quad (69)$$

the photon flux is

$$f = \frac{1}{0.15 k^2} \approx \frac{6.7}{k^2} \quad (70)$$

Normally the modulation is approximately 10% so

$$f \approx 670 \text{ photons/cm}^2/\text{sec}$$

A zero magnitude signal is about 10^6 photons/cm²/sec and considering that one magnitude is 4 db, 670 photons/cm²/sec is a 31.8 db difference or almost an 8 magnitude signal.

REFERENCES

Figure 16 has been included to give some indication of the problems involved, and as a key to a few of the references. This listing is an extension of that given in Photo Electric Observatory Report 3 and it includes some of the more recent papers.

Turbulence in the atmosphere has been discussed in a number of Meteorology Texts, special reference should be made to:

1. Brunt, Dynamical Meteorology
2. Sutton: Atmospheric Turbulence

The standard work on turbulence is:

3. Batchelor: Homogeneous Turbulence

One of the best reviews of seeing, including a very extensive Bibliography, is,

4. Folke Nettelblad: Studies of Astronomical Scintillation. (51)
5. Gaviola: On Seeing, Fine Structure of Stellar Images, and Inversion Layer Spectra. (29)

From the geometrical standpoint, and for an understanding of the problem, the following is basic:

6. Chandrasekhar: A Statistical Basis for the Theory of Scintillation. (12)

A different approach to the problem has also been used, and as a starting point the following papers are good.

7. Kellar: Astronomical "Seeing" and its Relation to Atmospheric Turbulence. (38)
8. Kellar and Hardie: Experimental Verification of a Recently Proposed Theory of Astronomical Seeing. (39)

One of the problems that is most difficult to investigate is that of low frequency components in stellar dancing. These are well discussed in

9. Land: Anomalies in Atmospheric Refraction. (43)

The paper that established the independence of scintillation and image motion is:

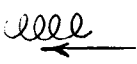
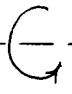
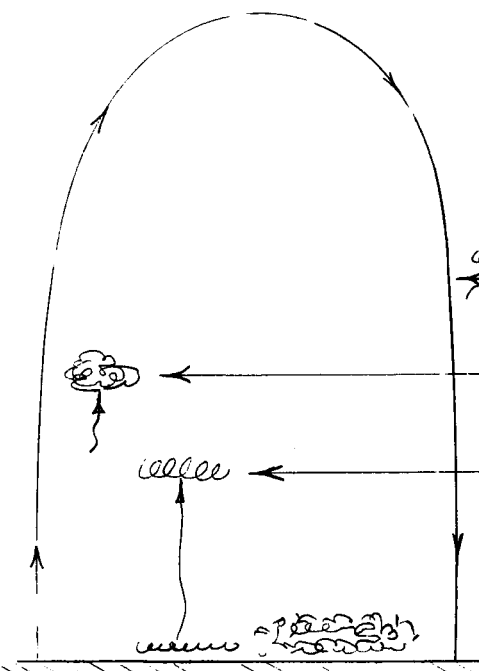
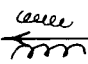


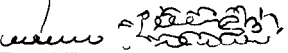
SITUATION	DESCRIPTION	REFERENCE
Tropopause	15-20 Km	
 turbulence carried by winds	Thin Layer, Scintillation	Keller (7)
Inversion Layer	1-10 Km (sometimes lower)	Gavioli (5)
 turbulent mixing of layers	defocusing, dancing	
		
Large Turbulent Convection		
cells, Benard cells		Brunt (1)
1-2 Km high		
2-6 Km horizontally		
	Wind forces (all levels)	Sutton (2)
	Occasional buoyant elements	Land (9)
	Buoyancy acting on thermal turbulence	Hosfeld (10)
	Thermal turbulence near ground	Portman (12)

Figure 16

10. Hosfeld: Comparison of Stellar Scintillation with Image Motion. (34)

One of the basic papers on avoiding the seeing problem is:

11. Platt: Increase of Telescope Resolution with Time Selection and Image Forming Stellar Interferometer. (52)

Other papers include that of Leighton in Scientific American, and Hardie, Seyfort, and DeWitt in Sky and Telescope.

Of the more recent work, three should be noted.

12. Portman, Elder, Ryznen, Noble: Some Optical Properties of Turbulence in Stratified Flow Near the Ground. (92)
13. Tatarski: Wave Propagation in a Turbulent Medium. (84)
14. Chernov: Wave Propagation in a Random Medium. (80)

There is also a good discussion of seeing in Amateur Telescope Making (Scientific American), and a recent article in The Transactions of the Professional Group on Military Electronics, IRE, which discusses seeing under daytime conditions.

BIBLIOGRAPHY

1. V. Barocas and R. Withers - Obs. 68, 153, 1948.
2. H. Booker, J. Radcliffe and D. Schinn - Phil. Trans. Roy. Soc. 242, 579, 1950.
3. H. G. Booker and W. E. Gordon - Proc. IRE 38, 401, 1950.
4. E. N. Bramley - Proc. Roy. Soc. A., 215, 515, 1954.
5. B. H. Briggs, G. J. Phillips and D. H. Shinn - Proc. Phys. Soc. B 63, 196, 1950.
6. B. H. Briggs and G. J. Phillips - Proc. Phys. Soc. B, 63, 907, 1950.
7. B. H. Briggs - Proc. Phys. Soc. B 64, 225, 1951.
8. H. E. Butler - Obs. 70, 235, 1950.
9. H. E. Butler - Obs. 71, 28, 1951.
10. H. E. Butler - Proc. Roy. Irish Acad. 54A, 321, 1952.
11. H. E. Butler - Nature 167, 287, 1951.
12. S. Chandrasekhar - Mon. Not. Roy. Ast. Soc. 112, 475, 1952.
13. S. Chandrasekhar - R. M. P., 15, 1, 1943.
14. A. Couder - Vistas in Astronomy, Vol. I, Revised, 1955.

15. A. Couder - C. R. 203, 609, 1936.
16. A. Danjon and A. Couder - Ch. V, P. 72, Lunettes et Telescopes, 1935.
17. A. Danjon - C. R. 174, 1408, 1922
18. M. A. Ellison and H. Seddon - Obs. 71, 26, 1951
19. M. A. Ellison and R. Wilson - MNRAS, 112, 475, 1952.
20. M. A. Ellison - Astronomical Optics, Ch. 31, Z. Kopal 1956.
21. M. A. Ellison - Nature 165, 664, 1950.
22. J. A. Fejar - Proc. Roy. Soc. A, 220, 455, 1953.
23. P. B. Fellgett - Astronomical Optics, Ch. 36, Z. Kopal 1956.
24. R. Furth - Astronomical Optics, Ch. 32, ed. Z. Kopal 1956.
25. R. Furth - Schwankungerscheinungen in der Physik, 1920.
26. R. Furth - Phys. Zs. 21, 582, 1920.
27. R. Furth - On the Theory of Stochastic Phenomena, Geophysical Bulletin V, Dublin Inst. for Adv. Stud. 1952.
28. R. Furth - Report of Conference on Physics of the Ionosphere, Physical Society (London) 1955.
29. E. Gaviola - A. J., 54, 155, 1949.
30. J. S. Hall - Astronomical Photoelectric Photometry Wood ed, 1953.
31. N. Hansson, H. Kristenson, F. Nettelblad, A. Reinz - Ann.
32. A. Hewish - Proc. Roy. Soc. A 209, 81, 1951.
33. A. Hewish - Proc. Roy. Soc. A 214, 494, 1952.
34. R. Hosfeld - JOSA 44, 284, 1954.
35. R. Hosfeld - AFCRC - TN-55-873.
36. T. R. Kaiser - Astronomical Optics Ch. 35, Z. Kopal ed. 1956.
37. G. Keller - A. J. 58, 113, 1953.
38. G. Kellar, R. H. Hardie - A. J. 59, 195, 1954.
39. G. Keller, Protheroe, Barnhat, Galli - Ohio State University, AFCRC Contract AF 19(609)-1409, Report No. 1.
40. G. Keller, Protheroes, Barnhat, Galli - AFCRC Contract AF 19(609)-1409, Final Report.
41. G. Keller - JOSA 45, 845, 1955.
42. G. Keller - Present and Future of Telescope of Moderate Aperture Ch. 10, Wood ed. 1958.
43. G. Land - A. J. 59, 29, 1954.
44. Leighton, Sci. American 194, No. 6, 157, June 1956.

45. C. G. Little - MNRAS 111, 289, 1951.
46. E. C. S. Megaw - Nature 166, 1100, 1950.
47. A. H. Mikesell, H. A. Hong, J. S. Hall - JOSA 41, 689, 1951.
48. A. H. Mikesell, Pub. U. S. Naval Obs. XVII Part IV, 139, 1955.
49. M. Minnaert - Nature 165, 664, 1950.
50. M. Minnaert and J. Houtgast - Zs f. Ap. 10, 86, 1935.
51. F. Nettleblad - Medd. fran Lunds. Astr. Obs. Sec. II No. 130, 1953.
52. J. Platt, Ap. J. 125, 601, 1957.
53. W. M. Protheroe - Perkins. Obs. Contr. Sec. 2, No. 4, 1955.
54. W. M. Protheroe - Present and Future of Telescope of Moderate Aperture Ch. 9, Wood ed. 1958.
55. W. M. Protheroe - JOSA 45, 851, 1955.
56. W. M. Protheroe - Contrib. Perkins Obs., II-4, 1955.
57. W. M. Protheroe and Kwan-Yu Chen - GRD TR-60-287.
58. J. A. Radcliffe - Nature 162, 9, 1948.
59. Lord J. W. S. Rayleigh - Phil. Mag. 36, 129, 1893.
60. J. Rosch - J. Physique Rad. 15, 395, 1954.
61. J. Rosch - Astronomical Optics Ch. 33, Z. Kopal ed. 1956.
62. J. Rosch - J. Physique Rad. 16, 545, 1955.
63. M. A. Ryle and A. Hewish - MNRAS 110, 381, 1950.
64. H. O. Sandig - A. N. 269, 269, 1939,
65. H. Seidentopf and W. Elsasser - Zf. Ap. 35, 21, 1954.
66. H. Seidentopf - Astronomical Optics, Ch. 34, Z. Kopal ed. 1956.
67. Smith, Saunders, Vatisia - JOSA 47, 755, 1957.
68. M. V. Smoluchowski - Sitzungsber. d. Akad. Wiss. Wien 123, 2381, 1914.
69. M. V. Smoluchowski - Sitzungsber. d. Akad. Wiss. Wien 124, 1915.
70. W. H. Stevenson - Vista in Astronomy, Vol. 1, A. Beer, 1955.
71. B. Stromgren - Matematisk Tidsskrift, Forste Del, 15, 1945.
72. F. Villars, V. Weisskopf - Phys. Rev. 94, 232, 1954.
73. F. Zwicky - PASP 62, 150, 1950.
74. A. M. Obukhov - Izvestia Akad. Nauk, Geophys. Series, No. 2, 1953, 155.
75. V. A. Kradilnikov - Dokl. Akad. Nauk 65, No. 3, 1949.
76. E. G. Kolchinsky - A. J. 29, No. 3, 1952.

77. V. A. Krasilnikov - Izv. Akad. Nauk SSSR, Series Geog. and Geophys. No. 1, 1949,
78. H. Seidentopf and F. Wisshak - Optik, Band 3, 1948.
79. F. Bellaire, F. Elder - Univ. of Michigan Res. Inst. Rept. 2900-134-T, 1960.
80. F. Bellaire, E. Ryzhar - Univ. of Michigan Res. Inst. Rept. 2900-293-T, 1961.
81. P. Bergmann - Phys. Rev. 70, 486, 1946.
82. M. A. Ellison - Quant. J. Royal Meteorol. Soc. 80, 246, 1954.
83. A. S. Gurvich; V. Tatarski and L. Cvang - Doklady, Akad. Nauk SSSR 123, 655, 1958.
84. V. I. Tatarski - Wave Propagation in a Turbulent Medium, McGraw-Hill, 1961.
85. Tatarski, Gurvich, Kallistratova, Terenteva - J. Soc. Ast. 2, 588 (A.I.P. Trans.).
86. Chernov - Wave Propagation in a Random Medium, McGraw-Hill, 1960.
87. Van Isacker - Quart. J. Royal Meteorol, Soc. 80, 251.

International Symposium on Fundamental Problems in Turbulence and their Relation to Geophysical. J. of Geophysical Research 67, No. 8, July, 1962. Especially the following papers:

88. R. Bolgiano - Structure of Turbulence in Stratified Media, 3015.
89. R. Deissler - Turbulence in the Presence of a Vertical Body Force and Temperature Gradient, 3049.
90. E. Spiegel - Thermal Turbulence at Very Small Prandtl Number, 3063.
91. Panofsky - Budget of Turbulent Energy in the Lowest 100 Meters, 3161.
92. Portman, Elder, Ryzhar, Noble - Some Optical Properties of Turbulence in Stratified Flow, 3223.
93. P. B. MacCready - Turbulence Measurements by Sailplane, J. G. P. Res. 67, p. 1041.
94. P. B. MacCready - Inertial Subrange of Atmospheric Turbulence, J. G. P. Res. 67, p. 1051.
95. Briggs - Diff. by an Irregular Screen of Limited Extent, Proc. Phys. Soc. LXXVII, p. 305.

96. Mercier - Diff. by Finite Irregular Objects, p. 318.
97. J. A. Hynek - Smithsonian Report No. 33, February 1, 1960, Effects of Image Motion on the Measurement of a Flashing Satellite.
98. R. A. Becker, "Effects of Atmospheric Turbulence on Optical Instrumentation", IRE Trans. on Mil. Elect., Vol. MIL-5, pp. 352-356; October 1961.
99. S. Q. Duntley, W. H. Culver, F. Richey and R. W. Preisendorfer, "Reduction of Contrast by Atmospheric Boil", Jr. Optical Society of America, Vol. 53, pp. 351-358; March 1963.

An introduction to the topic of scattering by clouds and fog can be obtained through the following books:

100. Middleton - Vision Through the Atmosphere, University of Toronto Press, 1952.
101. Handbuch der Physik Band XLVII, Geophysik II, Article by Middleton.
102. Minnaert - Light and Colour in the Open Air, Dover, 1954.
103. Van de Hulst - Light Scattering by Small Particles, Wiley, 1957.

For background data the following are convenient:

104. Handbook of Geophysics, Second Edition, MacMillan, 1960.
105. Allen - Astrophysical Quantities, University of London, 1955.

Sky structure is discussed by:

106. R. M. Miller, "A Limitation On the Photometry of Faint Objects", The Astrophysical Jr., Vol. 137, No. 4, pp. 1040-1056.

Part 3

LASER OPTICS

LASER OPTICS

I. Transmitting Optics

A laser is characterized by a beam divergence α ; this divergence being due to the imperfection of the device. Empirically for solid lasers an image can be formed of dimensions

$$h = f \alpha \quad (71)$$

where f is the focal length of the lens. This corresponds to a model in which a number of coherent wave fronts are emerging from the end of the laser, with the angle between the extreme rays being α . To narrow the divergence from α to α' , where $\alpha' < \alpha$, it is necessary only to use a telescope of power

$$P = \alpha / \alpha' \quad (72)$$

But this is also the ratio of entrance to exit pupil, so that if one takes the exit pupil to be the laser diameter, and the entrance pupil as the telescope aperture, we have

$$\alpha' = (d/D) \alpha \quad (73)$$

where

d - is the laser diameter

D - is the telescope aperture

Obviously it is not necessary to use the full aperture D , but if some optics are used with $D' < D$, then energy is lost in the system by the amount $D^2 - D'^2$, and there is no net gain in energy in the beam. It can also be readily shown that using this technique is the most efficient, if one focuses the beam it will diverge beyond the focus, and the formed image will be quite large.

Let us assume a laser of diameter d , divergence α , and an optical system telescope aperture of D , where we wish to place a maximum energy density ρ at some range r . If a Galilean telescope system is used to decrease the divergence we have $\rho \approx 1/\alpha'^2 r^2$ which with equation 73 becomes

$$\rho \approx \frac{D^2}{\alpha^2 d^2 r^2} \quad (74)$$

When we attempt to focus the beam, the system is similar to that of Figure 1, although of course it is not necessary to use real foci--instead a Galilean system could be used.

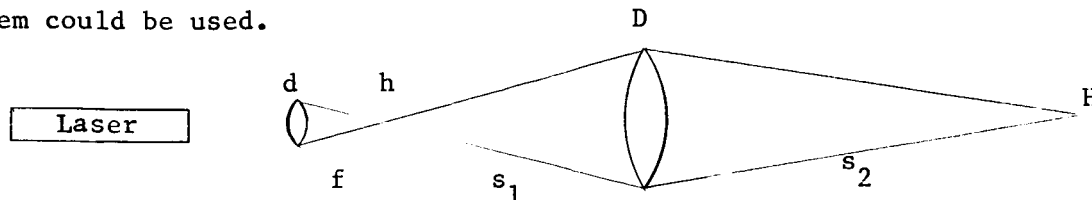


Figure 1. Laser System

The following relationships are given by Figure 1.

$$h = \alpha f \quad (75a)$$

$$H = (s_2/s_1) h \quad (75b)$$

$$d/f = D/s_1 \quad (75c)$$

$$\rho \approx 1/H^2 \quad (75d)$$

$$s_2 = r \quad (75e)$$

From which we see that

$$\rho \approx (s_1/r)^2 / \alpha^2 f^2 \quad (76)$$

and substitution of 75c gives

$$\rho \approx \frac{D^2}{\alpha^2 d^2 r^2} \quad (77)$$

Thus the inverted Galilean telescope operating to decrease divergence does so as efficiently as any other system.

Consider now what occurs when imperfect optics are used:

an incoming collimated beam will yield an image that is not a point, but rather has a characteristic dimension or quality c . If a point is then placed at this focus, it will have a divergence upon leaving the system, of $\theta = c/f$. Now if at the focus we place a laser with a divergence α and a diameter $d \gg c$, we will have our previous situation, with a resulting divergence of $\alpha' = (d/D)\alpha$. Now, there will be an additional divergence $\theta = c/f$ which will add to α' , so that the total divergence will be

$$\alpha d/D + c/f \quad (78)$$

As an example, consider using a 16" aperture $f/20$ telescope as a transmitter, with a laser beam of $1/2$ " diameter and divergence of 10^{-3} . This will have an output divergence of 3×10^{-5} if the instrument is diffraction limited ($c \sim .5 \times 10^{-3}$ inches, or an intrinsic divergence of the order of 10^{-6}). If however, we have $c \sim .5 \times 10^{-2}$, intrinsic divergence of 10^{-5} , the output divergence is 4×10^{-5} . This is not serious, but since energy density at the receiver goes down as the square of the divergence, any further drop in optical quality will bear a serious penalty. Obviously a drop in optical quality is equivalent to reducing the aperture of the telescope, so that further correction is hardly worthwhile after the two divergences are of the same order. If we set $\alpha (d/D) = k c f$, where k is a constant determining how important we let the losses due to imperfections to become (k will most likely be between

1 and 10) we see that

$$\alpha df = k c D \quad (79)$$

and thus aperture and optical quality are a direct trade where we let c represent the optical quality.

II. Receiving Optics

Similar considerations as with transmitting optics occur with receiving optics, and in the same manner the actual problem, including desired and possible divergences must be considered.

The receiver gathers the light and focuses it on some type of filter. The image will of course be that of a point source. Background radiation, coming as it does from an extended source, will be a function of the square of the f-ratio, while radiation from the transmitter will go as the square of the aperture. This implies that one desires as long a focal length as possible and of course, this immediately places constraints on the spectrograph or other wavelength and spatial filters. There is also no point in increasing the focal length beyond a certain point where seeing takes over. This means that at night, under good conditions, a maximum resolution of the order of two seconds of arc is the limit, while in the day time a limit of 5 to 10 times this is more reasonable. Unfortunately, it is in the day time that one wishes the best filtering (both spatial and frequency), so as to decrease the background noise, which is not critical at night. Much of this problem will be covered in the discussion of spectroscopic filters. The main point that can be made about optical quality is that the characteristic size c must be less than the angular resolution required. If this circle is larger than the acceptance area of the filter there will be an effective decrease in aperture, in a manner analogous to that of the transmitting system. Thus any use of low quality optics depends on the use of lower spatial resolution and wavelength resolution. The limitations are obvious.

Consider now the effects on phase coherence by the use of a non-ideal optical system. Fermat's principle states that, when light passes from one point to another, it follows paths or "rays" which are lines connecting the two points in such a way that the optical path has a maximum or minimum value. In other words, the rays are defined by the condition that the variation in optical path is zero for any infinitesimal deviation from the actual path. This implies that the optical paths from a point at infinity to an image point

must be equal. Thus we do not affect the coherence of a point in the image plane; rather, we distribute the energy over a number of points in the image plane, the optical paths to which must be different. However, this phase shift must be continuous, so that by selecting an arbitrarily small area we can obtain an arbitrarily small phase shift. This of course is equivalent to throwing away part of the aperture. As a first order approximation, the phase shift will be

$$\delta \lambda = x^2 / 2f \quad (80)$$

Assuming, for the sake of an example, that we have images of 1 mm, a 1 cm separation x , and a focal length of 1 meter, then we have

$$\delta \lambda = \frac{10^{-6}}{2} = .5 \times 10^{-6} \quad (1 \text{ mm}) \quad (81)$$

$$\delta \lambda = \frac{10^{-4}}{2} = .5 \times 10^{-4} = 50 \times 10^{-6} \quad (1 \text{ cm})$$

but we have a wavelength of the order of 0.5×10^{-6} , so that one millimeter implies a phase shift of one wavelength. Thus, if phase is important it is necessary to use high quality optics, and to limit the examined region of the focal plane. It should be noted that similar arguments apply to the phase shifts introduced by atmospheric turbulence.

III. Filtering

The problem of filtering is a complex one, since there are relations between spatial and frequency resolution. We will restrict ourselves here primarily to filters which utilize the phenomenon of interference, although the discussion can be extended to other types.

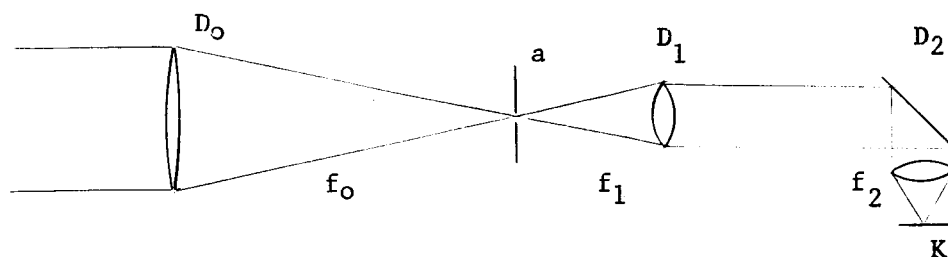


Figure 2. Telescope - Spectrograph Combination

Consider a telescope - spectrograph combination as shown in Figure 2 where

D_0 - is the diameter of the telescope aperture

f_o - is the telescope focal length
 a - is the slit width at the focus which controls
 both field of view and resolution
 D_1 - is the collimator aperture
 f_1 - is the focal length of the collimator

Notice that an angular deviation δ is converted to a linear displacement $f\delta$ at a , and again to an angular deviation by the collimator where

$$\delta' = (f_o/f_1) \delta \quad (82)$$

so that in general there will be a net magnification of the angular deviation. The collimated light is reflected from the grating with some angular dispersion, α - Angstroms/radian. This angular dispersion is thus converted into a linear dispersion by the spectrograph camera D_2 , with the linear dispersion K_2 - Å/mm, where $K_2 = 1/\alpha f_2$. The resolution is set by either the resolution element size, R , or the size of the image of the slit at the detector, $w = \frac{f_2}{f_1} a$, whichever is larger. Note that if we can make R arbitrarily small the camera characteristics do not enter into the problem. Let us also introduce a quantity $a = D_1/D_o$.

We may now set up a number of constraints and relations on the system, as follows:

$$a) \quad D_o/f_o = D_1/f_1 \quad (83a)$$

$$b) \quad \beta f_2 (D_1/D_o) = \beta/q \alpha k = \beta f_2/q \quad (83b)$$

where β is the angular field of view, and the others are defined above

$$c) \quad \text{Size of image at slit } \beta f_o \quad (83c)$$

$$d) \quad \text{Size of slit at detector } w = a(f_2/f_1) \quad (83d)$$

$$e) \quad \text{Spectral resolution } K R \quad (83e)$$

Now, we set $R = w = a(f_2/f_1)$. Note that if $R < w$, spectral resolution is not increased, and if we are using a photomultiplier we are throwing away some of the light. This loss of light does not hold of course for an imaging detector. If $R > w$, spectral resolution is decreased. Since in the type of application under discussion we would have R as a mask ahead of a photomultiplier this assumption is justified.

It now follows that

$$\Delta \lambda = K R = \frac{1}{\alpha f_2} \frac{f_2}{f_1} a = a/\alpha f_1 \quad (84)$$

Furthermore, we set $a = \beta f_o$, that is, the slit defines the field of view. We note that if $a > \beta f_o$, extra sky light is admitted, limiting the signal to noise. If $a < \beta f_o$, light is not admitted by our system, and the field of view is restricted.

It now follows that a number of relations can be set up on the basis of this last relation. We have

$$w = \frac{f_2}{f_1} \quad a = \frac{\beta f_2}{q} \quad (85a)$$

$$\beta = \frac{a}{f_1} \quad q = \frac{a}{f_1} \frac{D_1}{D_o} \quad (85b)$$

$$\text{and since } \beta f_o = a, \quad \beta = \frac{a}{f_o}$$

This last gives

$$\frac{a}{f_o} = \frac{a}{f_1} (D_1/D_o) \quad , \quad D_o/f_o = D_1/f_1 \quad (86)$$

which we have already assumed. Obviously our assumptions are not completely independent.

We now have two equations

$$\beta = \frac{a}{f_o} = \frac{a}{f_1} \times \frac{D_1}{D_o} \quad \text{and} \quad (87a)$$

$$\Delta \lambda = a / \propto f_1 \quad (87b)$$

Note that this depends on our assumptions involving R.

Now

$$a/f_1 = \propto \Delta \lambda \quad (88a)$$

$$\beta = \propto \Delta \lambda (D_1/D_o) \quad (88b)$$

Thus setting β and $\Delta \lambda$ sets D_1/D_o , or vice versa. Further note that if we assume a given value of $\Delta \lambda$,

$$\Delta \lambda = a / \propto f_1 \quad (89)$$

Thus a/f_1 is fixed, and

$$\beta = (a/f_1) (D_1/D_o) \quad (90)$$

If we assume D_o/f_o is fixed, and thus D_1/f_1 is fixed,

$$\beta \sim \frac{a}{D_o} \quad (91a)$$

but also

$$\Delta \lambda \sim \frac{a}{f_1} \quad (91b)$$

Thus

$$\beta = q_1 a/D_o \quad (92a)$$

$$\Delta \lambda = q_2 a/f_1 \quad \text{or} \quad a = f_1 \Delta \lambda / q_2 \quad (92b)$$

and

$$\begin{aligned} \beta &= (q_1/q_2) f_1 \Delta \lambda / D_o \\ &= q_3 f_1 \Delta \lambda / D_o \end{aligned} \quad (93)$$

Thus β is proportional to $\Delta \lambda$, and β is inversely proportional to D_o . Also, since f_1 is proportional to D_1 , we have

$$\beta \sim \Delta \lambda (D_1/D_o) \quad (94)$$

Now, α is of the order of 10^{-3} to 10^{-4} . Taking 10^{-4} ,

$$\beta = \Delta \lambda 10^{-4} \frac{D_1}{D_o} \quad (95)$$

D_1/D_o will be less than 1, say of the order of .1, then

$$\beta \sim \Delta \lambda 10^{-5} \quad (96)$$

and for a resolution of .1 Å, then $\beta = 10^{-6}$, or less than one second of arc.

For a practical system we must include a number of other considerations, especially that of background illumination and the resulting signal to noise ratio.

Assume that we are attempting to observe a monochromatic point source with N_s photons / cm²/second. Assume further that we have a background of N_v photons / cm²/second/steradian.

Thus, we collect $1/4 \pi D_o^2 N_s$ photons/second for the signal, and $1/4 \pi D_o^2 N_v \Omega$ photons/second background, when Ω is the field of view in steradians. If our field of view is β radians, then it will be β^2 steradians (depending of course on the actual aperture shape). Thus the signal to noise ratio is with equation 90 included

$$\frac{1/4 \pi D_o^2 N_s}{1/4 \pi D_o^2 N_v \beta^2} = \frac{N_s D_o^2}{N_v (a/f_1)^2 D_1^2} \quad (97)$$

Obviously, the signal to noise against the sky is set only by the field of view, or, analogously, the focal length and slit of the telescope. The question now is, how much of the noise, and how much of the signal are passed by the spectroscope.

The spectral resolution of the sky light will be set by the slit width. However, the spectral resolution on the point source will depend on its angular diameter, as set by seeing or similar phenomenon. As a problem let us assume that the sky noise can be represented by $N = f(\lambda) \Delta \lambda$, where $\Delta \lambda$ will be set by the telescope/spectrograph combination.

$$\Delta \lambda = (\beta/\alpha) (D_o/D_1) = a/\alpha f_1 \quad (98)$$

Thus, the noise at the detector will be limited to a $\Delta \lambda$ which is a function of β , and will also be a function of β from field of view combinations. Thus we have

$$\begin{aligned} N &= 1/4 \pi D_o^2 f(\lambda) \Delta \lambda \beta^2 \\ &= 1/4 \pi D_o^2 f(\lambda) (a/f_1)^3 (D_1/D_o)^2 / \alpha \end{aligned} \quad (99)$$

and our signal is

$$S = 1/4 \pi D_o^2 N_s$$

So thus, the Signal/Noise ratio is

$$S/N = \frac{\alpha N_s}{f(\lambda)} (f_1/a)^3 (D_o/D_1)^2 \quad (100)$$

Therefore we see that the Signal/Noise ratio is proportional to $(D_o/D_1)^2$. Note that this is quite different than our previous result D_1/D_o .

Under sky light conditions our limit is set by the noise in the background, under dark sky conditions it will be set by the photon noise in the signal, and this of course will be proportional to D_o , so that the signal/noise is set by D_o .

Practical Design

Now, to tie these formulas down let us consider a concrete design. Assume that our receiver is fixed as a 16" f/20 Cassegrain telescope. This is the type of instrument which will be installed in the Radio-Optical Observatory in early 1964. Furthermore, assume that we are trying to observe a weak laser signal limited by the night sky, the day sky, the moon's surface, and scattered light near the moon. These cover a great variety of conditions.

Before continuing further let us examine the dispersion of a grating more closely. We have used α - radians/Ångstroms. From the theory of

diffraction we have

$$\alpha = \frac{d\theta}{d\lambda} = \frac{m}{s \cos \theta} \quad (101)$$

where s is the spacing between lines, m is the order, and θ is the angle of diffraction. If the lines are spaced about one micron, then $s = 10^4 \text{ \AA}$, and α is of the order of 10^{-4} . It must be noted that the dispersion is distinct from the resolution of a grating, which increases with the order and with the total number of lines, and will in general be greater than that of our instrument, since we are limited by the slit.

We will assume in what follows that α is of the order of 10^{-4} , and that the grating is blazed for the first order in the red.

Taking $D_0 = 400 \text{ mm}$, $f_0 = 8000 \text{ mm}$, $D_0/f_0 = 1/20$, then $D_1/f_1 = 20$ also. Our selection of D_1 will now depend on the spectral resolution required and on the angular field.

Now, remembering that angular resolution is

$$\beta = (a/f_1) (D_1/D_0)$$

so that referring to formula 100 for Signal/Noise we have

$$S/N = \frac{\alpha N_s}{f(\lambda) \beta^3} (D_1/D_0) \quad (102)$$

We wish β to be small, and D_1 to be large. Assume that we use a 150 mm grating. Then we are limited to a 150 mm collimator, so $D_1 = 150 \text{ mm}$, and $f_1 = 20 \times 150 = 3000 \text{ mm}$. Thus $(D_1/D_0) = 15/40 = 3/8$, and $S/N = 3/8 \times 10^{-4} 1/\beta^3 N_s/f(\lambda)$. Thus, if we know the necessary S/N , N_s , and $f(\lambda)$, we may set β .

Consider a 1 mill field of view, and a signal to noise of 1. Then

$$f(\lambda) = 3/8 \times 10^{-4} \times 10^9 \times N_s \sim 5 \times 10^4 N_s$$

or

$$N_s = .2 \times 10^{-4} f(\lambda)$$

$f(\lambda)$ may be taken as the average number of photons at the wavelength of interest, per \AA , per steradian. Thus, for a 1 mill field we have the required signal for a given background.

The daytime sky in these units is roughly 10^9 . Thus in the daytime we have

$$N_s = .2 \times 10^{-4} \times 10^9 = 2 \times 10^4 \text{ photons/second} \quad (103)$$

Consider now a field of 10^{-2} mills, roughly two seconds of arc. This is a minimum field of view from the stand point of seeing. Then

$$f(\lambda) \sim .5 \times 10^{-4} \times 10^{-15} N_s = 5 \times 10^{20} N_s$$

or

$$\begin{aligned} N_s &= 10^{-10} = 2 \times 10^{-11} f(\lambda) \\ &= 2 \times 10^{-2} \text{ photons/second} \end{aligned} \quad (104)$$

The variation of 10^6 between the two follows the $1/\beta^3$ response. This last value might be regarded as being close to a minimum one.

The night sky is down by a factor of 10^7 from the day time sky, and since this is a straight decrease in noise, it modifies the signal to noise ratio by that amount. The surface of the moon is an order of magnitude brighter than the day time sky, and allowing for some scatter in the telescope, at night the sky near the moon will be 10^3 down from the day time sky. These factors, which are of course only order of magnitude, are directly applicable to the signal to noise calculations given previously.

Note that we have not explicitly given the resolution of the spectro-scope, which is implied by the field of view. Knowing equation 98 and substituting in the assumed values we have that

$$\Delta \lambda = \beta \times 10^4 \times 8/3 \quad (105)$$

For

$$\beta = 10^{-3}, \text{ then, we have}$$

$$\Delta \lambda = 10 \times 2.67 = 26.7 \text{ \AA}$$

and for

$$\beta = 10^{-5} \text{ we have}$$

$$\Delta \lambda = .267 \text{ \AA}$$

Let us now summarize the relations

S/N (sky limited)

$$S/N = \frac{\alpha N_s}{f(\lambda) \beta^3} (f_1/a)^3 (D_o/D_1)^2 \quad (100)$$

$$= \frac{\alpha N_s}{f(\lambda) \beta^3} (D_1/D_o) \quad (102)$$

S/N (photon limited)

$$S/N = D_o \sqrt{1/4\pi} N_s$$

$$\Delta \lambda = (\beta/\alpha) (D_o/D_1) \quad \beta = \alpha \Delta \lambda (D_1/D_o)$$

$$\Delta \lambda = (a/f_1)/\alpha$$

$$\beta = (a/f_1) (D_1/D_o)$$

These relations somewhat conceal the dependence on focal length, and the practical factors involved in the camera design.

Dielectric Filters

Dielectric interference filters are frequently used. With this type of filter we need to consider the filter center frequency, λ_o , the bandwidth $\Delta \lambda$, and the shifted center frequency $\lambda \theta$ when the light comes in at some angle θ to the normal. Consider the system in the accompanying Figure 3.

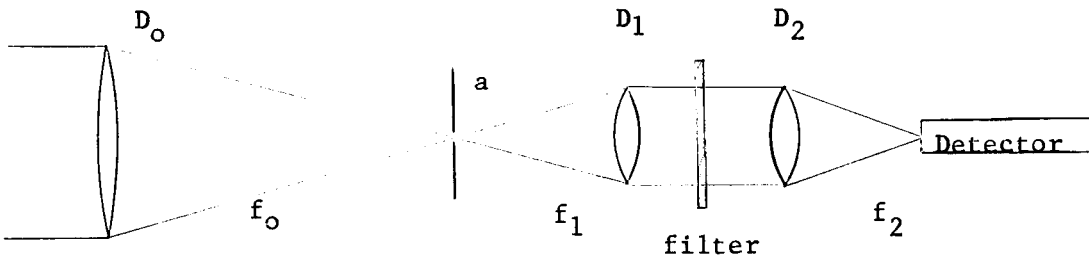


Figure 3. A Dielectric Interference Filter

This is quite similar to the previous one. Here the aperture "a" will serve as a spatial filter, and the collimator will minimize the divergence of the beam. The camera lens is not critical. The divergence at the filter, θ , will be defined by

$$a = f_1 \theta \quad (106)$$

and the field of view of the telescope will be given by

$$a = f_o \alpha \quad (107)$$

$$\text{so that} \quad \theta/\alpha = f_o/f_1 \quad (108)$$

but we also have

$$D_o/f_o = D_1/f_1 \quad (109)$$

so that

$$\theta/\alpha = D_o/D_1 \quad (110)$$

Since $D_1 < D_0$, we must have $\theta > \alpha$, and this ratio is set by the available filter size. In most practical systems there will be an order of magnitude difference between α and θ .

The wavelength shift, λ_θ , can be determined from the equation

$$\lambda_\theta / \lambda_0 = \sqrt{1 - (\sin \theta / n)^2} \quad (111)$$

where θ is the angle from the normal, not the total angle as before. For 10° , this value is typically of the order of .995, and our wavelength are of the order of 10,000 Å, so that a 1° field of view, resulting in a 10° divergence, would deviate the center wavelength by 50 Å. In this region the relationship is approximately linear, so that to obtain an Angstrom shift the field of view would have to be near a minute of arc. Note that this is the shift in center frequency, so that the bandpass must be appreciably wider.

One point that is frequently overlooked in calculations with this type of filter is the width of wings; the percentage transmission in the wings may be large, since they extend thru the spectrum and can result in the admission of a strong background signal.

IV. Detection of Faint Sources

As a final point let us consider the problem of the detection of a faint object. In this we will follow the direction of Baum (Astronomical Techniques, Ed. W. A. Hiltner, U. of Chicago, 1962). At first we will assume that seeing fluctuations can be ignored, and then we will examine this assumption.

In the wavelength interval of interest, let n_s be the number of photons from the source, n_b the number of photons of background per unit solid angle, ϵ the quantum efficiency, δt the time interval of observation, and D the effective aperture of the telescope. By absorbing system losses and $1/4\pi$ in D we simplify the discussion. We then have

$$N_s = n_s D^2 \epsilon \delta t \quad (112)$$

as the number of signal events. The number of background events in the same area of the detector will be

$$N_b = n_b D^2 \epsilon \alpha^2 \delta t + n_n D^2 \epsilon \alpha^2 \delta t \quad (113)$$

where n_n is the number of instrumental noise events projected thru the optics,

$$n_n = (f/D)^2 \beta / \epsilon \quad (114)$$

where β is the number of instrumental noise events (dark current, etc.) per second per unit area. Thus we have

$$\begin{aligned} N_b &= (n_b + n_n) D^2 \epsilon \alpha^2 \delta t \\ \text{or} \\ N_b &= (n_b D^2 \epsilon + \beta f^2) \alpha^2 \delta t \end{aligned} \quad (115)$$

There is another noise that should be added to this formulation -- one which we might term scanning noise. This we shall consider later.

Now, in one element we have a signal $N_s + N_b$, and in an adjacent element a noise N_b . Assuming a Poisson distribution we have fluctuations in N_b of $\sqrt{N_b}$, and in $N_s + N_b$, $\sqrt{N_s + N_b}$. For detection N_s must stand out above the noise, so we might write

$$N_s = k \sqrt{N_b} \quad (116)$$

Actually, our criterion should be that the envelope of $N_s + N_b$ with noise $\sqrt{N_s + N_b}$ stand out beyond the envelope of the background N_b with noise $\sqrt{N_b}$. However, since we are dealing with limiting detection this distinction may be absorbed into the definition of k without affecting the argument. Thus we may write

$$N_{so} = (n_s D^2 \epsilon \delta t)_o = k \left\{ (n_b + n_n) D^2 \epsilon \alpha^2 \delta t \right\}^{1/2} \quad (117)$$

The assumption thus far lies primarily in the definition of ϵ and the independence of the events, plus the type of noise considered.

We have two forms that the relation can take.

$$\begin{aligned} N_{so} &= (n_s D^2 \epsilon \delta t)_o = k \left\{ (n_b + n_n) D^2 \epsilon \alpha^2 \delta t \right\}^{1/2} \\ N_{so} &= (n_s D^2 \epsilon \delta t)_o = k \left\{ (n_b D^2 \epsilon + \beta f^2) \alpha^2 \delta t \right\}^{1/2} \end{aligned} \quad (118)$$

solving for n_s , and taking logs of each side we obtain a ready solution for either form.

$$\log n_s = \log k + 1/2 \log n_b + 1/2 \log (1 + n_n/n_b) + \log \alpha - 1/2 \log D^2 \epsilon \delta t$$

$$\log n_s = \log k + 1/2 \log n_b + 1/2 \log (1 + \beta f^2/n_b D^2 \epsilon) + \log \alpha - 1/2 \log D^2 \epsilon \delta t \quad (119)$$

If the time constant of the detector τ is less than the shortest pulse length, $\tau < \delta t$, these formulas are valid. If it is not, it is apparent that there will be a loss of sensitivity. This follows from setting the minimum pulse length as δt , and the integration time for noise as τ . We then obtain

$$\begin{aligned} \log n_s &= \log k + 1/2 \log n_b + 1/2 \log (1 + n_n/n_b) + \log \alpha \\ &\quad - 1/2 \log D^2 \epsilon + 1/2 \log \tau - \log \delta t \\ &= \log k + 1/2 \log n_b + 1/2 \log (1 + n_n/n_b) + \log \alpha \\ &\quad - 1/2 \log D^2 \epsilon + \log \sqrt{\tau} / \delta t \end{aligned} \quad (120)$$

The use of the term $(1 + n_n/n_b)$ can be somewhat misleading, since there are then two variables when sky brightness changes, n_b and $(1 + n_n/n_b)$. We thus can put the equation into another form,

$$\log n_s = \log k + \log \alpha + 1/2 \log (n_b + n_n) - 1/2 \log D^2 \epsilon \delta t \quad (121)$$

The argument so far has neglected photon noise, this was implicit in the manner in which k was defined. Let us now examine this point a little more fully. We had assumed that

$$N_s = k \sqrt{N_b}, \quad (122)$$

but we might instead take

$$N_s - N_b = k (N_s + N_b)^{1/2} \quad (123)$$

yielding

$$n_s = \frac{k \{ (n_b + n_n) D^2 \epsilon \alpha^2 \delta t + n_s D^2 \epsilon \delta t \}^{1/2} + (n_b + n_n) D^2 \epsilon \alpha^2 \delta t}{D^2 \epsilon \delta t} \quad (124)$$

This form is not as amenable to a simple solution as the former. However, in the limit as $(n_b + n_n)$ becomes negligible it goes into the form

$$\log n_s = \log k^2 - \log D^2 \epsilon \delta t \quad (125)$$

which is the formula for pure photon noise limiting.

We might best summarize these relations using magnitudes instead of logarithms. We then obtain

$$m_{so} = 0.5 m_b - 2.5 \log \alpha - 2.5 \log k + 1.25 \log D_\epsilon^2 \int t \\ - 1.25 \log (1 + R) + \text{constant} \quad (126)$$

$$\text{where} \quad 1 + R = 1 + \beta f^2 / n_b D_\epsilon^2 = 1 + n_n / n_b$$

or, in a somewhat more convenient form

$$m_{so} = 0.5 m_{(b+n)} - 2.5 \log \alpha - 2.5 \log k + 1.25 \log D_\epsilon^2 \int t \\ + \text{constant} \quad (127)$$

the sign reversal and the factor 2.5 of course come from the definition of stellar magnitude, and the constant is simply one to establish the zero point of the magnitude scale. The magnitude of the sky including the projected detector noise is simply m_{b+n} .

For practical purposes it would seem to be a good idea to define a magnitude scale using 0 magnitude as equivalent to 10^6 photons. In this case the available astronomical data could be readily used.

In using photomultipliers as detectors these equations will be followed fairly closely, except that there will be some additional noise caused by the fluctuation in output pulse height. These should not cause an error by a factor of two. A larger source of error will be scintillation noise, which the previous equation assumed to be negligible. This is of course not an additive noise, but rather will be a rapid fading. This has been discussed previously. Since the suggested definition of magnitude matches the astronomical one reasonably closely, the cross-over between scintillation noise limiting and photon noise limiting will occur at between 5th magnitude and 7.5 magnitude (10^4 photons/cm²/second to 10^3 photons/cm²/second) independent of the telescope aperture. This statement of course applies to intensity measurements over extended integration periods.

What can we say about short pulses? We of course do not expect the scintillation to have components of high enough frequency to compare to pulse length. Thus the scintillation introduces a pulse height modulation which

will decrease as the aperture is increased. Assume that we have a percentage modulation index k which is typical of a one centimeter aperture. Then the actual modulation at the receiver will be $(1/D)k$, where D is the aperture in centimeters. Assume that we have a pulse of $D^2 \rho \tau$ photons, where ρ is the photon density in photons/cm²/sec. and τ is the pulse length. Then we expect modulation depths of $(k/D)D^2 \rho \tau$, and the signal to go from $D^2 \rho \tau$ to $D^2 \rho \tau - k D \rho \tau$. Similarly a like pulse will have photon noise of $\sqrt{D^2 \rho \tau}$. Setting the two equal we have

$$\sqrt{D^2 \rho \tau} = k D \rho \tau$$

or

$$k^2 \rho \tau = 1, \rho = 1/k^2 \tau \quad (128)$$

as the point at which photon noise becomes more important than scintillation noise. Note that this is independent of D .

Such arguments are of course of an order of magnitude nature, and great care should be taken in applying them. It appears that in most cases we must consider scintillation as a major noise, the photon noise is of course not independent of scintillation noise either. In many cases, we are more interested in the amount of noise, rather than the scintillation. As a first approximation it is permissible to assume that it will vary as $k D^{-1} \sec \theta$, when θ is the zenith distance. Typically, for a one centimeter aperture we might take k as .3, although it will go higher in cases of poor seeing. On the other hand, for large zenith distances the $\sec \theta$ term will yield terms that are too high.

Since scintillation yields a fading, the previous detection limit should be modified so that the minimum signal is increased to compensate for the worst scintillation.